NITROXIDE MEDIATED POLYMERIZATION: MICROEMULSION OF N-BUTYL ACRYLATE AND THE SYNTHESIS OF BLOCK COPOLYMERS

by

Wing Sze Jennifer Li

A thesis submitted to the Department of Chemical Engineering

In conformity with the requirements for

the degree of Master of Applied Science

Queen's University

Kingston, Ontario, Canada

September, 2012

Abstract

Living radical polymerization has proved to be a powerful tool for the synthesis of polymers as it allows for a high degree of control over the polymer microstructure and the synthesis of tailored molecular architectures. Although it has great potential, its use on an industrial scale is limited due to environmental and economical aspects. Nitroxide-mediated polymerization is explored to bring this technology closer to adoption in commercial applications.

One of the obstacles encountered using nitroxide-mediated polymerization in microemulsion systems is the difficulty in controlling both the particle size and target molecular weight. Due to the nature of the formulation, a decrease in the target molecular weight is coupled to an increase in the particle size. For many applications, it is important to be able to design polymer particles with both specifications independently. Strategies to decouple these two properties and processing conditions required for targeting a range of particle sizes and molecular weights for *n*-butyl acrylate latexes are presented. Furthermore, in an attempt to reduce the large amounts of surfactant typically used in microemulsions, these methods were explored at low surfactant to monomer ratios (0.2 to 0.5 by wt.) in order to reduce the costs associated with excess surfactant and post-processing steps for surfactant removal (high surfactant levels also give poor water-resistance in coatings). Stable nanolatexes with particle sizes <40 nm have been obtained by other groups using NMP in microemulsions with SG1 but have done so by using much higher surfactant to monomer ratios (~2.5 by wt.) and at much lower solids content (6-10 wt. %). In this work, molecular weights of 20,000 to 80,000 $g \cdot mol^{-1}$ were targeted and stable, *n*-butyl acrylate microemulsions with particle sizes ranging from 20-120 nm were prepared at a solids content of 20 wt. % using much lower surfactant concentrations. Although numerous studies have shown the effects of process parameters on particle sizes and methods to control the molecular weight, the decoupling of the molecular weight and particle size effect in NMP microemulsions under these conditions has not been done to this extent.

In copolymer systems, nitroxide-mediated polymerization also provides an efficient method to synthesize well-defined block copolymers. Random copolymers are widely used as protective colloids, but the use of block copolymers for these applications has not been well studied. It is unclear what effects do the importance of a narrow molecular weight distribution and purity of block copolymers have on their performance as protective colloids. In order to investigate this, a range of block copolymers with different properties would need to be synthesized for systematic analysis. The direct synthesis of polystyrene-*b*-poly(acrylic acid) copolymers of varying lengths and compositions was successful by use of nitroxide mediated polymerization in bulk and solution polymerization. The characterization of these amphiphilic block copolymers was explored by titration and nuclear magnetic resonance spectroscopy.

Statement of Co-Authorship

The bulk of the research was carried out independently by myself, under the supervision of Dr. Michael Cunningham. The preparation and editing of this thesis was conducted under the supervision of Dr. Michael Cunningham.

Acknowledgements

I would like to thank Dr. Michael Cunningham for his guidance and support in working towards my Masters degree at Queen's University and also for the many opportunities for further learning and travel.

I would like to thank my family and Jeff for their support, encouragement, and patience throughout my Masters. I would like to thank my friends Calista, Kevin, Julien, Lydia, Ki, Eric, Niels, Nicky, Jason, and Sandhya for the numerous fun times, random moments, awesome food adventures, and help in the past 2 years. Thanks to the many others in the polymer group and chemical engineering department for their advice and expertise. Thank you to all my friends who have supported me one way or another throughout all of this.

List of Abbreviations

AA	Acrylic Acid
ABC	Amphiphilic Block Copolymer
ATRP	Atom Transfer Radical Polymerization
BA	Butyl Acrylate
BB	BlocBuilder® MA
BB/Na_2CO_3	BlocBuilder® MA to Sodium Carbonate ratio
CMC	Critical Micelle Concentration
CRP	Controlled Radical Polymerization
CTAB	Cetyl trimethylammonium bromide
DIW	Distilled Deionized Water
DLS	Dynamic Light Scattering
DMSO	Dimethyl sulfoxide
DP	Degree of Polymerization
DP_n	Number Average Degree of Polymerization
DRI	Differential Refractive Index
GPC	Gel Permeation Chromatography
HMQC	Heteronuclear Multiple Quantum Correlation
LRP	Living Radical Polymerization
MMA	Methyl Methacrylate
MWD	Molecular Weight Distribution
NMP	Nitroxide Medicated Polymerization
NMR	Nuclear Magnetic Resonance
NOE	Nuclear Overhauser Effect
PAA	Poly(acrylic acid)
PDI	Polydispersity Index
PMMA	Poly(methyl methacrylate)
PSD	Particle Size Distribution
PSt	Polystyrene
RAFT	Reversible Addition Fragmentation Transfer
SG1	1-diethylphosphono-2,2-dimethylpropyl
St	Styrene
S/M	Surfactant to Monomer ratio
TEMPO	2,2,6,6-tetramethylpiperidine-1-oxyl
THF	Tetrahydrofuran
TMS	Trimethylsilyl
UV-VIS	Ultraviolet-Visible Spectroscopy

Nomenclature

α	Significance level in confidence interval
δ	Chemical shift [ppm]
κ	Debye-Hückel parameter
ρ	Polymer density [$g \cdot cm^{-3}$]
ρ_{BA}	Density of butyl acrylate [$g \cdot cm^{-3}$]
ρ_{PBA}	Density of poly(butyl acrylate) [$g \cdot cm^{-3}$]
a	Mark-Houwink Sakurada parameter
A_s	Area that one surfactant molecule occupies on the particle surface
C	Surfactant concentration at micellization [$mol \cdot L^{-1}$]
C_a	Concentration of surfactant added and adsorbed [$mol \cdot L_{latex}^{-1}$]
C_i	Initial surfactant concentration [$mol \cdot L_{latex}^{-1}$]
C_f	Concentration of unadsorbed soap in the latex solution at the CMC [$mol \cdot L^{-1}$]
D_p	Average particle diameter
K	Mark-Houwink Sakurada parameter [$dL \cdot g^{-1}$]
k_{act}	Rate coefficient of activation [s^{-1} or $L \cdot mol^{-1} \cdot s^{-1}$]
k_{deact}	Rate coefficient of deactivation [$L \cdot mol^{-1} \cdot s^{-1}$]
k_p	Rate coefficient of propagation [$L \cdot mol^{-1} \cdot s^{-1}$]
m	Polymer concentration [$mol \cdot L^{-1}$]
m_{BA}	Mass of butyl acrylate [g]
m_o	Initial polymer concentration [$g \cdot L_{latex}^{-1}$]
m_s	Mass of surfactant [g]
M	Monomer concentration [$mol \cdot L^{-1}$]
M_n	Number-average molecular weight [$g \cdot mol^{-1}$]
M_{pol}	Mass of polymer [g]
M_s	Surfactant molecular weight [$g \cdot mol^{-1}$]
M_w	Weight-average molecular weight [$g \cdot mol^{-1}$]
N	Number of samples
N_A	Avogadro's number
N_p	Number of particles [L^{-1}]
P●	Concentration of propagating polymer chain [$mol \cdot L^{-1}$]
P-X	Concentration of polymer chains capped by nitroxide [$mol \cdot L^{-1}$]
R_p	Rate of polymerization [$mol \cdot L^{-1} \cdot s^{-1}$]
s	Sample standard deviation
S_a	Surfactant concentration required to reach the CMC [$mol \cdot g_{polymer}^{-1}$]
S_i	Initial surfactant concentration [$mol \cdot g_{polymer}^{-1}$]
S_t	Surfactant concentration at micellization [$mol \cdot g_{polymer}^{-1}$]
$t_{1-\alpha/2,\ N-1}$	t-critical value from t-distribution tables
V_p	Particle volume [cm^3]
x	Conversion
X	Nitroxide concentration [$mol \cdot L^{-1}$]
$\bar{X}$	Sample mean

Table of Contents

List of Figures

Chapter 2

Chapter 3

Chapter 4

Appendices

List of Tables

Chapter 3

Chapter 4

Appendices

Chapter 1

Introduction

Living radical polymerization (LRP) has emerged as an effective and powerful tool to produce tailored polymers with advanced molecular architectures. Through the use of a mediating species in nitroxide mediated polymerization (NMP), a reversible termination process between growing polymer chains is established which enables the direct control of the resulting polymerization structure with narrow molecular weight distributions. As with conventional free radical polymerization, NMP can be employed in the dispersed phase, bulk, and solution polymerization. The synthesis of these polymers at an industrial scale remains a challenge due to economical and environmental constraints and it is necessary to explore different strategies to synthesize these polymers in a cost-effective and environmentally beneficial manner.

1.1 Overview

In this work, nitroxide mediated polymerization is explored in microemulsions to investigate the polymerization conditions at which specific polymer properties can be targeted and in copolymerizations to create amphiphilic block copolymers. One of the challenges include the correlation between the target molecular weight and particle size in controlled emulsion polymerizations, which is opposite in conventional emulsion polymerizations. Targeting both the molecular weight and particle size independently can be achieved in miniemulsion systems but the high costs associated with their implementation on an industrial scale makes microemulsion systems more attractive. Another challenge is the synthesis and characterization of low molecular weight amphiphilic copolymers of polystyrene and poly(acrylic acid) due to incompatibilities

between the nitroxide and the acid groups and the similarities in chemical structure thus making compositional analysis by NMR difficult.

A comprehensive literature review is presented in Chapter 2 which covers the mechanisms of NMP and the challenges associated with its implementation in the dispersed phase as well as difficulties with its use in the polymerization of acidic polymers. Traditional and novel methods for the controlled synthesis of well-defined polymers are reviewed.

The challenges of the coupling effect of target molecular weight and particle size in nitroxide mediated microemulsion polymerization are addressed in Chapter 3 and a range of polymerization conditions is explored in an attempt to decouple these two effects. Furthermore, in an attempt to reduce the large quantities of surfactant traditionally used in microemulsions in the interest of costs, these polymerizations are carried out at much lower than typical surfactant to monomer ratios (0.2 to 0.5 by wt.) with the use of a two-stage polymerization method. By varying process conditions and parameters, a range of particle sizes (20-100 nm) were obtained independent of the target molecular weight (from 20,000 to 80,000 $g \cdot mol^{-1}$) at moderate solids content of 20 wt. %.

The ability to tailor specific properties in polymers using living radical polymerization strategies is what makes these techniques so attractive. However, the importance of high purity and narrow molecular weight distributions from a performance point of view in commercial applications is not well documented. The push for the "ideal" polymer comes with high costs and the trade-offs in terms of performance is still not clear. In Chapter 4, the synthesis and characterization of amphiphilic block copolymers, specifically polystyrene-*b*-poly(acrylic acid), is discussed with the goal of producing a wide range of these copolymers at different molecular weights, polydispersities, compositions, and degrees of purity for performance analysis as

protective colloids in collaboration with BASF. Polystyrene-*b*-poly(acrylic acid) copolymers are synthesized with an overall degree of polymerization (DP_n) of 30 and polystyrene contents of 65-75%. These copolymers are characterized by titration, nuclear magnetic resonance (NMR) spectroscopy, and gel permeation chromatography (GPC) for structure and composition.

A summary of the thesis and recommendations for future work are discussed in Chapter 5. In this work, a combination of strategies to synthesize polymer nanolatexes with both tunable molecular weight and particle size is presented. This will allow for the development of new and a wider range of materials for use in specialized coating and drug delivery applications. The methods discussed to synthesize and characterize amphiphilic block copolymers will allow for future investigation of their effectiveness for use as protective colloids compared to random copolymers and can lead to new insights in the way protective colloids behave.

1.2 Research Objectives

- To determine a set of conditions in NMP microemulsion of *n*-butyl acrylate that will enable the molecular weight and particle size to be targeted separately.
- Determine the extent at which the effects of molecular weight and particle size can be decoupled.
- Synthesize polystyrene-*b*-poly(acrylic acid) copolymers of varying block lengths, polydispersity, and composition for analysis of effectiveness as protective colloids.
- Investigate techniques to characterize polystyrene-*b*-poly(acrylic acid) copolymers for composition and purity.

Chapter 2

Background and Literature Review

Conventional free radical polymerization is widely used in industry to produce a variety of polymers and materials used today. However, the nature of the polymerization mechanism does not allow for control over the polymer architecture, which limits its use in many specialized applications. Living radical polymerization has emerged as an effective and powerful tool to produce tailored polymers with advanced characteristics. The level of control this technique provides is achieved through the reversible termination of growing polymer chains. The three main types of living radical polymerization (LRP) are nitroxide mediated polymerization (NMP), atom transfer radical polymerization (ATRP), and reversible addition-fragmentation chain transfer polymerization (RAFT). All of these techniques allow for the production of polymers with tunable properties including molecular weight, structure, functionality, and composition.

2.1 Nitroxide Mediated Polymerization

Since the initial work by Rizzardo et al.[61] and Georges et al.[1] on the use of nitroxides as mediators in living radical polymerization of styrene, the kinetics and mechanisms of NMP has been extensively studied in many systems and much effort has been put into the synthesis of new nitroxides[2]. Nitroxide mediated polymerization allows for a high degree of control over the synthesis of tailored molecular architectures by making use of a stable free radical that acts as a regulator between propagating polymer chains to establish a reversible termination process. Control of the polymerization is attained through the activation-deactivation equilibrium of the nitroxide mediating species. This equilibrium between the dormant and active chains favours the

dormant species, so the concentration of active chains is generally lower than in conventional free radical polymerization. It has been proposed that for a successful nitroxide mediated polymerization to take place, the equilibrium constant should ideally be small, in the range of 10^{7}-10^{11} L·mol^{-1}[3]. The reaction mechanism for NMP using the nitroxide SG1 (1-diethylphosphono-2,2-dimethylpropyl) is shown in Figure 2.1.

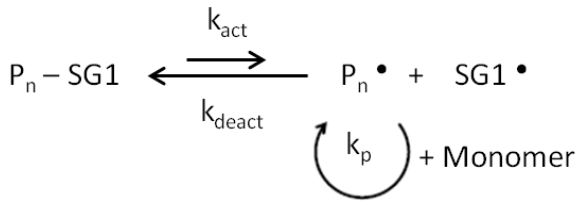

Figure 2.1: Reaction mechanism for nitroxide mediated polymerization. P_n represents a polymer chain of length *n*.

Propagation of the polymer chains proceeds through successive activation and deactivation cycles whereby monomer addition takes place when the growing chains are in their active state. The duration of each cycle is determined by the rate of chain deactivation by the nitroxide, and this can vary depending on the nitroxide used as well as the concentration of nitroxide in the system. Typically, a chain will be activated every ~10^{2}-10^{3} s and deactivated within ~10^{-4}-10^{-3} s, allowing it to add approximately 1-5 monomer units before becoming dormant[4]. This method allows for narrow molecular weight distributions to be attained (PDI<1.3)[5], especially if the polymer chains undergo many short cycles rather than fewer longer ones.

At steady state, the rate of polymerization is governed by the activation-deactivation equilibrium as those are the two main radical generation and radical loss events, which ultimately determine the concentration of the radical species [P•].

$$R_p = k_p[P\bullet][M] = k_p \frac{k_{act}}{k_{deact}} \frac{[P-X]}{[X]}[M] \tag{2.1}$$

where, k_p, k_{act}, k_{deact} are the rate coefficients of propagation, activation, and deactivation, respectively, and P, X, and M represent the polymer, nitroxide, and monomer concentrations, respectively.

Previous studies have shown that control and livingness depend not only on the equilibrium constant, but also on the propagation and termination rate constants[6]. The livingness of the polymerization is governed by the equilibrium constant but the control is dependent on the rate of initiation as well. Better control of the polymerization has been achieved with faster initiation rates[7]. In the past, the Cunningham group has worked with two nitroxides in heterogeneous systems, TEMPO (2,2,6,6-tetramethyl-1-piperidine-1-oxyl) and SG1 (1-diethyl-phosphono-2,2-dimethylpropyl). SG1 is a more reactive nitroxide compared to TEMPO but is more effective in the polymerization of acrylates because the instability actually helps to reduce its accumulation during the reaction[4]. The buildup of free nitroxide can lead to very slow polymerization times or even limit the conversion as the equilibrium is further shifted to the dormant state. The controlled polymerization of *n*-butyl acrylate has been challenging due to its high propagation rate constant and generally requires excess nitroxide to maintain control. However, the SG1-based alkoxyamine from Arkema, also known as BlocBuilder® MA, has been shown to give controlled polymerizations in the absence of excess SG1. In comparison to

TEMPO, SG1 has a higher coefficient of deactivation and a lower coefficient of activation[8] and as a result yields much faster polymerization rates.

2.2 Polymerizations in the Dispersed Phase

Water based dispersions are much preferred over solvent based polymerizations due to environmental benefits and suitability for large scale applications[9]. The use of water instead of volatile organic solvents eliminates the need for solvent recovery processes after the polymerization, which is also advantageous in terms of costs. Compared to that of bulk systems, emulsions provide better heat transfer as heat generated from the exothermic polymerization reactions are dissipated to the aqueous phase. In bulk systems, the viscosity of the reaction mixture can increase significantly making it difficult for stirring and for efficient cooling.

2.2.1 Emulsion Polymerization

Emulsions are widely used in commercial polymerization processes such as in adhesives, paints, coatings, cosmetics, and drug delivery. Poly(butyl acrylate) emulsions can be used as binders for household paints. An emulsion is a kinetically stable mixture of two immiscible liquids. In a conventional oil-in-water emulsion polymerization system, monomer (the oil phase) is dispersed in the aqueous phase and is stabilized by surfactants. Emulsion polymerization consists of three main intervals. During Interval I, also termed the nucleation stage, monomer, initiator, and surfactant are added to the continuous aqueous phase. Monomer droplets will start to form and once above the critical micelle concentration, surfactant molecules will self-assemble and form micelles[10]. Monomer will then enter these micelles to form monomer-swollen micelles. Once the temperature for initiator decomposition is reached, initiator radicals will react with

monomer in the aqueous phase until the propagating chain reaches a critical chain length at which point it loses its solubility in water and enters a monomer-swollen micelle. In systems with surfactant concentrations higher than the CMC, this is the predominant form of particle nucleation, also termed micellar nucleation. Another mechanism for particle nucleation is droplet nucleation whereby the oligomeric radicals enter monomer droplets rather than micelles. Although these z-meric oligomers can enter a monomer droplet as well, they are more likely to enter a micelle due to the greater number of micelles and the greater surface area they provide for radical capture as compared to monomer droplets[11]. For butyl acrylate, the minimum critical chain length is 2 to 3 units for persulfate derived radicals[12]. This oligomeric radical will continue to propagate to form a latex particle. As the concentration of free surfactant in the system diminishes, no new particles will be nucleated and Interval I ends. Monomers that are more hydrophilic will have a longer critical chain length and may also undergo aggregative nucleation because of this. As they are able to add more monomer units in the aqueous phase while maintaining water solubility, they can combine with other oligomeric radicals to form small particles and these particles then further combine to form a polymer particle. In Interval II, propagating radicals continue to grow in the latex particles as monomer is replenished by the monomer droplets via diffusion through the aqueous phase. Interval III begins once all the monomer droplets have been depleted. The polymerization will continue in the polymer particles until nearly all of the monomer has reacted.

As the polymerization proceeds, there will be a slow buildup of the nitroxide species in the system which will slow down the polymerization. This is due to the persistent radical effect (PRE), which explains the cross reactions between a persistent radical (the nitroxide) and a

transient radical (the propagating species)[13]. Even though irreversible bimolecular termination of the transient radicals is kept to a minimum, these reactions are still possible and will further shift the equilibrium to the dormant species. The work by Marque et al.[6] showed that there is a critical value for the rate of deactivation for which the persistent radical effect collapses and indicated that $k_d \geq 10^{-3}\ s^{-1}$ is desirable.

In an emulsion system, individual polymer particles stabilized by surfactant are dispersed in the aqueous phase. As long as the polymer chains within the particles are sufficiently hydrophobic, partitioning to the aqueous phase is kept to a minimum. Compartmentalization effects in NMP refers to the segregation effect on termination and the confined space effect on deactivation[14]. Individual polymer particles are segregated from one another and this leads to lower rates of termination resulting in increased livingness but poorer control. The segregation effect comes into play when the physical separation of propagating radicals from one another enhances the rate of polymerization due to reduced probabilities of termination between chains[15]. This leads to a slower build up of free nitroxide. On the other hand, the confined space effect explains the events that occur from the close proximity of radicals within an individual particle[15]. In this case, the rate of biradical termination increases, and the rate of polymerization decreases as a result of an increase in the rate of deactivation. The control of the polymerization is improved under this influence because the radicals undergo a higher number of activation-deactivation cycles so that fewer monomer units are added per activation cycle since the length of each cycle is decreased. This leads to a lower PDI as the number of added units by each radical per cycle is more even. In living radical systems, the overall effect is a reduction in the rate of propagation

because the confined space effect has a stronger influence on the rate than segregation. So with smaller particles, slower rates are usually observed.

Compartmentalization effects have been extensively studied in NMP and LRP emulsion systems by the groups of Zetterlund, Okubo, and Cunningham[15][14,16,17][18][19][20,21] in an attempt to exploit these effects to improve the control and livingness of nitroxide mediated emulsion polymerization systems.

2.2.2 Electrostatic Stabilization of Polymer Colloids

The stability of polymer latexes is often a concern as coagulation is generally undesirable in end-use applications. The tendency for particles to adhere to one another is the result of dipole-dipole interactions, also known as van der Waals interactions[22]. The strength of the interactions between a polymer particle and the aqueous phase will determine whether a colloidal state is achieved or not. If the interaction between a polymer particle and the medium is stronger than the interaction between two particles, then the polymer particles will be dispersed in the medium, otherwise, they will aggregate.

Electrostatic stabilization is the result of interactions among charged particles at close proximity to each other and is considered to be thermodynamically metastable. The surface potential, electrolyte concentration, and valency of the ions all play a role in influencing the extent of repulsion experienced by the particles[22]. Ions on the surface of a particle form the Stern layer and provide a surface charge which help to overcome van der Waals forces of attraction. These ions are more or less fixed on the particle surface. Ionic surfactant can either be bound to or adsorbed on the particle surface to provide these charges. The amount of surfactant adsorbed

onto the surface depends on the adsorption equilibrium between the surface of the particle and the medium[23]. Based on the principle of electroneutrality, the presence of surface ions must be accompanied by ions of the opposite charge, resulting in two parallel layers of charge surrounding the particle. This second layer of counterions is termed the diffuse layer and they move under the influence of the surface ions. The Stern and diffuse layer form the electrical double layer (EDL)[24]. The thickness of the double layer is influenced by the concentration of electrolyte in the medium and the valency of the ions. As two particles move closer together, their double layers start to overlap one another once they reach a separation distance of less than twice the Debye length (denoted as the inverse of the Debye-Hückel parameter, κ), where repulsive forces take over as the double layers are compressed together[22].

One measure of stability in colloidal systems in an electrostatically stabilized system is the zeta potential. The zeta potential is the potential at the Stern plane and it depends on the surface charges of the polymer particle as well as the properties of the surrounding medium[10]. As a general approximate value for colloidal systems, a zeta potential value of -30 mV indicates the border between a high surface charge and a low surface charge. The higher the value of the zeta potential, the stronger the electrostatic repulsion between particles and the more stable the latex. The pH of the continuous phase (water phase) can impact the zeta potential by changing the surface charge of the particle. End groups that are ionically dissociable will affect the stability of the system as well. To coagulate an electrostatically stabilized system, ~0.01 M of electrolyte is usually sufficient[25].

As electrostatic stabilization relies on ionic charges, the ionic strength of the medium plays a very important role in determining the stability of the polymer colloid as it influences the interaction energy between the particles and the medium. The thickness of the electrical double

layer decreases with an increase in ionic strength because the free ions decrease the surface potential causing the diffuse layer to contract, allowing van der Waals forces to dominate. The addition of salts or acids is used to destabilize aqueous latex by surface charge reduction due to protonation of acidic groups at low pH. Whenever there is a change in the ionic strength of a system, the ionic species will redistribute themselves, altering the colloidal interactions[23].

2.2.3 Microemulsions

Microemulsions differ from conventional emulsions in that they are thermodynamically stable oil-in-water dispersions[26]. Much smaller particle sizes (20-40 nm)[4] can be obtained from microemulsion polymerization due to the low interfacial tensions achieved using high quantities of surfactants and in some cases the use of cosurfactants as well. They are optically translucent compared to emulsions which appear milky white. These microemulsions are extremely desirable for many applications such as adhesives, drug delivery, and microencapsulation as they provide a very large internal interfacial area for further functionalization[27]. The surfactant to monomer ratios used in microemulsions are much higher than emulsions and are typically in the range of 1 to 3.3 by weight[28]. The high surfactant concentrations result in high micelle concentrations, which drive nucleation in micelles. The concentration of micelles is approximately 1000 times greater than that of particles that form and so the final polymer latex typically consists of nanoparticles and empty micelles[29]. Due to the large concentration of micelles, the probability of a radical entering a particle rather than a monomer-swollen micelle is very slim and therefore, biradical termination is almost negligible. However, this also depends on the hydrophobicity of the monomer. Monomers with higher water solubility will propagate to a greater degree of polymerization before partitioning into a micelle and so will remain in the aqueous phase for a

longer period of time, increasing the chances of termination[26]. Depending on the monomer used, the amount of surfactant required for stabilization varies. The hydrophobicity or hydrophilicity of the monomer affects surface properties and this will change the percentage of surfactant coverage required. Methyl methacrylate has a more hydrophilic surface so only about 20% coverage is sufficient. Butyl acrylate on the other hand, has a more hydrophobic surface so more than 50% coverage is required for stability[30].

One disadvantage of using such a large quantity of surfactant in the microemulsion process is that it can hinder end-use performance of the final product. Whether it is an issue of increased foaming or decreased adhesion and water resistance, these kinds of performance limitations drive the need to explore other ways to achieve stability. Some methods include varying pH, agitation speed, temperature, and monomer feed conditions. Previous work in the Cunningham group with methyl methacrylate and styrene have shown that very small particles (20-30 nm) are obtainable using low surfactant to monomer ratios (0.13-0.28 wt/wt)[31]. Previous work by the groups of Pan and Rempel[32][33] in the low surfactant ranges by free radical polymerization have also shown successful polymerization of styrene and MMA and latexes with particle sizes in the 20 nm range using surfactant to monomer ratios as low as 0.05 by wt.

Nitroxide mediated polymerization has been successfully applied in microemulsion systems to yield controlled and living polymerizations[16,34,35]. Compartmentalization effects comprising of the segregation effect and the confined space effect have been shown to operate in these systems as demonstrated by Tomoeda et al.[35].

2.3 Target Molecular Weight and Particle Size

In conventional emulsion polymerization systems, an increase in the initiator concentration results in a decrease in particle size. This is due to the stabilizing effect provided by the charged initiator end groups as well as a higher number of micelles nucleated in Interval I. In NMP emulsion systems, the opposite effect is observed where an increase in the initiator concentration results in an increase in particle size. The initiator concentration is changed when targeting different molecular weights. When going from a high molecular weight target to a low molecular weight target with the same concentration of monomer, additional initiator radicals are required to generate a higher quantity of shorter chains. This increase in initiator concentration can affect colloidal stability in several ways. First, the resulting higher concentration of short oligomers promotes superswelling, as the diffusion of monomer from the monomer-swollen micelles to nucleated particles is enhanced because of the lower monomer chemical potential in the particles. Through theoretical simulations in emulsion systems, Luo et al.[36] showed that some of the early formed particles can undergo superswelling and swell to approximately 1 μm causing colloidal instability resulting in very large particles. The superswelling effect is shown to be more pronounced in systems with slow nucleation and fast monomer transport[37]. Second, for electrostatically stabilized systems, the charged initiator end groups can increase the overall ionic strength in the system causing the electrical double layer to contract, lowering colloidal stability. Any modifications in the ionic strength of the system will cause the ionic species to redistribute themselves, which will change the colloidal interactions as well.

To address the superswelling problem, Charleux's group demonstrated a multi-step approach for nitroxide mediated emulsion polymerization using a water-soluble alkoxyamine

initiator as shown in Figure 2.2[38]. BlocBuilder® MA, the SG1-based alkoxyamine from Arkema, requires ionization with a base to convert it into its water soluble form. In the two-step method shown in Figure 2.3, a living seed latex is first produced by combining water, initiator, surfactant, and a low concentration of monomer. This step is then followed by a semi-batch addition of the remaining monomer. The results of the SG1-mediated emulsion polymerization of *n*-butyl acrylate and styrene obtained by Charleux's group using this approach showed fast, living polymerizations with good control and colloidal stability with solids content up to 26 wt% [38]. This two-step approach was also demonstrated by Ming et al. [39] in free radical microemulsion polymerizations to achieve very small particle sizes (< 20 nm) using low surfactant concentrations.

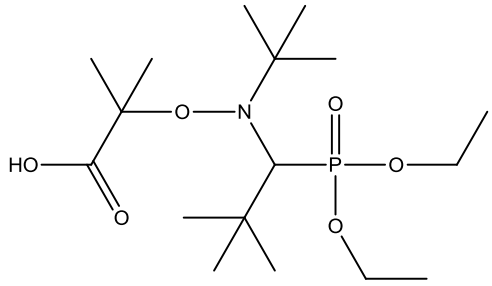

Figure 2.2: BlocBuilder® MA from Arkema Inc.

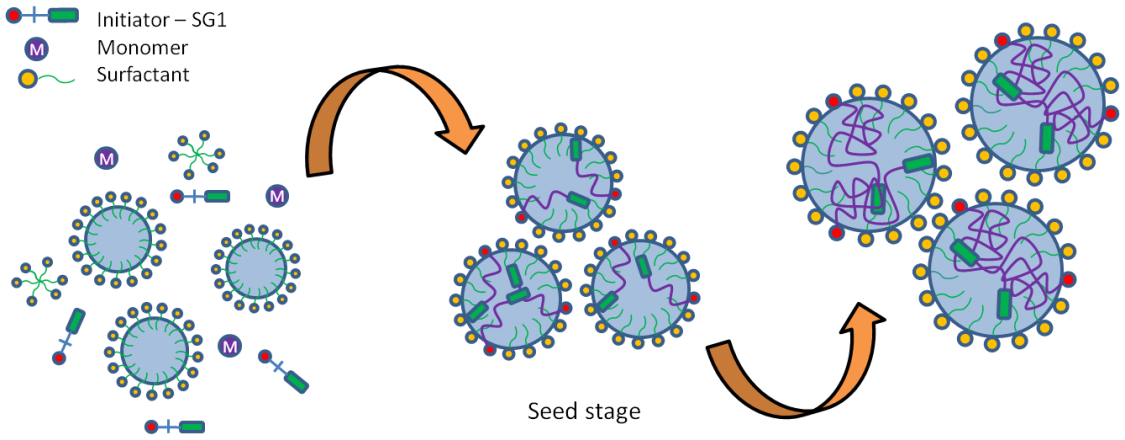

Figure 2.3: Two-stage polymerization process [38].

The strong correlation between the initiator concentration and particle size makes it difficult to tune both molecular weight and particle size simultaneously. When customizing nanoparticles for advanced applications, it is crucial that all properties can be targeted at the same time. One of the ways this can be achieved is through miniemulsion polymerization. The particle size is established through the dispersion of monomer droplets in the aqueous phase through the application of high shear, such as sonication. These droplets range from 50-500 nm[40] and are stabilized by surfactant and co-stabilizer, which help to reduce the thermodynamic driving force for monomer transport in the system. The independent control of molecular weight and particle size can be achieved using this method but in terms of implementation on an industrial scale, the sonication process is impractical and is not easily or cheaply adopted. Microemulsion on the other hand can produce very small particles and does not require such energy intensive processes, which make them easier to carry out on an industrial scale. However, the molecular weight and particle size effects in microemulsions are strongly coupled so it is challenging to target both properties simultaneously. The work presented in this thesis serves to explore this correlation and

to lay out a set of conditions that will allow the particle size and molecular weight to be targeted separately in order to determine the extent to which these two effects can be decoupled using commercially available materials.

Previous work with SG1-mediated emulsion polymerization in the Cunningham group has explored the effects of the initiator concentration on the particle size as well as the effects of ionic strength, pH, buffer, and surfactant concentration on the 1st stage latex particle size[41]. As mentioned previously, when targeting a lower molecular weight, an increase in the number of initiating groups is necessary. With NMP using BlocBuilder® MA, it was observed that the increase in BlocBuilder concentration increased the particle size even with additional surfactant in the system.

The increase in BlocBuilder concentration is suspected to cause an increase in the particle size by contributing to a higher ionic strength. As it requires ionization with a base to convert it to its water soluble form, the ionic strength contribution from the base will also negatively affect the colloidal stability. Depending on the type of base used, the ionic strength contribution can vary significantly. This was explored by Thomson et al.[41] who compared the use of Na_2CO_3 and NaOH and found that there was a significant difference in the particle sizes obtained. An increase of approximately 130 nm in particle diameter was observed when using NaOH compared to Na_2CO_3. It was suggested that because NaOH is a strong base, its apparent ionic strength in the system is higher than that of Na_2CO_3, a weak base, so the influence on the thickness of the electrical double layer is stronger. Another important role of the base is to provide buffering capacity to the system. As SG1 is unstable at low pH, buffering of the aqueous phase is necessary

to retain the surface charges of BlocBuilder. Otherwise, polymerization kinetics can be compromised as the nitroxide is consumed and cannot effectively mediate the reaction leading to high polydispersities[42]. As a result, the ratio of BlocBuilder to base plays a critical role in obtaining stable and controlled polymerizations. In a butyl acrylate emulsion polymerization using Di-BlocBuilder, it was found that particle nucleation occurred at a specific pH range and that the z-meric length may increase with increasing pH as it changes the surface activity of the water soluble oligomers[41]. All of these parameters have an effect on the colloidal stability of the system, directly influencing the final particle size. By changing these as well as other process parameters, an attempt to decouple the molecular weight and particle size is presented.

2.4 Amphiphilic Block Copolymers as Protective Colloids

Amphiphilic block copolymers (ABCs) possess the necessary properties that enable them to be compatible with two different environments at the same time. The properties and functionalities of each block allow for these polymers to establish a link between the two environments. ABCs are widely used as dispersing agents in a range of dispersion applications such as pigment dispersions in paints and coatings, compatibilizers in polymer blending processes, and protective colloids in emulsion systems. They are also used for drug delivery applications in the area of microencapsulation. In emulsion systems, these copolymers consist of a hydrophobic and a hydrophilic block allowing them to act as effective dispersing agents.

Protective colloids are water-soluble polymers which achieve stability by steric stabilization. In this stabilization mechanism, one end of the polymer chain is adsorbed onto the surface of a polymer particle and acts as an anchor, while the other end extends out into the

dispersion medium[43]. As like charges repel each other, the stabilizing groups on an amphiphilic block copolymer are mutually repulsive, helping to keep the particles from aggregating. Amphiphilic copolymers used as protective colloids are usually low molecular weight species. The length of each homopolymer block determines the polymer properties. Varying the composition of the block copolymer can enable different properties to be obtained and thus allowing them to be tailored to specific applications. Of particular interest is the polystyrene-*b*-poly(acrylic acid) amphiphilic copolymer. Much research in recent years has focused on the synthesis of this copolymer using controlled living radical polymerization techniques and its self-assembly in aqueous media.

2.5 Synthesis of Copolymers by Living Radical Polymerization

Usually, amphiphilic block copolymers are prepared via anionic polymerization, which allows for narrow molecular weight distributions to be achieved with polydispersities as low as 1.05[44]. The emergence of CRP has led to new techniques to synthesize well-defined block copolymers with low polydispersities as well, although still not as low as that achieved through anionic polymerization, from 1.1 to 1.5[45]. The suppression of the termination step in CRP allows for the re-initiation of the polymer chains that enables the controlled addition of different types of monomer to produce homopolymer blocks in a desired sequence.

The synthesis of the acrylic acid block of the PSt-*b*-PAA block copolymer has proved to be challenging in the past using CRP techniques such as NMP and ATRP due to the incompatibility between the acid and the control agent (e.g. nitroxide or metal catalyst)[46][47]. In ATRP, the acrylic acid would react with the metal complex to form metal carboxylates, which

destroys the metal catalyst, thus disabling the deactivation step[48]. In NMP, the nitroxide would be consumed through side reactions with the initiator, which was enhanced under acidic conditions, resulting in a loss of control of the polymerization[47][49]. In recent years, the controlled polymerization of acrylic acid has been successfully carried out using nitroxide mediated polymerization with excess free nitroxide to maintain control of the polymerization[50]. Couvreur et al.[50] found that a 9 mol % of free nitroxide with respect to the initiator was optimal for maintaining good control of the kinetics. The copolymerization of styrene and acrylic acid by NMP is well documented by several groups[51-53] and successful polymerizations have been carried out using NMP provided that appropriate polymerization conditions are selected. The use of 1,4-dioxane as solvent at a reaction temperature of 120°C appear to give well controlled conditions. However, at low initiator concentrations, chain transfer to 1,4-dioxane was observed at higher conversions and polymerization to low conversions (~30%) was recommended to minimize this transfer reaction.

2.5.1 Properties of Block Copolymers

It is of interest to compare the performance of block and random copolymers of polystyrene and poly(acrylic acid) as protective colloids since the distribution of each polymer in the overall copolymer can drastically influence its properties. The overall copolymer composition will also play an important role. It is often desirable to produce copolymers with a very narrow molecular weight distribution and high purity, but this is associated with higher costs. Most studies of phase behaviour uses diblock copolymers with PDI less than 1.1 and with negligible compositional heterogeneity between the chains[45]. However, the degree of purity and narrowness of the MWD have never yet been quantified in relation to the performance of the

copolymer in a systematic way. Previous studies by Laruelle et al.[51] with PSt-*b*-PAA copolymers consisting of short polystyrene blocks have looked into the effects of copolymer composition on their stabilization properties. In studies of self-assembly, they observed that the longer the poly(acrylic acid) block is, the stronger the electrostatic repulsion and that a higher concentration is required for self-aggregation with higher hydrophilic content during micellization. Burguière et al.[54] studied these copolymers synthesized by ATRP and looked at micellization behaviour from varying the length of the polystyrene block from 10 to 16 units and the poly(acrylic acid) block from 21 to 100 units. They found that those block copolymers with a high acid content behaved very similar to low molecular weight surfactants and prevented a good control of the number of particles, and those with a low acid content formed micelles for direct nucleation allowing a good estimate of the number of particles. Davis et al.[55] looked at the synthesis of low molecular weight polystyrene-*b*-poly(acrylic acid) copolymers (M_n ~10,000 g·mol^{-1}) with low PDI ranging between 1.1 and 1.3 and targeted polystyrene content from 5 to 20 mol % by ATRP, and compared the efficiency of the micellar solutions to act as a seed in emulsion polymerizations with styrene. Synthesis of the acrylic acid block was done by hydrolysis of poly(*t*-butyl acrylate). The synthesis of these diblock copolymers by RAFT and their use as stabilizers has also been discussed by several groups. With a styrene block of 5 units and an acrylic acid block of 20 to 60 units, the synthesized PAA-*b*-PSt macroRAFT agents were found to be most effective when the DP_n of acrylic acid is higher than 20, but control of the molecular weight was lost when DP_n of acrylic acid was around 60[56]. Wang et al.[57] synthesized PSt-b-PAA macro-RAFT agents consisting of styrene and acrylic acid blocks of 5 and 27 units, respectively. It has also been noted from block copolymer self-assembly studies that the morphology is dependent on the length of the blocks, chain length ratios, polydispersity, and composition[58]. With diblock polydispersity

indices of ~2.0, well-ordered lamellar or hexagonally packed cylindrical morphologies were observed in solvent-cast films of these using PSt-*b*-PAA copolymers[45]. In a study involving the use of block copolymers in polymeric microemulsions, it was suggested that polydispersity improves flexibility of copolymer monolayers and suppresses attractive interactions caused by van der Waals forces, which improves polymerically stabilized colloidal suspensions[59]. In simulation work for compatibilizers, it was found that the incorporation of compositional polydispersity into block copolymers improves their efficiency[44]. All of these studies show that the performance of block copolymers is highly dependent on the specific application and depending on the application, the restrictions on the block copolymer properties may not need to be that tight. Since there is yet to be a complete assessment of the effects of purity and breadth of the molecular weight distribution on the effectiveness of the block copolymer, it is therefore useful to analyze this relationship in order to produce an effective, economically viable copolymer. For many applications with which polystyrene-*b*-poly(acrylic acid) is used, it is still unclear as to how narrow the molecular weight distribution and how high the purity needs to be in order to give good dispersing properties.

2.5.2 Bulk Polymerization

Bulk polymerizations offer the advantage that it enables the production of polymer with a minimal level of contamination. It is typically carried out with monomer, a soluble initiator, and in some cases a chain transfer agent for controlling the molecular weight distribution. When the reaction mixture is heated to a sufficiently high temperature for initiator decomposition, radicals will form and react with the monomer. These oligomeric chains continue to propagate until the supply of monomer in the system is depleted. Bulk polymerizations are highly exothermic and

heat transfer becomes challenging as the viscosity of the reaction mixture increases with conversion. Proper mixing of the reactor contents is extremely important or runaway reactions can occur. Polymerizations of ethylene, styrene, and methyl methacrylate are usually carried out in bulk on an industrial scale[60].

2.5.3 Solution Polymerization

Unlike bulk polymerization, solution polymerizations are carried out in a solvent rather than in the monomer. Chain transfer to solvent can become an issue with this type of polymerization so the solvent must be carefully chosen. The copolymerization of styrene and acrylic acid is carried out in 1,4-dioxane. This solvent was chosen as both polystyrene and poly(acrylic acid) are fully soluble in it[53]. However, chain transfer to 1,4-dioxane for poly(acrylic acid) has been identified in this system and is high enough to limit the molecular weights achievable[50]. This event can be minimized by polymerizing to low conversions or increasing the monomer concentration.

2.6 Synthesis of Block Copolymers for Further Studies

In collaboration with BASF, polystyrene-*b*-poly(acrylic acid) copolymers will be prepared at different purity levels and compositions, with varying polydispersities to be analyzed for effectiveness as an amphiphilic copolymer for protective colloids. In this part of the project, the synthesis and characterization of polystyrene-*b*-poly(acrylic acid) copolymers by nitroxide mediated polymerization will be discussed. The polydispersity index of the styrene and acrylic acid blocks will be varied from narrow (1.1 to 1.2) to broad (1.5 to 1.7) in order for future assessment of the impact of the breadth of the molecular weight distribution on final block

copolymer performance. The block copolymer composition will be varied between 65-75% polystyrene. The homopolymer impurity will also be varied by incorporating known amounts of both polystyrene and poly(acrylic acid) homopolymers during the synthesis. The techniques for synthesizing these block copolymers and their characterization by nuclear magnetic resonance, gel permeation chromatography, and titration will be discussed in detail.

References

[1] M. K. Georges, R. P. N. Veregin, P. M. Kazmaier, G. K. Hamer, *Macromolecules.* **1993**, *26*, 2987-2988.

[2] J. Nicolas, Y. Guillaneuf, C. Lefay, D. Bertin, D. Gigmes, B. Charleux, *Progress in Polymer Science.*

[3] L. Tebben, A. Studer, *Angew.Chem.Int.Ed.* **2011**, *50*, 5034-5068.

[4] M. F. Cunningham, *Prog.Polym.Sci.* **2008**, *33*, 365-398.

[5] R. P. N. Veregin, M. K. Georges, G. K. Hamer, P. M. Kazmaier, *Macromolecules.* **1995**, *28*, 4391-4398.

[6] S. Marque, C. Le Mercier, P. Tordo, H. Fischer, *Macromolecules.* **2000**, *33*, 4403-4410.

[7] F. Chauvin, P. Dufils, D. Gigmes, Y. Guillaneuf, S. R. A. Marque, P. Tordo, D. Bertin, *Macromolecules.* **2006**, *39*, 5238-5250.

[8] J. Sobek, R. Martschke, H. Fischer, *J.Am.Chem.Soc.* **2001**, *123*, 2849-2857.

[9] M. J. Monteiro, M. F. Cunningham, *Macromolecules.* **2012**, *45*, 4939-4957.

[10] P. C. Hiemenz, R. Rajagopalan, *Principles of colloid and surface chemistry*, 3 , rev a expa edition, Marcel Dekker, New York 1997, p. 650.

[11] F. J. Schork, Y. Luo, W. Smulders, J. P. Russum, A. Butté, K. Fontenot, **2005**, *175*, 129-255.

[12] I. A. Maxwell, B. R. Morrison, D. H. Napper, R. G. Gilbert, *Macromolecules.* **1991**, *24*, 1629-1640.

[13] H. Fischer, *Macromolecules.* **1997**, *30*, 5666-5672.

[14] P. B. Zetterlund, *Macromol.Theory Simul.* **2010**, *19*, 11-23.

[15] P. B. Zetterlund, M. Okubo, *Macromolecules.* **2006**, *39*, 8959-8967.

[16] P. B. Zetterlund, J. Wakamatsu, M. Okubo, *Macromolecules.* **2009**, *42*, 6944-6952.

[17] P. B. Zetterlund, *Macromolecular Reaction Engineering.* **2010**, *4*, 663-671.

[18] P. B. Zetterlund, *Polym.Chem.* **2011**, *2*, 534-549.

[19] H. Maehata, C. Buragina, M. Cunningham, B. Keoshkerian, *Macromolecules.* **2007**, *40*, 7126-7131.

[20] R. W. Simms, M. F. Cunningham, *Macromolecules.* **2008**, *41*, 5148-5155.

[21] M. E. Thomson, M. F. Cunningham, *Macromolecules.* **2010**, *43*, 2772-2779.

[22] R. M. Fitch 1928-, *Polymer colloids : a comprehensive introduction*, Academic Press, San Diego 1997, p. 346.

[23] Z. Jia, C. Gauer, H. Wu, M. Morbidelli, A. Chittofrati, M. Apostolo, *J.Colloid Interface Sci.* **2006**, *302*, 187-202.

[24] T. F. Tadros, "General Principles of Colloid Stability and the Role of Surface Forces", in: *Colloid Stability: The Role of Surface Forces - Part I, Volume 1* Wiley-VCH, Weinheim 2007,.

[25] M. S. Romero-Cano, A. Martín-Rodríguez, F. J. d. l. Nieves, *Langmuir.* **2001**, *17*, 3505-3511.

[26] F. Bleger, A. K. Murthy, F. Pla, E. W. Kaler, *Macromolecules.* **1994**, *27*, 2559-2565.

[27] P. G. Sanghvi, S. Devi, *Int.J.Polym.Mater.* **2005**, *54*, 293-303.

[28] M. J. Monteiro, *Macromolecules.* **2010**, *43*, 1159-1168.

[29] J. O'Donnell, E. W. Kaler, *Macromol.Rapid Commun.* **2007**, *28*, 1445-1454.

[30] E. S. Daniels, E. D. Sudol, M. S. El-Aasser, *Polymer colloids : science and technology of latex systems*, American Chemical Society; Distributed by Oxford University Press, Washington, DC; Cary, NC 2002, p. 413.

[31] M. E. Thomson, J. S. Ness, S. C. Schmidt, M. F. Cunningham, *Macromolecules.* **2011**, *44*, 1460-1470.

[32] G. He, Q. Pan, G. L. Rempel, *Macromol.Rapid Commun.* **2003**, *24*, 585-588.

[33] G. He, Q. Pan, *Macromol.Rapid Commun.* **2004**, *25*, 1545-1548.

[34] J. Wakamatsu, M. Kawasaki, P. B. Zetterlund, M. Okubo, *Macromol.Rapid Commun.* **2007**, *28*, 2346-2353.

[35] S. Tomoeda, Y. Kitayama, J. Wakamatsu, H. Minami, P. B. Zetterlund, M. Okubo, *Macromolecules.* **2011**, *44*, 5599-5604.

[36] Y. Luo, X. Cui, *J.Polym.Sci.A Polym.Chem.* **2006**, *44*, 2837-2847.

[37] Y. Luo, J. Tsavalas, F. J. Schork, *Macromolecules.* **2001**, *34*, 5501-5507.

[38] J. Nicolas, B. Charleux, O. Guerret, S. Magnet, *Angewandte Chemie International Edition.* **2004**, *43*, 6186-6189.

[39] W. Ming, F. N. Jones, S. K. Fu, *Macromol.Chem.Phys.* **1998**, *199*, 1075-1079.

[40] P. A. Lovell, M. S. El-Aasser, *Emulsion polymerization and emulsion polymers*, J. Wiley 1997.

[41] M. E. Thomson. Controlled Radical Polymerization in the Dispersed Phase. Ph.D. Thesis, Queen's University, October 2010.

[42] M. F. Cunningham, *Progress in Polymer Science.* **2002**, *27*, 1039-1067.

[43] J. Shi, "Steric Stabilization", in: The Ohio State University, Columbus, OH 2002,.

[44] I. W. Hamley, "Developments in Block Copolymer Science and Technology", in: John Wiley & Sons Ltd., England 2004,.

[45] D. Bendejacq, V. Ponsinet, M. Joanicot, Y. -. Loo, R. A. Register, *Macromolecules.* **2002**, *35*, 6645-6649.

[46] K. A. Davis, K. Matyjaszewski, *Macromolecules.* **2000**, *33*, 4039-4047.

[47] J. Qiu, B. Charleux, K. Matyjaszewski, *Progress in Polymer Science.* **2001**, *26*, 2083-2134.

[48] T. E. Patten, K. Matyjaszewski, *Adv Mater.* **1998**, *10*, 901-915.

[49] P. G. Odell, R. P. N. Veregin, L. M. Michalak, D. Brousmiche, M. K. Georges, *Macromolecules.* **1995**, *28*, 8453-8455.

[50] L. Couvreur, C. Lefay, J. Belleney, B. Charleux, O. Guerret, S. Magnet, *Macromolecules.* **2003**, *36*, 8260-8267.

[51] G. Laruelle, J. François, L. Billon, *Macromol.Rapid Commun.* **2004**, *25*, 1839-1844.

[52] B. Lessard, S. C. Schmidt, M. MaricÌ • , *Macromolecules.* **2008**, *41*, 3446-3454.

[53] L. Couvreur, B. Charleux, O. Guerret, S. Magnet, *Macromol.Chem.Phys.* **2003**, *204*, 2055-2063.

[54] C. Burguière, C. Chassenieux, B. Charleux, *Polymer.* **2003**, *44*, 509-518.

[55] K. A. Davis, B. Charleux, K. Matyjaszewski, *Journal of Polymer Science Part A: Polymer Chemistry.* **2000**, *38*, 2274-2283.

[56] R. Wei, Y. Luo, P. Xu, *Journal of Polymer Science Part A: Polymer Chemistry.* **2011**, *49*, 2980-2989.

[57] X. Wang, Y. Luo, B. Li, S. Zhu, *Macromolecules.* **2009**, *42*, 6414-6421.

[58] W. Jakubowski, N. V. Tsarevsky, P. McCarthy, *Material Matters.* **2010**, *5*, 16.

[59] R. B. Thompson, M. W. Matsen, *Phys.Rev.Lett.* **2000**, *85*, 670-673.

[60] G. Odian, *Principles of Polymerization*, John Wiley & Sons 2004.

[61] D.H. Solomon, G. Waverly, E. Rizzardo, W. Hill, P. Cacioli., U.S. Patent, 4,581,429, **1986.**

Chapter 3

Decoupling Molecular Weight and Particle Size in Nitroxide Mediated Microemulsion Polymerization of *n*-Butyl Acrylate

Abstract

A strong correlation between the effect of varying target molecular weight and particle size exist in nitroxide-mediated microemulsion systems where a decrease in target molecular weight results in an increase in particle size. Using a two-step microemulsion polymerization method, a range of conditions to decouple these two effects were investigated in a system of *n*-butyl acrylate and BlocBuilder® MA. By varying processing conditions and parameters, the particle size was successfully decoupled from target molecular weight effects by changing the monomer and surfactant feed conditions, and surfactant, monomer, and nitroxide concentrations. Conditions for obtaining particle sizes of 20 to 100 nm for target molecular weights from 20,000 to 80,000 $g \cdot mol^{-1}$ were achieved at a 20 wt. % solids content.

3.1 Introduction

Living radical polymerization has emerged as an effective and powerful tool to produce tailored polymers with advanced characteristics. Nitroxide mediated polymerization makes use of a stable free nitroxide radical to mediate the polymerization by acting as a regulator between the propagating polymer chains to establish a reversible termination process. The first nitroxide mediated polymerizations were reported using TEMPO (2,2,6,6-tetramethylpiperidine-1-oxyl) in styrene polymerizations. For the polymerization of acrylates, other nitroxides such as SG1 (1-diethylphosphono-2,2-dimethylpropyl) have been proven to be more effective in mediating the polymerization.

In conventional emulsion polymerizations, an increase in the initiator concentration results in a decrease in particle size due to the greater stabilization provided by the charged initiator end groups and the increase in the number of micelles[1]. In NMP emulsion systems, the opposite effect is observed where an increase in the initiator concentration results in an increase in particle size[2]. There are several reasons for this behaviour. The first one is due to superswelling, which is caused by a high concentration of short oligomers resulting in enhanced diffusion of monomer from monomer-swollen micelles to nucleated particles because of a reduced monomer chemical potential in the particles[3]. The second reason has to do with the ionic strength contribution from the charged initiator end groups when using electrostatically stabilized systems. An increase in the ionic strength in the system can cause the electrical double layer of the particles to contract, lowering the repulsive forces between the particles. To address the superswelling problem, a two-stage polymerization approach[4,5] can be used which consists of creating a first stage living seed latex using initiator, nitroxide, water, surfactant, and a small

amount of monomer. A semi-batch addition of the remaining monomer is then introduced to the system.

In many applications, it is desirable to be able to produce particles with independent control of molecular weight and particle size. One way this can be achieved is through the use of miniemulsions where the particle number and size are established at the beginning of the polymerization and are allowed to grow. However, this method is not easily implemented on an industrial scale as the droplet formation process is a challenge on an industrial scale. Microemulsions on the other hand can produce very small particles without the use of such energy intensive processes. Microemulsions are thermodynamically stable oil-in-water dispersions and can be used to produce very small nanoparticles (<50 nm)[6] due to the large quantities of surfactants typically used in microemulsions allowing very low interfacial surface tensions to be achieved. Microemulsions are desirable for many applications such as adhesives, drug delivery, and microencapsulation as they provide a very large internal interfacial area for further functionalization[7]. Microemulsion polymerizations have been carried out using much lower than normal surfactant to monomer ratios in the past in an attempt to reduce the high costs associated with large quantities of surfactant and post-processing steps. Surfactant to monomer ratios typically used in microemulsions are 1 to 3.3 (wt/wt)[8] as an extremely large amount of surfactant is required to stabilize a large number of small particles. In a methyl methacrylate and styrene system, very small particles (~20-30 nm) have been achieved at surfactant to monomer ratios of 0.13-0.28 (wt/wt)[2,5,9-11]. Other work in free radical polymerizations have obtained particles as small as 20 nm using much lower surfactant to monomer ratios[2,5,9-11]. The use of such a low concentration of surfactant is enabled by the use of a two-stage differential monomer

addition technique[4][5] as described previously. The establishment of the first stage seed latex allows colloidal stability in our systems to be maintained even though our systems are not thermodynamically stable once a polymer chain is formed, as governed by kinetic exchange processes. Most work on microemulsions of *n*-butyl acrylate using SG1 or TEMPO by other groups have shown successful polymerizations of stable latexes with particle sizes in the range of 20-60 nm but using much higher surfactant to monomer ratios (~2.5 % by wt.) and lower solids content (6-10 wt.%) compared to that in our systems[12][13]. In this work, stable *n*-butyl acrylate latexes are prepared by nitroxide mediated microemulsion polymerization using very low surfactant to monomer ratios (0.2 to 0.5 by wt.) at moderate solids content (20 wt. %).

An attempt to decouple the target molecular weight and particle size in nitroxide mediated microemulsion polymerizations is presented. Previous work in the Cunningham group has investigated this behaviour in relation to effects of ionic strength, pH, buffer, and surfactant concentration on the 1st stage particle size[10]. This work seeks to present a range of polymerization conditions that will allow the independent control of both particle size and target molecular weights in *n*-butyl acrylate microemulsions using commercially available materials.

3.2 Experimental Section

3.2.1 Materials

The compounds *n*-butyl acrylate (BA, Aldrich, 99%), 2-((tert-butyl(1-(diethoxyphosphoryl)-2,2-dimethylpropyl)amino)oxy)-2-methylpropanoic acid (BlocBuilder® MA or BB, supplied by Arkema, 99%), Dowfax™ 8390 (Dow Chemicals, 35 wt% solution in

water), sodium carbonate (Na_2CO_3, Aldrich, >99%) were used as received. Distilled, deionized water purified by a Millipore Synergy ion exchange unit was used for all experiments.

3.2.2 Microemulsion Polymerization of *n*-Butyl Acrylate

A two-stage polymerization method was used as described by Charleux and coworkers[14]. BlocBuilder® MA (0.432 g, 1.134 mmol), Na_2CO_3 (0.300 g, 2.830 mmol), and DIW (8 g) were mixed overnight to form the ionized alkoxyamine initiator in solution. The 1st stage latex was prepared with butyl acrylate (3.6 g, 28.08 mmol), Dowfax™ 8390 solution (28.3 g, 15.40 mmol), DIW (225 g), and the ionized BlocBuilder solution in a 1L RC1 reaction calorimeter from Mettler Toledo (LM06). Butyl acrylate, Dowfax™8390, and DIW were combined in the reactor and sealed. Following a 30 minute purge of the reactor and a 10 minute purge of the ionized BB solution, the reactor was heated to 90°C at which point the ionized BB solution was added. The reactor was then heated to 120°C. Butyl acrylate was purged with nitrogen for 20 minutes prior to being pumped into the reactor over one hour at a rate of 0.70 $mL \cdot min^{-1}$. The reactor contents were mixed by an anchor impeller at a rotation speed of 200 RPM. The polymerizations proceeded for 6 hours with samples withdrawn periodically.

3.2.3 Characterization

Monomer conversions were determined gravimetrically. Samples were withdrawn periodically and cooled in an ice water bath to stop polymerization. Subsequently, the samples were dried under air overnight at room temperature, then for 4 hours at 85°C in a ventilated oven. Molecular weight and polydispersity of the polymer samples were measured using gel permeation chromatography (GPC). Distilled THF was used as the eluent at a flow rate of 1 $mL \cdot min^{-1}$. A

Waters GPC equipped with a Waters 2960 separation module containing four Styragel® columns (HR 0.5, HR 1, HR 3, HR 4) coupled with a Waters 410 differential refractive index detector calibrated with polystyrene standards ranging from 347 to 441,000 $g \cdot mol^{-1}$ was used. Mark-Houwink parameters used for the polystyrene standards are $K = 1.14x10^{-4}$ $dL \cdot g^{-1}$, $a = 0.716$[15] and for *n*-butyl acrylate are $K = 1.22x10^{-4}$ $dL \cdot g^{-1}$, $a = 0.70$[16], respectively. Particle size and zeta potential measurements were performed on a Malvern Zetasizer Nano ZS using a glass cuvette (83301-03) for particle size analysis and a universal dip cell (ZEN1002) for zeta potential. Particle size analysis using dynamic light scattering was done at 25°C and an angle of 173°, with dilution of samples with DIW prior to measurement. Reported intensity-average values are the average of 12 runs each. The refractive index for water used for the measurements is 1.330. The pH of the polymer latexes were measured with a Fisher Scientific AR25 pH meter calibrated with aqueous standards (pH 4, 7, and 10). Surface tension measurements were obtained using a TensioCAD tensiometer at room temperature by the Wilhelmy Plate method. Surfactant coverage analysis was done using the soap titration method by Maron et al.[17] with 3 min of stirring after each addition of surfactant.

3.3 Results and Discussion

SG1-mediated microemulsion polymerizations of butyl acrylate were carried out using a two-step approach, with the first stage latex prepared using approximately 8% of the total monomer. Low surfactant to monomer ratios were used ranging from 0.2 to 0.5 (wt/wt), and BlocBuilder® MA to Na_2CO_3 (buffer) ratios ranged from 0.4 to 1.0 (mol/mol). The effects of varying feed conditions, surfactant, monomer, and nitroxide concentrations, and target molecular weights on the final particle size were investigated in an attempt to reduce the coupling effects

between molecular weight and particle size. The molecular weights obtained are discussed in Section 3.3.5. Stable microemulsions of 20 wt % solids were achieved with monomodal particle size distributions and mean particle sizes ranging from 20 to 100 nm.

3.3.1 Effect of Varying Overall Surfactant Concentration and Ionic Strength

The surfactant to monomer ratio was varied to examine the effect on the final particle size when targeting different molecular weights. In colloidal systems, the stabilization required for the polymer particles and monomer droplets to be evenly dispersed in the aqueous phase without coagulation is provided by the surfactant. Theoretically, with the same amount of monomer, the particle size should decrease as the surfactant concentration is increased because of the ability to stabilize a higher number of smaller particles (i.e. higher overall particle surface area). The concentration of initiator is usually varied to target different polymer molecular weights. However, in varying the initiator concentration, the ionic strength of the system is also altered. When targeting lower molecular weights, an increase in the number of initiating groups is necessary to obtain a higher number of polymer chains. In our NMP system, this means an increase in BlocBuilder and base required for its ionization. This introduces more charged species into the system which raises the overall ionic strength of the system. This increase in ionic strength leads to an increase in particle size due to a decrease in the thickness of the electrical double layer of the particles[10][18]. Hence, it may be possible to reduce the effect of increased particle size with lower target molecular weights by providing the system with more stabilizing groups. However, the opposite trend was observed in our microemulsions where we obtained larger particle sizes as the surfactant concentration was increased.

This unusual behaviour has been previously observed by Tauer et al.[19] in a conventional free radical microemulsion polymerization of *n*-butyl acrylate. The authors described this correlation using particle nucleation theory, suggesting that the low monomer concentration caused by such a high amount of surfactant in the system causes short oligomers to grow out of the micelles with a lower average chain length and because more of them are needed to form a nucleus, the higher number of chains per critical nucleus results in larger nuclei. The increase in particle size with surfactant concentration was also observed by Loh et al.[20] in a methyl methacrylate emulsion system using CTAB (cetyl trimethylammonium bromide) at surfactant to monomer ratios exceeding 1.72, but not in an isobutyl methacrylate system. Gan et al.[21] also observed the same trend in MMA microemulsion latexes but thought it was due to the interaction between CTAB micelles and polymer particles as measured by dynamic light scattering. The possibility that the high surfactant concentration leads to a reduced number of micelles as they form higher order structures resulting in larger particles has also been suggested but no evidence was provided[22]. These studies show that depending on the type of monomer and surfactant used, the effect of increased surfactant concentration on the mechanisms and kinetics can be very different in microemulsion polymerizations.

In an effort to reduce the required amount of surfactant to achieve a specified particle size, SG1-mediated microemulsion polymerizations were carried out at low surfactant to monomer ratios, from 0.2 to 0.5 (wt/wt). In the **S** series of experiments, the overall surfactant concentration was varied while keeping all other variables the same, except for the amount of BlocBuilder, which was varied to target different molecular weights (Table 3.1). The amount of monomer at the seed stage was kept constant.

Table 3.1: Summary of the final particle sizes and zeta potentials obtained for the butyl acrylate microemulsion experiments by varying the surfactant to monomer ratio from 0.2 to 0.5 (wt/wt) at target M_n of 20,000 to 80,000 g·mol^{-1} at 20 wt. % solids.

Expt.	Target M_n (g·mol^{-1})	S/M (wt/wt)	Particle Diameter[a] (nm)	ζ-potential (mV)	N_p/L_{aq}	Conversion
S21	20,000	0.2	70.0	-37.9	$9.27x10^{17}$	0.90
S22	20,000	0.5	104.2	-15	$2.64x10^{17}$	1.00
S41	40,000	0.2	41.5	-69.3	$4.63x10^{18}$	0.92
S42	40,000	0.3	49.4	--	$2.85x10^{18}$	0.97
S43	40,000	0.5	64.9	-44.5	$1.19x10^{18}$	0.99
S81	80,000	0.2	37.1	-53.7	$6.63x10^{18}$	0.82
S82	80,000	0.5	51.9	-36.8	$2.34x10^{18}$	0.95

[a] particle size listed is the intensity average particle size (d_z) from the Malvern Nanosizer

For a target M_n of 40,000 g·mol^{-1}, the mean particle size increased from 42 to 65 nm as the S/M ratio increased from 0.2 to 0.5 (expt. S41-S43, Table 3.**1**), opposite to what was expected. Lowering the surfactant to monomer ratio to 0.1 (wt/wt) led to a bimodal particle size distribution with particle diameters of 42 nm and 350 nm. This is likely due to an insufficient amount of surfactant to stabilize all the growing particles, causing some particles to aggregate. It is suspected that at the low surfactant concentration range studied, the ionic strength of the system plays a more important role in colloidal stability, resulting in an increase in particle size. If there is a sufficient amount of surfactant present, the excess surfactant molecules that are not adsorbed onto the surface of the particles will remain free in the aqueous phase, or form micelles with other surfactant molecules above the CMC. With a higher number of excess surfactant molecules, the ionic strength contribution would be greater, thus exerting a larger influence on the thickness of the electrical double layer. Comparatively, a lower amount of excess surfactant would impart lower ionic strength effects and would result in a thicker double layer.

Surface tension experiments were carried out in order to determine the percentage of surfactant coverage on the surface of the polymer particles. A soap titration method developed by Maron et al.[17] was used by which surfactant was added to diluted latex samples until the air-latex surface tension reached a minimum, indicating the formation of micelles. Comparing the percent coverage of two different S/M runs, a slightly lower surfactant coverage was found for the run with a higher surfactant to monomer ratio at 76 % for S/M = 0.5 (S43) and 83 % for S/M = 0.2 (S41). It can be calculated from this that a larger total particle surface area is covered in S41 with smaller particles than in S43 with larger particles. This means that there is more excess surfactant in the aqueous phase in S43 which will contribute to a higher ionic strength. The same trend of increased particle size with an increase in surfactant was observed for target molecular weights of 20,000 and 80,000 g·mol^{-1} as shown in Figure 3.1.

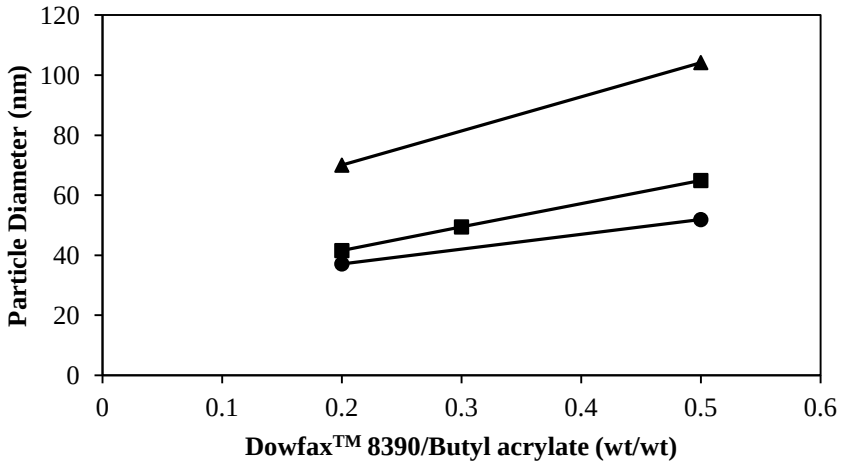

Figure 3.1: Particle sizes obtained from varying the surfactant-to-monomer ratio at target M_n of 20,000 g·mol^{-1} (▲), 40,000 g·mol^{-1} (■), and 80,000 g·mol^{-1} (●).

Looking at the final number of particles obtained in Figure 3.2, consistent with the particle size observations, the runs at a higher surfactant concentration had a lower number of

particles. Even though a higher surfactant concentration is able to support more particles, it appears that this is not the case as fewer particles were obtained. One possibility could be the fact that even though a higher number of micelles are generated at the beginning of the polymerization and become nucleated particles, the ionic strength contribution from the excess surfactant is sufficient to cause the electrical double layer to contract and allow the particles to aggregate more easily, resulting in a fewer number of larger particles. Another possibility could be that there is insufficient monomer in the seed stage to nucleate a larger number of particles. So even though the larger amount of surfactant can theoretically support more particles, there aren't enough nucleated particles to use all of the surfactant to the fullest during the seed stage. Thus, the number of particles established is lower. The number of particles was calculated using equation (3.1),

$$N_p = \frac{\left[\left(\frac{m_{BA}x}{\rho_{PBA}}\right) + \left(\frac{m_{BA}(1-x)}{\rho_{BA}}\right)\right]}{V_p} \tag{3.1}$$

where m_{BA} is the total mass of butyl acrylate in the sample, x is the conversion, ρ_{PBA} and ρ_{BA} is the density of poly(butyl acrylate) and butyl acrylate monomer, and V_p is the volume of the particle.

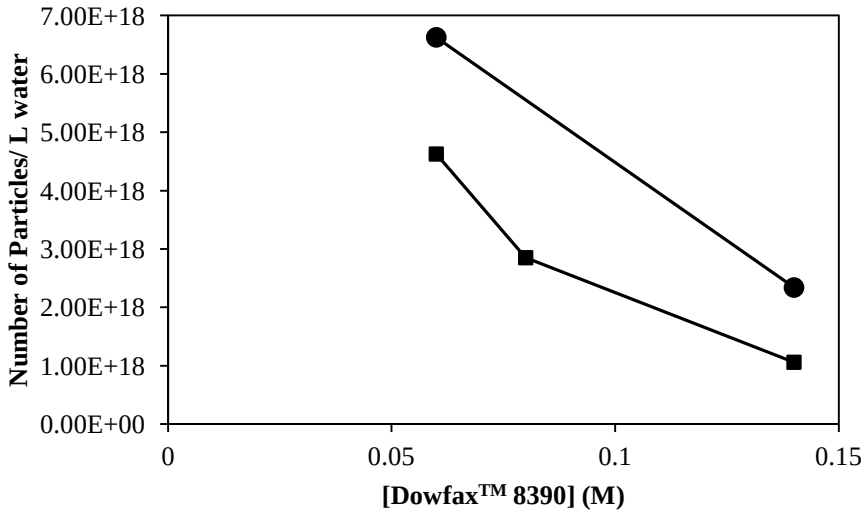

Figure 3.2: Number of particles obtained for target M_n of 40,000 g·mol^{-1} (■), and 80,000 g·mol^{-1} (●) at different Dowfax™ 8390 concentrations.

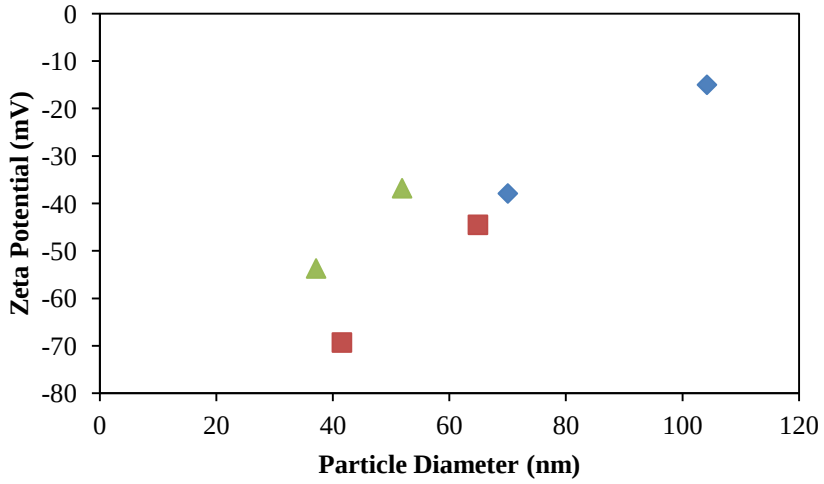

Figure 3.3: A plot of zeta-potential vs. particle diameter obtained from the microemulsion polymerization of n-butyl acrylate using a surfactant to monomer ratio of 0.2 and 0.5 at a target M_n of 20,000 g·mol^{-1} (▲), 40,000 g·mol^{-1} (◆), and 80,000 g·mol^{-1} (■).

The increase in particle size was accompanied by an increase in the zeta-potential as can be observed in Figure 3.3. As the electrical charge of the double layer is affected by the ionic strength of the system, the zeta-potential can give a good indication of the ionic strength influence between the different surfactant concentration experiments. The zeta-potential is the potential at the Stern plane of the EDL and changes with the surface charges on the polymer particles and the properties of the surrounding medium. An increase in the ionic strength of the medium will lower the zeta-potential as the free ions decrease the surface potential. The higher the zeta-potential, the stronger the electrostatic repulsion between the particles and the more stable the latex. Table 3.1 shows that the zeta-potential indeed decreases from -69.4 mV to -44.5 mV with an increase in the surfactant concentration. The drop in the zeta-potential when going from S/M = 0.2 to S/M = 0.5 indicates a thinner electrical double layer of the particles in the higher surfactant run and is likely caused by an increase in ionic strength from the additional Dowfax™ 8390. The structure of Dowfax™ 8390 is shown in Figure 3.4.

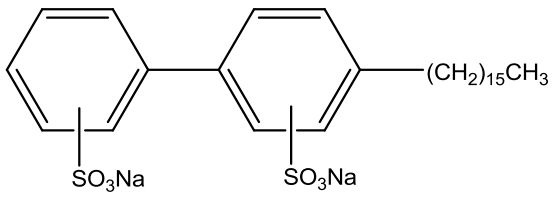

Figure 3.4: Structure of the anionic surfactant Dowfax™ 8390.

Dowfax™ 8390 is an anionic disulfonated surfactant, having a higher local charge density compared to monosulfonated surfactants. It is possible that the effect of the ionic strength contribution from the surfactant is higher than the effect of the stabilization it provides under these conditions causing the particle size to increase. Minute amounts of impurities in the

Dowfax™ 8390 solution can negatively affect colloidal stability. The certificate of analysis indicates that other than the active ingredients (disodium hexadecyldiphenyloxide disulfonate and disodium dihexadecyldiphenyloxide disulfonate), 0.2% NaCl and 0.5% Na_2SO_4 are also present. In order to investigate the ionic strength contribution from Dowfax™ 8390, a substitution experiment was carried out. In the **SB** series of experiments, the ionic strength effect from increasing the surfactant to monomer ratio of 0.2 to 0.5 (wt/wt) was compared by substituting the difference in surfactant concentration with a molar equivalent of a salt.

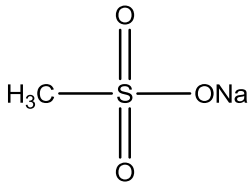

Figure 3.5: Structure of sodium methanesulfonate.

Sodium methanesulfonate (CH_3SO_3Na), depicted in Figure 3.5, and sodium chloride (NaCl) were chosen to mimic the ionic strength effects of Dowfax™ 8390. Sodium methanesulfonate was chosen as it has the same sulfonate end as Dowfax™ 8390 but without the long alkyl chain that provides stabilization. This allows the non-stabilizing effects of the surfactant to become apparent. The **SB** series of experiments were performed at a molecular weight target of 40,000 $g \cdot mol^{-1}$. Without substitution with a salt, the difference in particle diameter between the run with S/M = 0.2 (expt. SB1, Table 3.2) and that with S/M = 0.5 (expt. SB2, Table 3.2) was approximately 25 nm. With the substitution of CH_3SO_3Na (expt. SB4, Table 3.2), the particle diameter was about 10 nm larger than that of SB2. This difference is likely attributable to the stabilization provided by the additional Dowfax™ 8390 in SB2 compared to

SB4. The same experiment was carried out using NaCl (expt. SB3) and the effect on particle size is almost identical to that using CH_3SO_3Na as seen in Figure 3.6.

Table 3.2: Formulations for the salt substitution microemulsion polymerizations of *n*-butyl acrylate at a solids content of 20 wt. %.

Expt	S/M (wt/wt)	Salt	BA:Dowfax™ 8390:BB ratio	[Dowfax™ 8390] (M)	[Salt] (M)	Particle Diameter[a] (nm)
SB1	0.2	--	309:13:1	0.06		40.4
SB2	0.5	--	309:31:1	0.14		64.9
SB3	0.2	NaCl	309:13:1	0.06	0.08	78.1
SB4	0.2	CH_3SO_3Na	309:13:1	0.06	0.08	76.8

The alkoxyamine initiator BlocBuilder® MA (BB) was added to the aqueous phase in its carboxylated form, neutralized with Na_2CO_3 at a molar ratio of BB/Na_2CO_3 of 0.4.
[a] Particle size listed is the intensity average particle size (d_z) from the Malvern Nanosizer.

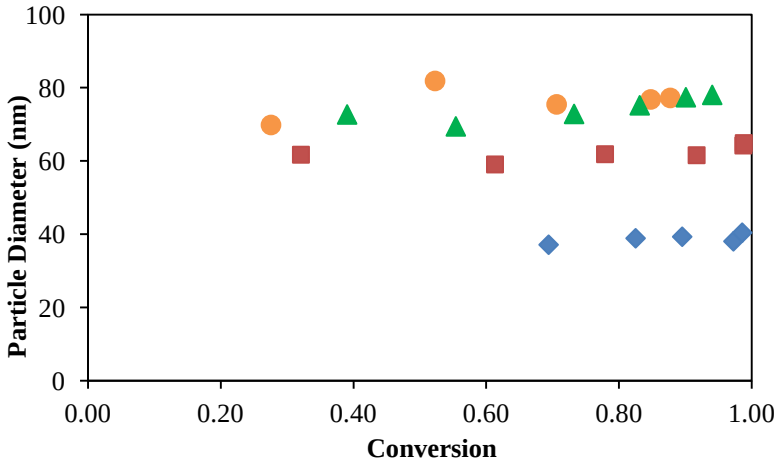

Figure 3.6: Particle size evolution for the salt-substituted microemulsion polymerizations SB1-SB4. The molar difference in additional surfactant was substituted with a molar equivalence of salt to mimic the higher surfactant concentration runs. S/M = 0.2 (SB1, ◆), S/M = 0.5 (SB2, ■), S/M = 0.2 with NaCl (SB3, ▲), S/M = 0.2 with CH_3SO_3Na (SB4, ●).

From these experiments, it is believed that the increase in ionic strength from the additional Dowfax™ 8390 causes the thickness of the electrical double layer of the particles to decrease, resulting in the aggregation of the particles and leading to larger particle sizes. The addition of salts is known to aid coagulation in polymer colloids and the similarity between the effect of CH_3SO_3Na and NaCl show that Dowfax™ 8390 is likely to increase the overall ionic strength in the system enough to cause some particles to aggregate.

From these experiments, it is believed that the ionic strength contribution is increased due to an increase in charged species and contaminants from the additional Dowfax™ 8390. The increase in ionic strength leads to a decrease in electrostatic repulsion due to an accumulation of counterions near the particle surface, which is the reason for a lower value of the zeta-potential as observed in our experiments. The accumulation of counterions close to the surface of the polymer particles causes the surface charges to be screened, thus reducing the surface potential and allowing the particles to coalesce more easily[20]. The decrease in the thickness of the electrical double layer of the particles allows van der Waals forces to take over, resulting in the aggregation of the particles and leading to larger particle sizes.

The number of particles formed in the system is also consistent with the particle sizes obtained as observed in Figure 3.7. Experiment SB1 yielded the smallest particle size and had the most number of particles, while the runs with the larger particle sizes (SB2-4) had a lower number of particles in the system. This is in good agreement with the observation that the number of particles decreases as the surfactant concentration increases leading to larger particles. Both the rate of free radical generation and the ionic strength have a large effect on the particle number[23].

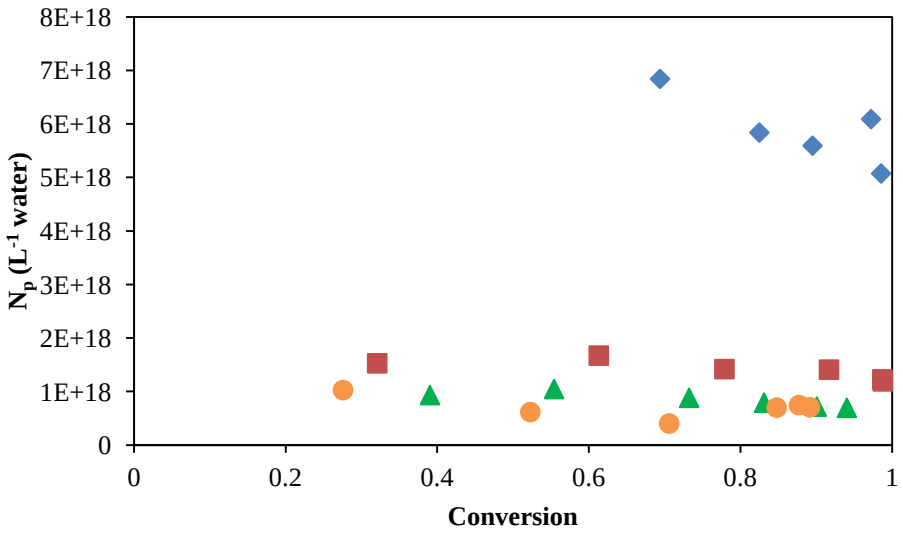

Figure 3.7: Number of particles vs. conversion profiles for the salt-substituted microemulsion polymerizations SB1-SB4. The molar difference in additional surfactant was substituted with a molar equivalence of salt to mimic the higher surfactant concentration runs. S/M = 0.2 (SB1, ◆), S/M = 0.5 (SB2, ■), S/M = 0.2 with NaCl (SB3, ▲), S/M = 0.2 with CH_3SO_3Na (SB4, ●).

This series of experiments show that the overall ionic strength contribution plays a major role in determining the minimum particle size achievable in microemulsions using very low concentrations of surfactant. Beyond a certain surfactant to monomer ratio, further increase in available surfactant ceases to result in a higher number of particles. This is mostly due to the fact that the monomer in the system already experiences maximum stabilization and the further addition of surfactant no longer aids in the generation of new particles. Since the interfacial tension cannot decrease beyond the minimum possible, the excess free surfactant molecules will result in an accumulation of free ions in the system, hence increasing the ionic strength.

3.3.2 Effect of Monomer Concentration at the Seed Stage

In the **S** series of experiments, the monomer content in the first stage was kept constant while varying the concentration of BlocBuilder, meaning that the number of monomer units available to add to each alkoxyamine group varied between the different target molecular weight experiments. As the particle nucleation process is extremely sensitive in the seed stage, the interactions between the surfactant, nitroxide, initiator, and monomer can vary significantly with changes in their proportions. The extent to which the final particle size can be varied within a target molecular weight range by changing the initial monomer content, while keeping the overall monomer content the same, was explored in an attempt to further decouple the two effects.

Depending on the target molecular weight of the experiment, the number of butyl acrylate units available to add on to each chain will vary. In the **M** series of experiments, the monomer content in the seed stage was varied from 4 to 16 wt. %, while the overall monomer content remained constant.

Table 3.3 shows the corresponding 1^{st} stage monomer contents, the final particle sizes achieved, and final conversion. It is important to note that while the overall surfactant to monomer ratio is kept the same, varying the initial monomer concentration changes this ratio in the seed stage. Increasing the monomer content from 4% to 16% in the 1^{st} stage decreases the surfactant to monomer ratio from 5.4 to 1.4 (wt/wt) in the 1^{st} stage for overall S/M = 0.2 and from 12.4 to 3.1 for overall S/M = 0.5.

Table 3.3: Microemulsion formulation and polymerization results for the M series experiments. The monomer content in the 1st stage was varied from 4 to 16 % for surfactant to monomer ratios of 0.2 and 0.5 (wt/wt) at target M_n of 20,000 to 80,000 g·mol^{-1} and solids content of 20 wt. %.

Expt.	S/M (wt/wt)	Initial BA/BB (mol/mol)	Particle Diameter[a] (nm)	PDI[b]	Conversion
M21	0.2	12	70.0	0.142	0.90
M22	0.2	18	53.6	0.097	0.93
M23	0.2	25	45.0	0.109	0.95
M24	0.5	12	104.2	0.069	1.00
M25	0.5	18	75.0	0.031	1.00
M26	0.5	25	57.7	0.043	1.00
M41	0.2	12	66.4	0.135	0.78
M42	0.2	25	41.5	0.179	0.92
M43	0.2	37	32.3	0.274	0.92
M44	0.2	50	27.4	0.288	0.98
M45	0.5	25	64.9	0.059	0.99
M46	0.5	37	44.7	0.062	0.98
M47	0.5	50	39.8	0.082	1.00
M81	0.2	25	41.4	0.218	0.86
M82	0.2	50	37.1	0.204	0.82
M83	0.2	74	20.8	0.388	0.92
M84	0.5	25	68.2	0.115	0.98
M85	0.5	50	51.9	0.137	0.95
M86	0.5	74	42.7	0.095	0.97

M21-M26 have target Mn=20,000 g·mol^{-1}
M41-M47 have target Mn=40,000 g·mol^{-1}
M81-M86 have target Mn=80,000 g·mol^{-1}
[a] Particle size listed is the intensity average particle size (d_z) from the Malvern Nanosizer.
[b] PDI values are based on the width of the Gaussian distribution of the intensity correlation function. A value less than 0.2 indicates monodispersity.

For all target molecular weights, increasing the initial monomer seed content led to a decrease in the final particle size. In addition, larger particle sizes were obtained with higher surfactant concentration, consistent with the trend observed in the **S** series of experiments, as shown in Figure 3.8, Figure 3.9, and Figure 3.10. The decrease in particle size with increasing monomer concentration in the seed stage is likely due to an increase in the number of particles

nucleated. This was indeed observed in the **M** series of experiments where increasing the monomer content led to an increase in the number of particles generated in the system. This trend was also consistent with both surfactant to monomer ratios of 0.2 and 0.5. Another interesting observation is that the difference in the particle sizes obtained between S/M ratios of 0.2 and 0.5 appear to decrease as the amount of initial monomer is increased. It could be possible that with enough initial monomer to begin with, this trend may be reversed.

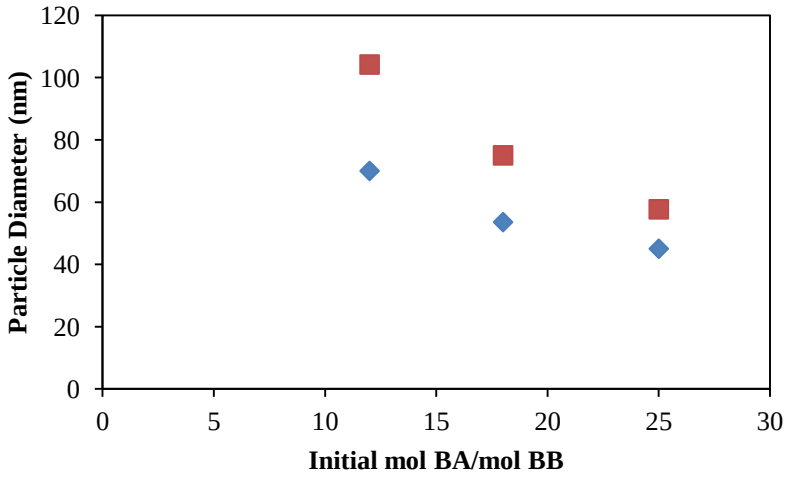

Figure 3.8: Final particle sizes for experiments M21-M26 at target M_n of 20,000 g·mol^{-1} and S/M=0.2 (◆) and S/M = 0.5 (■).

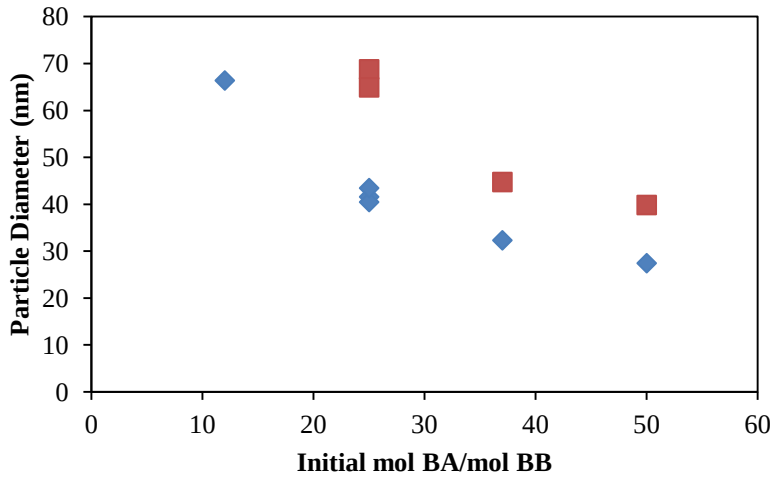

Figure 3.9: Final particle sizes for experiments M41-M47 at target M_n of 40,000 g·mol^{-1} and S/M=0.2 (◆) and S/M = 0.5 (■).

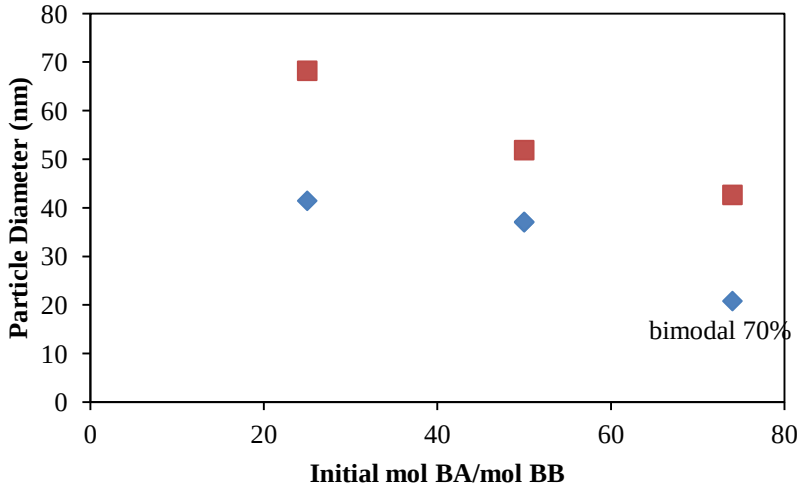

Figure 3.10: Final particle sizes for experiments M81-M86 at target M_n of 80,000 g·mol^{-1} and S/M=0.2 (◆) and S/M = 0.5 (■).

As the number of chains is fixed by the amount of BlocBuilder added to the system, the increased monomer available in the 1st stage could mean that chains can nucleate particles faster as the oligomeric radicals can reach the critical length for entry sooner. The higher rate of

monomer addition can also ensure that the growing chains are sufficiently water insoluble so they remain inside the monomer swollen micelles for nucleation. If there is not enough monomer, the oligomeric radicals may still be sufficiently water soluble to exit micelles and remain in the aqueous phase, leading to a lower number of seed particles prior to further monomer addition. The more seed particles generated, the smaller each particle will be, provided there is sufficient surfactant to stabilize all the growing polymer particles.

It is evident that the segregation effect[24-26] is in play here as the higher number of particles achieved with higher 1st stage monomer concentration led to an increase in the rate of polymerization as observed in the conversion-time profiles in Figure 3.11, Figure 3.12, and Figure 3.13. The larger number of smaller-sized particles results in increased segregation of the radicals leading to reduced chances of termination. The increased monomer concentration in the seed stage also helps to maximize the number of chains generated in the system by reducing the likelihood of biradical termination early on in the polymerization. The more monomer available means that the oligomeric radicals are more likely to react with a monomer unit than with another oligomeric radical in the aqueous phase before entry into a micelle. However, too much monomer present in the seed stage could possibly lead to superswelling of the particles resulting in decreased colloidal stability and larger particle sizes[3].

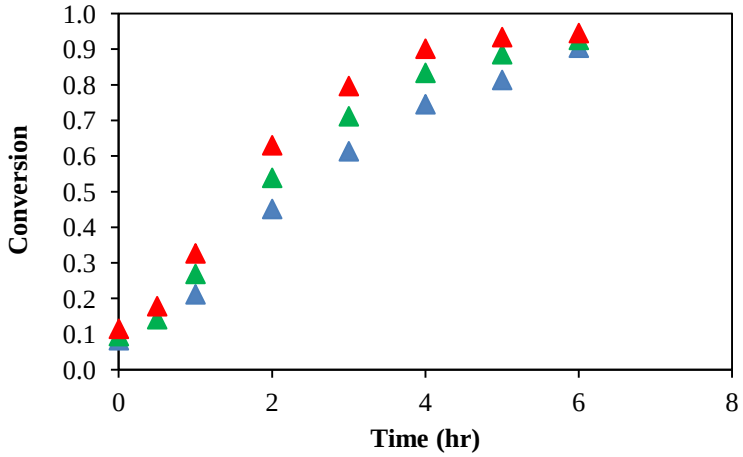

Figure 3.11: Conversion-time profiles for butyl acrylate microemulsion experiments M21-M23 carried out at target M_n = 20,000 g·mol^{-1} at initial monomer contents of 8% (M21, ▲), 12% (M22, ▲), and 16% (M23, ▲) at S/M = 0.2.

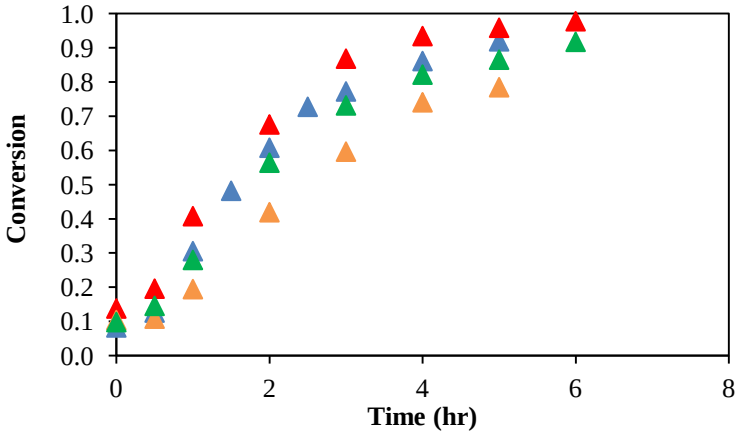

Figure 3.12: Conversion-time profiles for butyl acrylate microemulsion experiments M41-M44 carried out at target M_n = 40,000 g·mol^{-1} at monomer contents of 4% (M41, ▲), 8% (M42, ▲), 12% (M43, ▲), and 16% (M44, ▲) at S/M = 0.2.

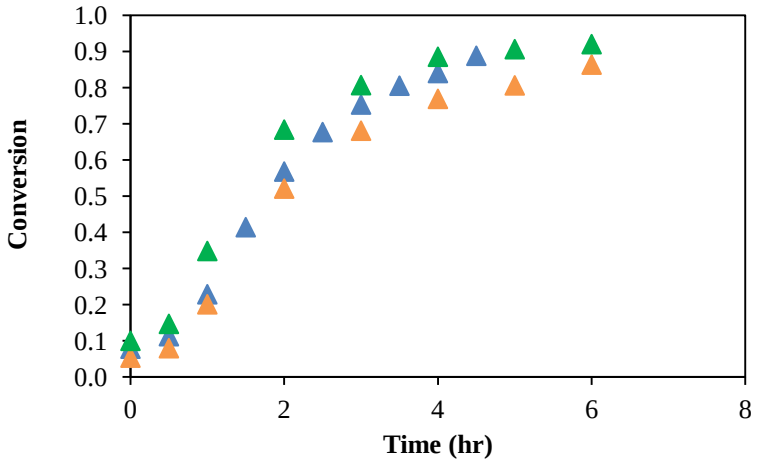

Figure 3.13: Conversion-time profiles for butyl acrylate microemulsion experiments M81-M83 carried out at target M_n = 80,000 g·mol^{-1} at monomer contents of 4% (M81, ▲), 8% (M82, ▲), and 12% (M83, ▲) at S/M = 0.2.

By varying the monomer content in the seed stage from 4% to 16% at an overall surfactant to monomer ratio of 0.2, particle sizes from 45-70 nm, 28-66 nm, and 21-44 nm can be obtained at target molecular weights of 20,000 g·mol^{-1}, 40,000 g·mol^{-1}, and 80,000 g·mol^{-1} respectively (expts. M21-M23, M41-M44, M81-M83,

Table 3.3). Figure 3.14 shows the particle size ranges at surfactant to monomer ratios of 0.2 and 0.5 (wt/wt) that were obtained by this method. This further broadens the range of particle sizes obtainable at different target molecular weights and is another technique that can be used to decouple the two effects.

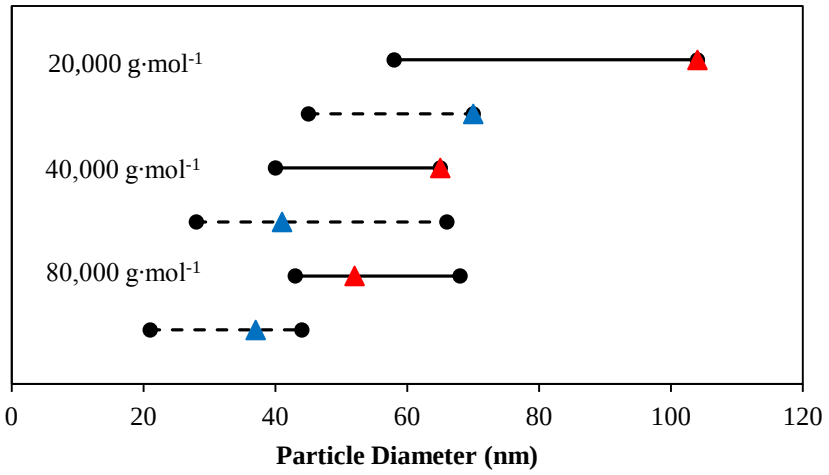

Figure 3.14: Range of particle sizes obtained at target M_n of 20,000, 40,000, and 80,000 g·mol^{-1} by varying the first stage monomer content at S/M = 0.2 (–) and S/M = 0.5 (---). Particle sizes obtained at 8% monomer content at the seed stage are indicated by (▲).

3.3.3 Effect of Semi-Batch Addition of Surfactant

Experiments were conducted while varying the feed of Dowfax™ 8390 to the reactor to examine the effects on the final particle size. Similar to the way the monomer is fed, in the **F** series of experiments (Table 3.4), a series of four experiments were carried out while varying the continuous feed of surfactant at 0%, 25%, 50%, and 75% of the total surfactant (expts. F1, F2, F, and F4). The surfactant concentrations at the seed stage for all experiments are above the CMC. The results obtained were expected, with the smallest particle sizes obtained with all of the surfactant present in the reactor at the beginning (F1, 0% feed) and the largest particle sizes obtained with the least amount of surfactant to begin with (F4, 75% feed). Figure 3.15 shows a significant particle size difference of approximately 40 nm between runs F1 and F4. There is however, not a significant difference between the particle sizes obtained from surfactant feeds of 25% and 50% of the total surfactant concentration as seen in Figure 3.15. The initial

concentration of surfactant in the system is crucial in establishing the number of particles as it dictates the number of micelles generated, so a lower amount of surfactant will lead to a lower number of micelles and vice versa. The number of particles established in each of the four runs is shown in Figure 3.16 with respect to the initial Dowfax^{TM} 8390 concentration in the system and is in agreement with the particle sizes obtained, where the smallest particle sizes were achieved with the highest initial surfactant concentration with the highest number of particles.

Table 3.4: Summary of the final particle size and zeta potential measurements of butyl acrylate microemulsion experiments with semi-batch addition of Dowfax^{TM} 8390 (F series).

Expt	Surfactant Feed (%)	Particle Diameter[a] (nm)	Zeta potential (mV)
F1	0	40.4	-69.3
F2	25	51.8	-59.3
F3	50	53.2	-47.1
F4	75	74.0	-46.7

[a] Particle size listed is the intensity average particle size (d_z) from the Malvern Nanosizer.

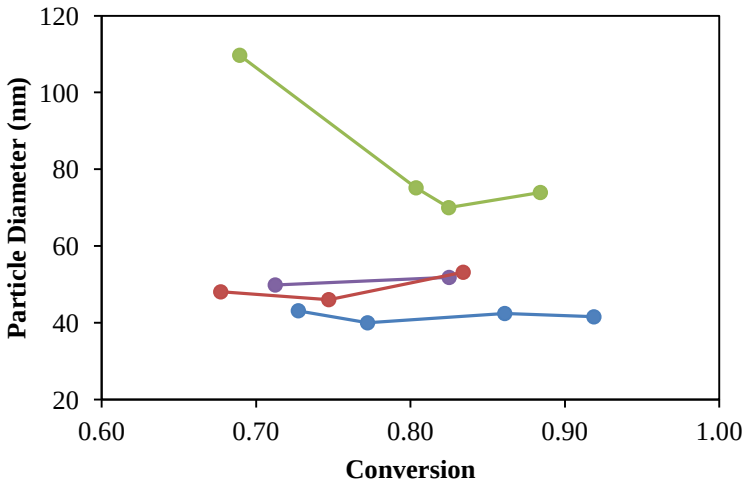

Figure 3.15: Particle size evolution for butyl acrylate microemulsion experiments with semi-batch addition of Dowfax™ 8390 at 0% (F1, ●), 25% (F2, ●), 50% (F3, ●), and 100% (F4, ●) of the total Dowfax™ 8390 content.

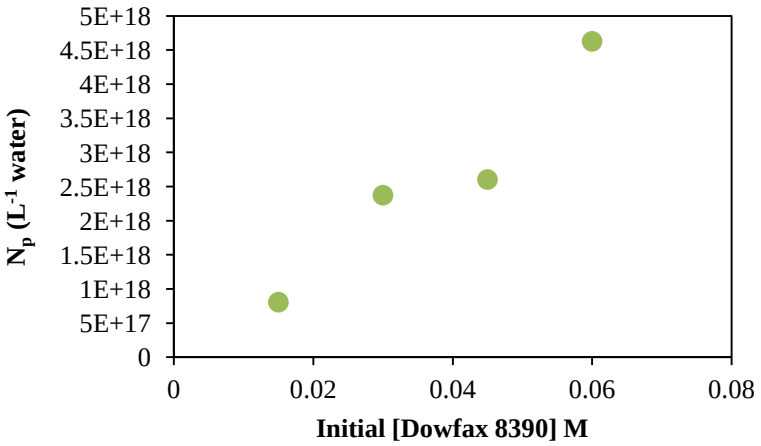

Figure 3.16: Number of particles attained by varying the initial surfactant concentration in the SG1-mediated microemulsion polymerization of *n*-butyl acrylate.

From Figure 3.15, it is clear that the subsequent feed of surfactant does not help to reduce the particle size back down to that of F1 even though the overall surfactant concentration in the system is the same. The difference is the surfactant concentration in the 1st stage latex. Most of

the activity during particle nucleation happens at the initial stage of the polymerization and it is the reactions that occur at this step that is crucial in establishing the particle number. Figure 3.15 shows that once the micelles and particles have been established, further addition of surfactant mainly helps with stabilization of existing particles and if present above the CMC, will form micelles but will not likely generate new particles.

It is important to note that in this series of experiments, the decrease in surfactant concentration in the first stage with the overall surfactant concentration in the system staying constant leads to larger particle sizes. In comparison to the **S** series of experiments where the decrease in overall surfactant concentration leads to smaller particles, the key difference between the two observed trends is the surfactant concentration in the first stage. With regards to experiments S1 to S3, the particle nucleation stage experiences the full amount of stabilization and ionic strength effects as all of the surfactant is present in the initial stage. Even though the number of micelles is expected to be greater in runs S42 and S43 in comparison to S41, the increase in ionic strength at this stage can cause the nucleated particles to aggregate early on resulting in larger than expected particles resulting in a lower particle number as well. In experiments F1 to F4, the particle nucleation stage is affected by only a partial amount of stabilization and ionic strength effects. The overall surfactant concentration remains the same so the degree of compression of the electrical double layer between the runs due to ionic strength effects is expected to be relatively the same. Once the particles have been established, additional surfactant fed to the system mainly provides stabilization to the growing particles and is not likely to contribute to new particle formation as all the chains have likely already gained entry into particles or micelles. As a result, the particle size cannot decrease from what was initially

established at the seed stage. Varying the feed of surfactant over time provides another way to control the particle size within the same formulation and still obtain stable latexes. The addition of surfactant using a semi-batch approach can be used to increase particle sizes at a given target molecular weight.

3.3.4 Effect of BlocBuilder to Na_2CO_3 Ratio

Several experiments were carried out at different molar ratios of BlocBuilder® MA to Na_2CO_3 for a series of target molecular weights and surfactant concentrations. As discussed previously, the addition of the base serves two purposes, to ionize the BlocBuilder and to provide buffering capacity for the system to prevent the pH from dropping too low. Thomson et al.[10] observed an increase in particle size with a decrease in pH when varying the buffer concentration in high solids nitroxide mediated emulsion polymerization using Di-BlocBuilder. Hence, the ratio of BlocBuilder to Na_2CO_3 in the system is crucial for a successful microemulsion polymerization that is stable, controlled, and living. Previous studies in the Cunningham group[10] have compared the use of different types of base to ionize BlocBuilder® MA and found that Na_2CO_3 is the most suitable for obtaining very small particles. Compared to the use of NaOH, the final particle size was approximately 130 nm smaller when using Na_2CO_3[10] due to the difference in ionic strength contribution.

Table 3.5: Influence of the BlocBuilder to Na_2CO_3 molar ratios of SG1-mediated microemulsion polymerizations of *n*-butyl acrylate (B series) on the final particle size and zeta potential at a solids content of 20 wt. %.

Expt.	**S/M**	**BB/Na_2CO_3**	**Particle Diameter[a] (nm)**	**ζ-potential (mV)**
B41	0.2	0.4	41.54	-69.3
B42	0.2	0.8	41.13	-69.6
B43	0.2	1	48.05	-71.3
B44	0.5	0.4	68.73	-44.5
B45	0.5	0.8	74.13	--
B46	0.5	1	93.66	--
B81	0.2	0.4	37.11	-53.7
B82	0.2	0.8	38.97	-69.6
B83	0.2	1	29.13[b]	-73.3
B84	0.5	0.4	51.87	-36.8
B85	0.5	0.8	51.12	-41.3
B86	0.5	1	54.27	-56.4

B41-B46 have target Mn=40,000 g·mol^{-1}
B81-B86 have target Mn=80,000 g·mol^{-1}
[a] Particle size listed is the intensity average particle size (d_z) from the Malvern Nanosizer.
[b] bimodal distribution (63%-29.13nm, 33%-275.7nm)

In the **B** series of experiments, the effect of the molar ratio of BlocBuilder to Na_2CO_3 on the final particle size of the microemulsions was investigated at three different values (Expt B1-B3, Table 3.5). There does not appear to be a significant impact when changing the BB/Na_2CO_3 ratio from 0.4 to 0.8 but an increase in particle size is observed when increasing from 0.8 to 1.0 as observed in Figure 3.17. The same trend is observed at different surfactant to monomer ratios as well for both target M_n of 40,000 and 80,000 g·mol^{-1}. One reason for the increase in particle size at higher BB/Na_2CO_3 ratios is the possible incomplete ionization of BlocBuilder. If there is insufficient sodium carbonate to convert the alkoxyamine to its water-soluble form, some of the alkoxyamine initiators will not be able to initiate chains in the aqueous phase leading to a

decrease in the number of chains in the system. This can lead to the nucleation of fewer particles and hence each particle will be larger in size. The initiator can also be buried inside empty micelles, eliminating them from the particle nucleation process, resulting in higher than expected molecular weights. The pH of the microemulsions dropped from ~8.8-9.1 to ~5.3-5.6 throughout the course of the polymerization mainly due to the hydrolysis of butyl acrylate and did not vary too much between the different BB/Na_2CO_3 ratios used. This indicates sufficient buffering of the system as the pH of all experiments was maintained above 5.0 at full conversion.

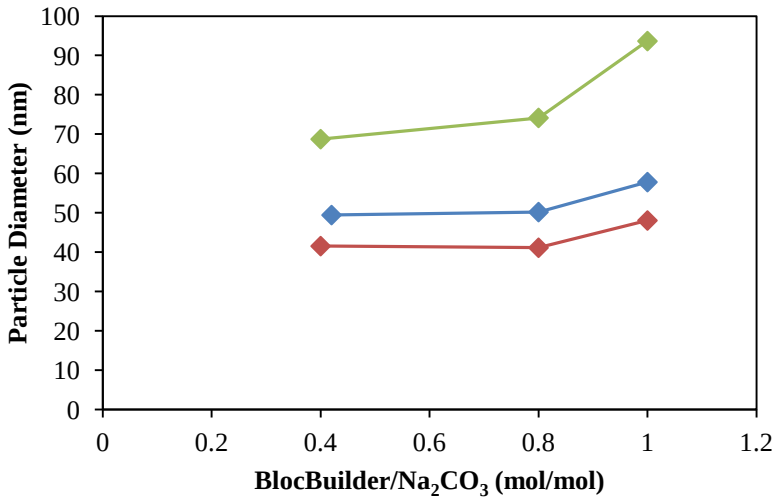

Figure 3.17: Particle sizes obtained by varying the BlocBuilder to Na_2CO_3 molar ratio at a target M_n of 40,000 g·mol^{-1} and at S/M=0.2 (◆), S/M=0.3 (◆), and S/M=0.5 (◆).

Increasing the amount of sodium carbonate over the range studied did not affect the particle size significantly but at even lower BB/Na_2CO_3 ratios, the particle size is expected to increase as the excess Na_2CO_3 contributes more to the ionic strength of the system. Similar to the effect of increased Dowfax™ 8390, additional Na_2CO_3 can contribute to colloidal instability causing the polymer particles to aggregate and form larger particles.

3.3.5 Molecular Weight Distributions

The molecular weight distributions show controlled and living behaviour with M_w/M_n maintained around 1.4 up to approximately 70% conversion, where it then increases to approximately 1.8 at higher conversions, likely caused by increased termination as the supply of monomer reaches depletion approaching full conversion. This is comparable to other SG1-mediated microemulsions of *n*-butyl acrylate[4][12]. Livingness is shown by a shift in the molecular weight distribution to the right with conversion. Tailing observed in the GPC traces at the low molecular weight end indicate termination of short chains early on in the polymerization. In some of the experiments, there is a slight overlap of the GPC traces at the low molecular weight end at higher conversions which indicate newly formed chains in the later stages of the polymerization. These molecular weight distributions are scaled proportional to conversion and are shown in Figure 3.18. In all the experiments carried out (**S, SB, M, F, B** series), the experimental M_n matched closely with the theoretical M_n except for the target M_n of 80,000 $g \cdot mol^{-1}$. Table 3.6 shows the molecular weights achieved for the different target M_n experiments.

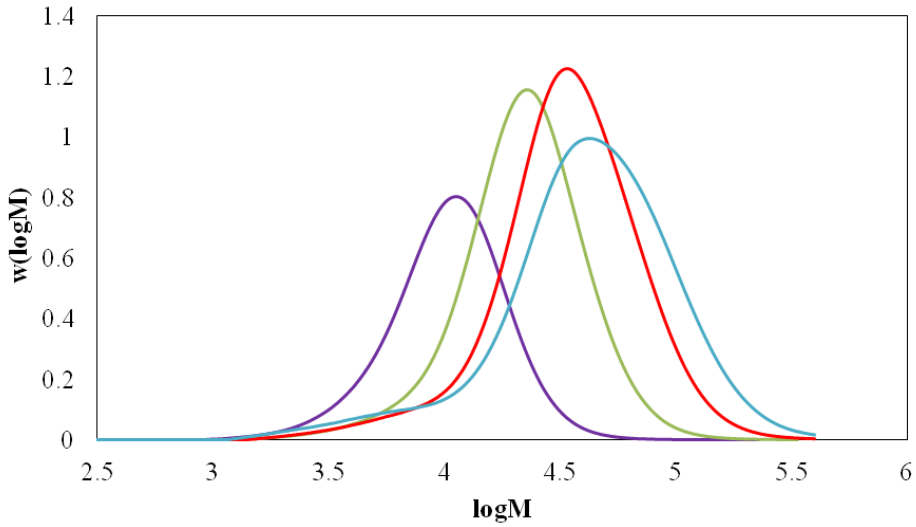

Figure 3.18: Molecular weight distribution scaled proportional to conversion showing the generation of new lower molecular weight species in the later stages of polymerization for expt. SB1. $M_{n,expt}$ = 30,500 g·mol^{-1}. $M_{n,theo}$ = 40,100 g·mol^{-1}. Conversions are at 45% (purple), 69% (green), 82% (red), and 99% (blue).

Table 3.6: Summary of the molecular weights and particle sizes obtained for all series of SG1-mediated microemulsion polymerizations of n-butyl acrylate at solids content of 20 wt. %.

Expt.	S/M (wt/wt)	BB/Na_2CO_3 (mol/mol)	Particle Diameter[a] (nm)	Conversion	$M_{n,\ theo}$ (g·mol^{-1})	$M_{n,\ expt}$ (g·mol^{-1})	PDI
S21	0.2	0.4	70.02	0.90	19000	20600	1.64
S22	0.5	0.4	104.20	1.00	20200	18400	1.71
S41	0.2	0.4	41.54	0.92	37000	44000	1.67
S42	0.3	0.4	49.43	0.97	41000	45800	1.83
S43	0.5	0.4	64.89	0.99	38800	31500	2.25
S81	0.2	0.4	37.11	0.82	65000	53300	1.94
S82	0.5	0.4	51.87	0.95	76300	50200	2.28
SB2	0.5	0.4	64.89	0.99	38800	31500	2.25
SB1	0.2	0.4	40.43	0.99	40100	30500	2.27
SB3	0.2	0.4	78.05	0.94	37500	30400	2.14

SB4	0.2	0.4	76.81	0.89	33900	38000	1.55
M21	0.2	0.4	70.02	0.90	19000	20600	1.64
M22	0.2	0.4	53.58	0.93	18900	26800	1.38
M23	0.2	0.4	45.03	0.95	19200	19100	1.64
M24	0.5	0.4	104.20	1.00	20200	18400	1.71
M25	0.5	0.4	75.02	1.00	19900	16600	1.95
M26	0.5	0.4	57.69	1.00	20200		
M41	0.2	0.4	66.35	0.78	33200	28300	1.69
M42	0.2	0.4	41.54	0.92	37000	44000	1.67
M43	0.2	0.4	32.27	0.92	36300	29300	1.66
M44	0.2	0.4	27.39	0.98	37800	31300	
M45	0.5	0.4	64.89	0.99	38800	31500	2.25
M46	0.5	0.4	44.70	0.98	39800		
M47	0.5	0.4	39.80	1.00	40600	50500	1.58
M81	0.2	0.4	41.44	0.86	70900	44600	2.51
M82	0.2	0.4	37.11	0.82	65000	53300	1.94
M83	0.2	0.4	20.80	0.92	72400		
M84	0.5	0.4	68.20	0.98	78300	40000	2.65
M85	0.5	0.4	51.87	0.95	76000	50200	2.28
M86	0.5	0.4	42.65	0.97	76000	45000	3.26
F1	0.2	0.4	40.40	0.92	37000	44000	1.67
F2	0.2	0.4	51.80	0.83	35100	39000	1.66
F3	0.2	0.4	53.20	0.83	35200	41000	1.83
F4	0.2	0.4	74.00	0.88	34300	37000	1.86
B41	0.2	0.4	41.54	1.67	37000	44000	1.67
B42	0.2	0.8	41.13	0.97	37400	40700	1.89
B43	0.2	1.0	48.05	0.89	36800	41000	1.83
B44	0.5	0.4	68.73	1.00	43300	49400	1.86
B45	0.5	0.8	74.13	1.00	40900	44000	1.88
B46	0.5	1.0	93.66	1.00	41200	42900	1.87
B81	0.2	0.4	37.11	0.82	65100	53400	1.94
B82	0.2	0.8	38.97	0.91	68000	47200	2.29
B83	0.2	1.0	29.13	0.86	68700	48500	2.18
B84	0.5	0.4	51.87	0.95	76300	50200	2.28
B85	0.5	0.8	51.12	0.98	78100	51200	2.47
B86	0.5	1.0	54.27	0.97	77400	44900	2.77

[a] Particle size listed is the intensity average particle size (d_z) from the Malvern Nanosizer.

For the runs carried out at a target M_n of 80,000g·mol^{-1}, the experimental M_n was always less than the theoretical M_n, reaching approximately 70-80% of the theoretical M_n at full conversion. The molecular weight distributions are also very broad for these, with $M_w/M_n > 2.0$. It is usually normal to observe a higher than expected molecular weight, especially with biradical termination by combination. However, a lower than theoretical M_n indicates that there are more chains in the system than theoretically possible, assuming the maximum number of chains is solely determined by the concentration of BlocBuilder in the system, or most of the chains are shorter than what they should be. Therefore, the observed result could possibly be due to thermal initiation or chain transfer to monomer. Thermal initiation will result in the generation of new radicals which can propagate and form new polymer chains, thus resulting in shorter chains as there are less monomer units available for each chain to add. Thermal initiation in *n*-butyl acrylate systems is possible but should not be too significant at temperatures below 140°C[27]. Since our experiments are carried out at 120°C, new chain formation from thermal initiation should be minimal. Dowfax^{TM} 8390 should be thermally stable at temperatures up to 180°C so thermal degradation should not be a problem in our experiments. Prior to use, butyl acrylate monomer was not purified by passing though an inhibitor removal column, so impurities from that may cause unwanted radical generation leading to new chain formation. Chain transfer to monomer results in one dead chain and a monomeric radical that can continue to propagate. This results in a dead polymer chain of length *n* and a new monomeric radical which can continue to propagate. This mechanism could be operational in our system and can be the reason for the generation of lower molecular weight species later on in the polymerization as observed in the overlapping GPC traces in Figure 3.18. The possibility of β-scission can also be a cause of dead chains in the system leading to higher polydispersities.

The thermal initiation of butyl acrylate was further investigated in an experiment carried out with just monomer, surfactant, and water. The microemulsion was left to react at 120°C for 5 hours. After just one hour, polymerization was clearly evident as the reaction mixture turned a slight milky white with a conversion of 12%, and reaching 37% in 5 hours. By comparison to the controlled polymerizations using BlocBuilder, the percent of thermally initiated chains is approximately 1-3 % of the total generated chains. The molecular weight of the poly(butyl acrylate) obtained cannot be compared to those from the NMP microemulsions as the polymerization is uncontrolled and so the rate of polymerization will be faster than those mediated by SG1. Whether the polymerization was a result of radicals generated from butyl acrylate or Dowfax^{TM} 8390, this explains why lower molecular weight species are created in the middle of the polymerization and why there are more chains formed than theoretically anticipated resulting in a lower than theoretical M_n, as well as broader molecular weight distributions.

Branching in the SG1-mediated microemulsions of butyl acrylate was also investigated as the presence of branched samples will result in deviations from the true molecular weight because their molecular density is higher than in linear chains. ^{13}C NMR was performed in order to identify the presence of branching in the polymer. Figure 3.19 shows a portion of the NMR spectrum obtained with peak assignments shown in Table 3.7, showing evidence of branching by chain transfer to polymer. The assignment of peaks was verified with previous chain transfer studies by NMR of *n*-butyl acrylate[28][29]. As the signal intensities do not necessarily reflect the abundance of carbon in the sample using a fast pulse interval due to different relaxation times and nuclear Overhauser effects (NOE), the extent of branching was quantified using NOE suppression by ^{13}C NMR with inverse gated decoupling using a slower pulse interval. The mole percent

branching was calculated by comparison of the integrations of the branched CH and CH_2 carbons to the total backbone carbons. Comparison of the quaternary carbon integral can also be made to the total backbone carbon integral but was found to be less accurate in a study by Ahmad et al.[28]. An interesting finding to note from that study is that the relative intensities of the CH and CH_2 carbon signals from a fast pulse spectrum reflect quite accurately the actual abundance of the corresponding carbons. This means that as long as the branching calculations incorporate the branched CH and CH_2 carbon signals and not the quaternary carbon signal, an inverse gated experiment with a slower pulse interval is not necessary. The mole percent branching was calculated using equation (3.2),

$$mol\ \%\ branching = \frac{{}^{1}/_{3}\,(branched\ CH + CH_2)}{total\ main\ chain\ CH + CH_2} = \frac{{}^{1}/_{3}\,(I[H+G])}{I[D+E]} \qquad (3.2)$$

where I[H+G] is the integration for regions **H** and **G** and I[D+E] is the integration for regions **D** and **E** according to Table 3.**7**.

Table 3.7: ^{13}C NMR peak assignments of poly(*n*-butyl acrylate) in $CDCl_3$ corresponding to the spectrum in Figure 3.19.

Peak	Chemical shift/ppm	Assignment	Integration
A	28.4-30.0	end group - $CH_2CH_2COO(CH_2)_3CH_3$	0.21
B	30.6	2-CH_2 in n-butyl side group	1.59
C	31.8	end group - $CH_2CH_2COO(CH_2)_3CH_3$	0.07
D	33.9-37.1	main chain CH_2	0.84
E	41-42.0	main chain CH	1.00
F	48.4	branch quaternary carbon	0.03
G	37.1-38.6	CH_2 adjacent to branch	0.04
H	38.6-40.0	CH adjacent to branch	0.11

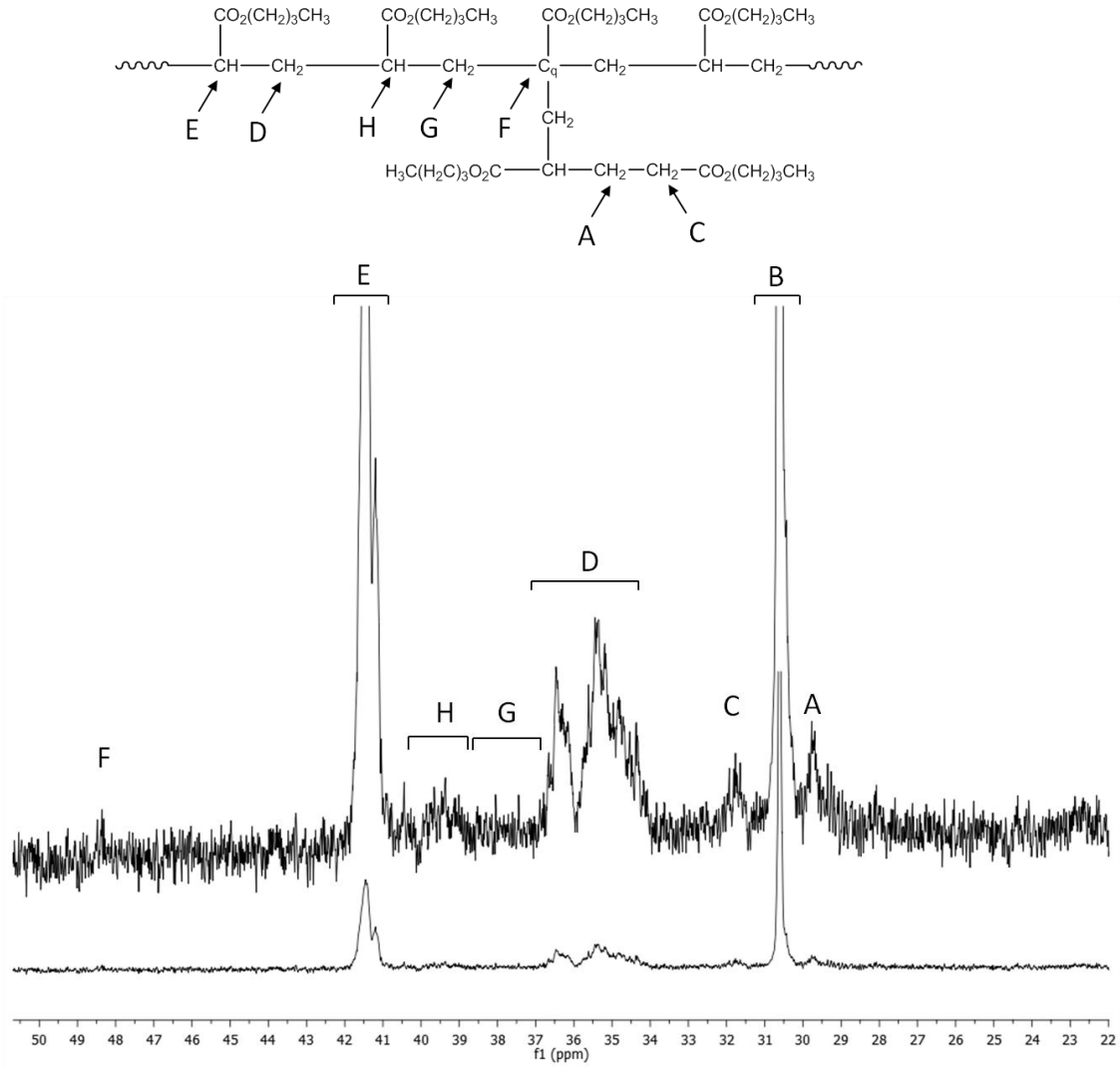

Figure 3.19: ^{13}C NMR spectrum of poly(*n*-butyl acrylate) M82 recorded using $CDCl_3$ as solvent. The assignments of the labeled peaks are given in Table 3.7.

The percent branching of sample M82 was calculated to be approximately 2.8 mol %. Although the extent of branching is small, it can cause slight discrepancies between the actual and theoretical molecular weights determined by GPC due to spatial orientation of the polymer chains

in solution. Molecular weight analysis by GPC is solely based on physical separation by size, and depending on how tightly the polymer chains coil up in solution will determine their effective size as they pass through the separation columns. Longer polymer chains coil up and form larger spheres in solution, but small branches along the linear chains might not add to the effective volume as much as in the linear form and as a result, will appear to have a lower molecular weight.

3.3.6 Replicate Runs

In order to ensure that the particle sizes obtained from varying the process parameters are significantly different, three sets of replicate runs were carried out to determine the standard deviation between the measurements. Figure 3.20 shows the replicate runs for target molecular weights of 40,000 and 80,000 $g \cdot mol^{-1}$. As observed, there is minimal batch to batch variation between the final particle sizes obtained.

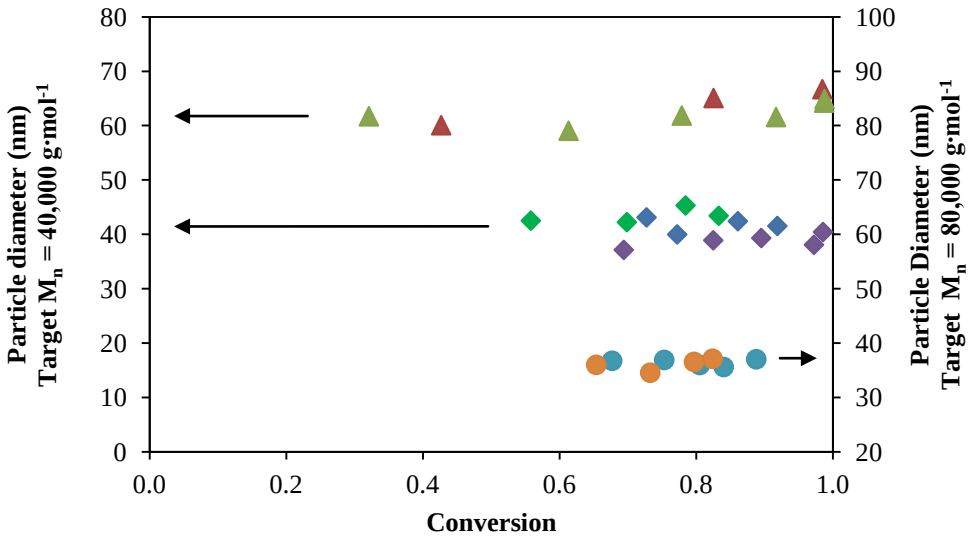

Figure 3.20: Replicate runs showing consistent results with minimal batch to batch variation in particle sizes achieved at target M_n of 40,000 g·mol^{-1} at S/M=0.5 (▲) and S/M=0.2 (◆), and target M_n of 80,000 g·mol^{-1} at S/M=0.2 (●).

3.3.7 Decoupling Target Molecular Weight and Particle Size

Combining all the different methods used to alter the particle size at different target molecular weights, the extent to which the particle size can be decoupled from the target molecular weight with respect to the different strategies used is shown in Figure 3.21.

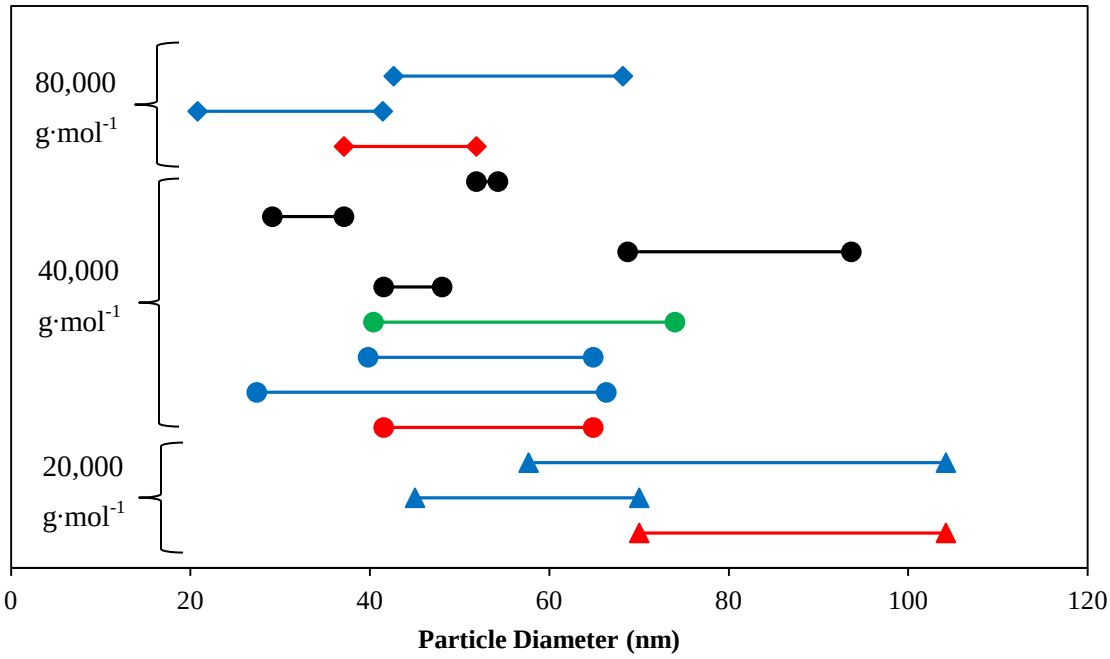

Figure 3.21: Range of particle sizes achieved by SG1-mediated microemulsion polymerization of *n*-butyl acrylate at target M_n of 20,000 g·mol^{-1} (▲), 40,000 g·mol^{-1} (●), and 80,000 g·mol^{-1} (◆) by varying the surfactant to monomer ratio (wt/wt) (S series, red), by varying the monomer content in the seed stage (M series, blue), by semi-batch addition of surfactant (F series, green), and by varying the BlocBuilder to Na_2CO_3 molar ratio (B series, black).

3.4 Conclusion

Stable poly(*n*-butyl acrylate) latexes were obtained by nitroxide-mediated microemulsion polymerization at a solids content of 20 wt. % using the alkoxyamine initiator, BlocBuilder® MA, and the anionic surfactant, Dowfax™ 8390. The particle size was successfully decoupled from the target molecular weight to a significant extent by varying the surfactant to monomer ratio (wt/wt), by varying the BlocBuilder to Na_2CO_3 ratio (mol/mol), by varying the monomer content in the seed stage, and by a semi-batch addition of the surfactant. At the target molecular

weights of 20,000, 40,000, and 80,000 g·mol^{-1}, the particle size was successfully varied from ~45 to 105 nm, ~25 to 95 nm, and 20 to 70 nm, respectively. Increasing the surfactant to monomer ratio from 0.2 to 0.5 (wt/wt) led to an increase in the particle size due to the increase in ionic strength from the additional surfactant. Increasing the initial monomer content in the seed stage from 4 to 16 wt. % resulted in a decrease in the final particle size as a result of an increased availability of monomer allowing for more particles to be nucleated in the seed stage. By semi-batch addition of the surfactant, larger particle sizes can be obtained by increasing the portion of surfactant fed into the system over time. Over the range studied, the molar ratio of BlocBuilder to Na_2CO_3 did not lead to a drastic change in the final particle size, although a minimum ratio must be kept in order to maintain the buffering capacity of the system. A large excess of Na_2CO_3 is expected to cause an increase in the particle size as a result of increased ionic strength contributions. The polymerizations showed controlled and living behaviour with M_w/M_n maintained around 1.4 up to about 70% conversion, and increasing to ~1.8 at high conversions. For target molecular weights of 20,000 and 40,000 g·mol^{-1}, the $M_{n,expt}$ matched that of the $M_{n,theo}$, but the $M_{n,expt}$ for target molecular weight of 80,000 g·mol^{-1} were less than that of the $M_{n,theo}$. The polydispersity of these microemulsions were also very high at over 2.0. This was likely caused by chain transfer to polymer leading to branching, chain transfer to monomer and free radical generation from impurities in Dowfax^{TM} 8390 resulting in the creation of short chains throughout the polymerization.

To our knowledge, the decoupling of the target molecular weight and particle size of *n*-butyl acrylate microemulsions has not been done to this extent. The strategies presented here can be used to produce polymer latexes with specified molecular weight and particle size via

nitroxide-mediated microemulsion polymerization. Although there are still some difficulties in extending the particle size range down to 20 nm for the low target molecular weights (< 20,000 $g \cdot mol^{-1}$), the range achieved in this work covers the typical size requirements usually desired (40 to 80 nm). In addition, this work shows that controlled, stable microemulsions of *n*-butyl acrylate can be obtained using much lower surfactant to monomer ratios than conventionally used in microemulsion systems and at higher solids content than typically reported for NMP microemulsions.

Acknowledgements

Financial support from the Natural Sciences and Engineering Research Council of Canada, Ontario Research Chair Program, and Queen's University, and materials from Arkema Inc. is gratefully acknowledged.

References

[1] R. G. Gilbert, *Emulsion polymerization: a mechanistic approach*, Academic Press 1995.

[2] M. E. Thomson, J. S. Ness, S. C. Schmidt, M. F. Cunningham, *Macromolecules.* **2011**, *44*, 1460-1470.

[3] Y. Luo, J. Tsavalas, F. J. Schork, *Macromolecules.* **2001**, *34*, 5501-5507.

[4] J. Nicolas, B. Charleux, O. Guerret, S. Magnet, *Angewandte Chemie International Edition.* **2004**, *43*, 6186-6189.

[5] G. He, Q. Pan, *Macromol.Rapid Commun.* **2004**, *25*, 1545-1548.

[6] F. Bleger, A. K. Murthy, F. Pla, E. W. Kaler, *Macromolecules.* **1994**, *27*, 2559-2565.

[7] P. G. Sanghvi, S. Devi, *Int.J.Polym.Mater.* **2005**, *54*, 293-303.

[8] M. J. Monteiro, *Macromolecules.* **2010**, *43*, 1159-1168.

[9] G. He, Q. Pan, G. L. Rempel, *Macromol.Rapid Commun.* **2003**, *24*, 585-588.

[10] M. E. Thomson. Controlled Radical Polymerization in the Dispersed Phase. Ph.D. Thesis, Queen's University, October **2010**.

[11] M. E. Thomson, M. F. Cunningham, *Macromolecules.* **2010**, *43*, 2772-2779.

[12] S. Tomoeda, Y. Kitayama, J. Wakamatsu, H. Minami, P. B. Zetterlund, M. Okubo, *Macromolecules.* **2011**, *44*, 5599-5604.

[13] P. B. Zetterlund, *Macromolecular Reaction Engineering.* **2010**, *4*, 663-671.

[14] J. Nicolas, B. Charleux, S. Magnet, *J.Polym.Sci.A Polym.Chem.* **2006**, *44*, 4142-4153.

[15] S. Beuermann, M. Buback, T. P. Davis, R. G. Gilbert, R. A. Hutchinson, A. Kajiwara, B. Klumperman, G. T. Russell, *Macromolecular Chemistry and Physics.* **2000**, *201*, 1355-1364.

[16] S. Beuermann, D. A. Paquet, J. H. McMinn, R. A. Hutchinson, *Macromolecules.* **1996**, *29*, 4206-4215.

[17] S. H. Maron, M. E. Elder, C. Moore, *J.Colloid Sci.* **1954**, *9*, 104-112.

[18] F. Caruso, *Colloids and Colloid Assemblies: Synthesis, Modification, Organization and Utilization of Colloid Particles*, Wiley 2006.

[19] Tauer. K., Ramírez. A.G., López. R.G., *Comptes Rendus Chimie*. **2003**, *6*, 1245-1266.

[20] S. Loh, L. Gan, C. Chew, S. Ng, *Journal of Macromolecular Science, Part A.* **1995**, *32*, 1681-1697.

[21] L. M. Gan, C. H. Chew, S. C. Ng, S. E. Loh, *Langmuir*. **1993**, *9*, 2799-2803.

[22] R. P. Moraes, I. Zavecs, P. Lauvernier, N. M. B. Smeets, R. A. Hutchinson, T. F. L. McKenna, *J.Polym.Sci.A Polym.Chem.* **2012**, *50*, 944-956.

[23] S. Krishnan, A. Klein, M. El-Aasser, E. D. Sudol, *Macromolecules.* **2003**, *36*, 3152-3159.

[24] P. B. Zetterlund, M. Okubo, *Macromolecules.* **2006**, *39*, 8959-8967.

[25] P. B. Zetterlund, *Macromol.Theory Simul.* **2010**, *19*, 11-23.

[26] P. B. Zetterlund, *Polym.Chem.* **2011**, *2*, 534-549.

[27] C. Quan. High-Temperature Free-Radical Polymerization of n-Butyl Acrylate. Ph. D. Thesis, Drexel University, December **2002**.

[28] N. M. Ahmad, F. Heatley, P. A. Lovell, *Macromolecules.* **1998**, *31*, 2822-2827.

[29] C. Former, J. Castro, C. M. Fellows, R. I. Tanner, R. G. Gilbert, *Journal of Polymer Science Part A: Polymer Chemistry.* **2002**, *40*, 3335-3349.

Chapter 4

Synthesis and Characterization of Polystyrene-*b*-Poly(acrylic acid) Copolymers

Abstract

Amphiphilic copolymers are an attractive class of functional polymers because of their ability to be compatible with two different chemical environments at the same time. Industrially, these are often produced in the form of random copolymers but the emergence of living radical polymerization has sparked interest in their performance as block copolymers. The synthesis and characterization of polystyrene-*b*-poly(acrylic acid) copolymers by nitroxide mediated polymerization is investigated in order to enable a range of these block copolymers to be made for analysis of their effectiveness as protective colloids. The direct synthesis of these block copolymers and their characterization by titration, GPC, and NMR methods are discussed. Polystyrene-*b*-poly(acrylic acid) copolymers were synthesized with a polystyrene content of 65-75% and polydispersities ranging from 1.17 to 1.46 and an overall degree of polymerization of 30.

4.1 Introduction

Amphiphilic block copolymers are used as dispersants, emulsifiers, compatibilizers, and protective colloids in a wide range of applications. Their success in these applications lies in their hydrophilic and hydrophobic properties which allow them to support the co-existence of two different chemical environments. The wide variability of their structure determined by the type of monomers and the length of each polymer block allows for their use in any corresponding interface and is not limited to only the oil/water interface[1]. Because of this, much interest in the performance of these amphiphilic block copolymers have been expressed.

Polystyrene-co-poly(acrylic acid) copolymers are used as protective colloids in thin film applications to prevent particles from coalescing or agglomerating during the film formation process. These copolymers are easily synthesized on an industrial scale using free radical polymerization. Anionic polymerization is usually used to synthesize block copolymers with very narrow molecular weight distributions as low as 1.05[2]. With the emergence of living radical polymerization techniques such as NMP, ATRP, and RAFT, well-defined block copolymers can be synthesized with low polydispersities ranging from 1.1 to 1.5[3]. It is often desirable to produce copolymers with very narrow molecular weight distributions and high purity, but this is associated with higher costs. However, the importance of such narrow molecular weight distributions is still unclear in terms of the performance of these copolymers in commercial applications. Further, block copolymers are expected to behave differently than random copolymers and their performance also depends on the overall copolymer composition. The work presented here aims to provide the techniques necessary to synthesize and characterize

PSt-*b*-PAA copolymers of varying polydispersities, compositions, and degree of impurities for the analysis of their effectiveness as protective colloids.

The difficulties of synthesizing acidic polymers using NMP and ATRP in the past have been resolved in recent years. Incompatibility between the acid and the control agent (e.g. nitroxide or metal catalyst) has resulted in poorly controlled polymerizations[4][5]. Side reactions resulting in the consumption of the nitroxide species in NMP[5] and destruction of the metal catalyst from the formation of metal carboxylates in ATRP[6] have posed major obstacles in the use of these polymerization techniques with acrylic acid. Methods to tackle these problems have been used including the synthesis of poly(*tert*-butyl acrylate) followed by hydrolysis to obtain poly(acrylic acid). However, the multi-step procedure can be quite time consuming. Couvreur et al.[7] has successfully demonstrated the use of NMP to directly synthesize poly(acrylic acid) in well-controlled conditions using the SG1 nitroxide (1-diethylphosphono-2,2-dimethylpropyl). Since then, the copolymerization of styrene and acrylic acid by NMP have been well documented by several groups[8-10] and successful polymerizations have been carried out provided appropriate polymerization conditions are selected. It was found that a 9 mol % excess of free nitroxide with respect to the initiator and polymerization to low conversions (~30 %) were optimal for maintaining good control of the kinetics and minimizing transfer to solvent reactions[7][10].

The synthesis and characterization of polystyrene-*b*-poly(acrylic acid) copolymers will be discussed with the goal of preparing these copolymers at different purity levels and compositions, with varying polydispersities for analysis of their effectiveness as amphiphilic copolymers for protective colloids.

4.2 Experimental Section

4.2.1 Materials

The compounds acrylic acid (AA, Aldrich, 99%), 2-((tert-butyl(1-(diethoxyphosphoryl)-2,2-dimethylpropyl)aminoxy)-2-methylpropionic acid (BlocBuilder® MA or BB, supplied by Arkema, 99%), 1,4-dioxane (Aldrich, >99%), trimethylsilyldiazomethane (TMS-diazomethane, Acros, 2 M solution in hexanes), methanol (Fisher) were used as received. Styrene (St, Aldrich, >99%) was purified by passing through an inhibitor remover column (Aldrich). Deuterated chloroform ($CDCl_3$, Acros, 99.8% D) and deuterated acetone (acetone-d_6, Acros, 99.8% D) were used as received.

4.2.2 Synthesis of PSt-*b*-PAA Copolymers

4.2.2.1 Bulk Polymerization of Styrene

The NMP of styrene was carried out in bulk using BlocBuilder® MA in a 100 mL three-necked round-bottom flask. Styrene (50 g, 480 mmol) was purged with nitrogen for 20 min while stirring at a speed of 250 RPM using a magnetic stir bar prior to the addition of BlocBuilder® MA (3.2 g, 8.4 mmol). The resulting reaction mixture was purged for 10 min and then immersed in a hot oil bath at 90°C. The polymerization proceeded for 6 to 12 hours with samples withdrawn periodically. After polymerization, the reaction mixture was precipitated in methanol, filtered, and dried under air for 1 day. The resulting SG1 end-capped polystyrene was used as a macroinitiator for the copolymerization with acrylic acid. The M_n of the polystyrene macroinitiators ranged from 1,500 to 2,300 $g \cdot mol^{-1}$ with polydispersities from 1.17 to 1.42.

4.2.2.2 Acrylic Acid Block Extension in Solution Polymerization

Synthesis of the acrylic acid block was carried out in 1,4-dioxane using the purified polystyrene macroinitiator. The polystyrene macroinitiator (7 g, 3 mmol) was dissolved in 1,4-dioxane ([1,4-dioxane] = 9 $mol \cdot L^{-1}$) and purged with nitrogen for 30 min. The reaction mixture was then immersed in a hot oil bath at 90°C. Acrylic acid (8 g, 0.11 mol) was added to the reactor by a single injection or via a syringe pump over time at 4 or 6 $mL \cdot min^{-1}$. Polymerization proceeded for 4 to 6 hours with samples withdrawn periodically. The resulting copolymer was dried under air overnight, in a ventilated oven at 60°C for 1 day, then in a vacuum oven at room temperature for 2 days.

4.2.3 Methylation of PSt-*b*-PAA Copolymer

For GPC analysis, the carboxylic acid groups of the dried copolymers were methylated using trimethylsilyldiazomethane (TMS diazomethane) using a procedure described by Couvreur et al.[7]. Using this method, 50 mg of each copolymer sample was dissolved in 10 mL of a mixture of THF and water. The proportion of water was relative to the amount of acid groups in order to get solubilization at room temperature. TMS diazomethane, yellow in colour, was then added dropwise to the solution. Upon addition, the solution became colourless and bubbles formed. Dropwise addition of the methylation agent continued until the solution became yellow and stopped bubbling. Excess TMS diazomethane was then added and the solution was stirred for 3 more hours before drying under air overnight and in a vacuum oven at 70°C for 1 day.

4.2.4 Characterization

Monomer conversions were determined gravimetrically. Samples were withdrawn periodically and cooled in an ice water bath to stop polymerization. Subsequently, the samples were dried under air overnight at room temperature, then for 4 hours at 85°C in a ventilated oven.

Copolymer composition was determined by NMR spectroscopy and titration. ^{1}H NMR, ^{13}C NMR, and Heteronuclear Multiple Quantum Correlation (HMQC) spectroscopy were performed on a 400 MHz Bruker Avance Instrument (Bruker BioSpin GmbH) in $CDCl_3$ or acetone-d_6 in 5 mm tubes at room temperature. For ^{1}H NMR, 150 scans per spectrum were obtained. For ^{13}C NMR, 30,000 scans per spectrum were obtained using a 45° flip angle and a pulse delay of 0.5 s. For HMQC, 25 scans per spectrum were obtained. The references for the NMR spectrum obtained were set according to the solvent chemical shifts in Table 4.1.

Table 4.1: NMR solvent chemical shifts (δ)[11].

Solvent	^{1}H Chemical Shift (ppm from TMS)	^{13}C Chemical Shift (ppm from TMS)
Chloroform-d	7.24	77.23
Acetone-d_6	2.05	29.92

Titrations were carried out using phenolphthalein as indicator. To 100 mg of dried copolymer sample, 4.5 mL THF, 4.5 mL acetone, 1 mL DIW, and 0.02 mL of phenolphthalein were added and the solution stirred. A 1M NaOH solution was added to the mixture at 0.02 mL or 0.025 mL additions until the solution turned bright purple, signalling the equivalence point of the titration.

Molecular weight and polydispersity of the polystyrene samples were measured using gel permeation chromatography (GPC). Methylation of the copolymer samples were done prior to GPC analysis. Distilled THF was used as the eluent at a flow rate of 1 $mL \cdot min^{-1}$. A Waters GPC equipped with a Waters 2960 separation module containing four Styragel® columns (HR 0.5, HR 1, HR 3, HR 4) coupled with a Waters 410 differential refractive index detector calibrated with polystyrene standards ranging from 347 to 441,000 $g \cdot mol^{-1}$ was used. Mark-Houwink parameters used for the polystyrene standards are $K = 1.14x10^{-4}$ $dL \cdot g^{-1}$, $a = 0.716$[12] and for methyl acrylate are $K = 9.5x10^{-5}$ $dL \cdot g^{-1}$, $a = 0.719$[13], respectively. The final molecular weights of polystyrene-*b*-poly(methyl acrylate) were adjusted to reflect that of polystyrene-*b*-poly(acrylic acid).

4.3 Results and Discussion

The copolymerizations of polystyrene and poly(acrylic acid) were carried out in two steps. First, the polymerization of styrene was carried out in bulk with BlocBuilder® MA to approximately 30% conversion. After purification, the SG1-capped polystyrene was used as a macroinitiator for the polymerization of acrylic acid in 1,4-dioxane. The overall composition of the polystyrene-*b*-poly(acrylic acid) copolymer was varied from 65-75% polystyrene while maintaining an overall DP_n of 30. The PDI of the block copolymers was varied from 1.1 to 1.5. Figure 4.1 show the structures of the polystyrene macroinitiator and the final PSt-*b*-PAA copolymer. The synthesis and characterization of these blocks will be discussed.

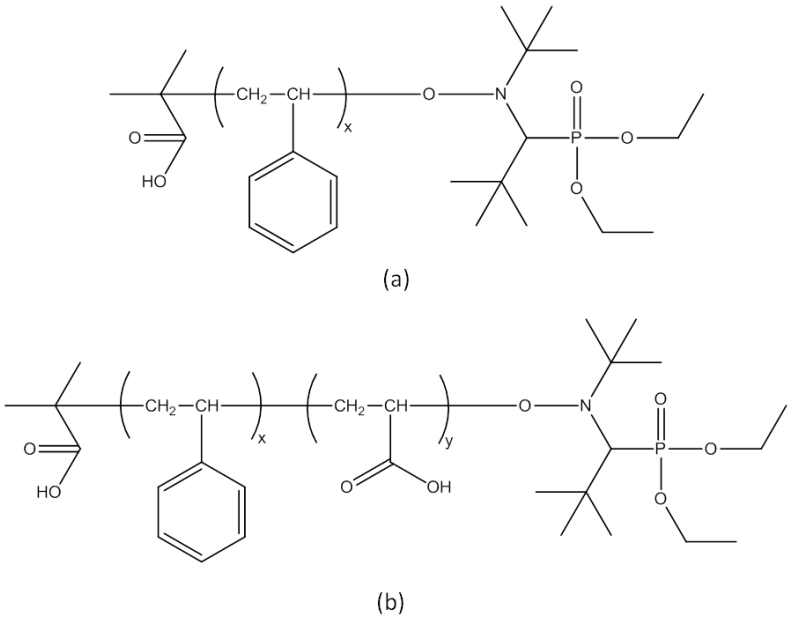

Figure 4.1: Chemical structures of (a) polystyrene macroinitiator capped by SG1 and (b) PSt-*b*-PAA block copolymer capped by SG1.

4.3.1 Synthesis and Characterization of Polystyrene Macroinitiator

The target degree of polymerization for the synthesized block copolymer is 30 with a polystyrene block composition of 65-75%. Table 4.2 shows the styrene compositions and the corresponding chain lengths and molecular weights desired.

Table 4.2: Desired block copolymer compositions and degree of polymerization for the polystyrene macroinitiators.

Styrene Composition %	**DP_n**	**M_n ($g \cdot mol^{-1}$)**
65	20	2030
70	21	2187
75	23	2343

As a range of polydispersities for the styrene block also need to be targeted, different conversions of the polymerization are needed. Lower polydispersities can be obtained by polymerizing to low conversions. As the monomer supply depletes with conversion, there is a higher chance that chains will react with another chain than with a monomeric unit (i.e. increased termination). This will increase the polydispersity. Several experiments were carried out to determine the ideal conversions for the targeted degrees of polymerization. Figure 4.2 shows a conversion vs. time profile for the bulk polymerization of styrene mediated by BlocBuilder. Depending on the amount of BlocBuilder used, different chain lengths were obtained at different conversions. Care was taken to keep the concentration of BlocBuilder the same as much as possible between experiments for reproducibility. As can be observed, there is a slight variation in the rates of polymerization due to the slight differences in BlocBuilder concentration from batch to batch. As the targeted chain lengths are quite short, a small variation in the obtained chain length can have a large impact on the final block compositions.

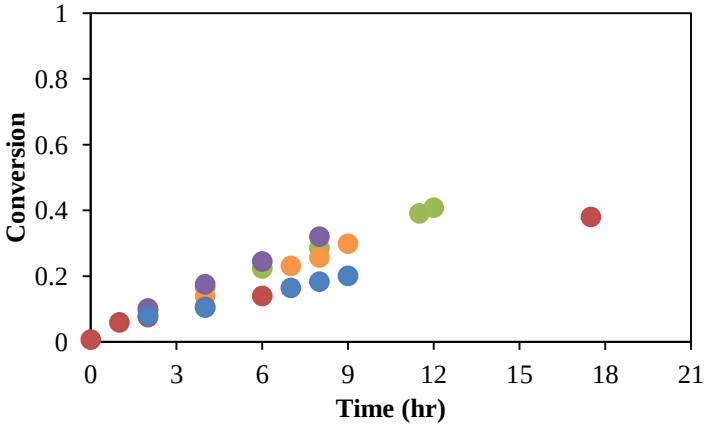

Figure 4.2: Typical conversion vs. time profiles for the bulk polymerization of styrene at 90°C by NMP using BlocBuilder® MA. Corresponding polystyrene block properties are found in Table 4.3 with reference to the following codes: PS651 (green), PS652 (orange), PS751 (red), PS1 (purple), PS2 (blue).

In order to achieve a low polydispersity, the bulk polymerization of styrene was carried out to approximately 30%. Polymerization to slightly higher conversions was done to obtain a broader molecular weight distribution. The PDI of the polystyrene block was varied from 1.17 to 1.46 with chain lengths from 15 to 23 units. The synthesized polystyrene macroinitiators are summarized in Table 4.3. The purified polystyrene macroinitiators were characterized by GPC for molecular weight and ^{1}H NMR in $CDCl_3$ for fraction of polymer, with the remainder of the sample being primarily monomer.

Table 4.3: Summary of the conversions and molecular weights of the polystyrene macroinitiators synthesized by NMP in bulk using BlocBuilder at 90°C.

Expt.	**Polymerization Time (hrs)**	**Conversion**	**M_n ($g \cdot mol^{-1}$)**	**PDI**	**DP_n**	**Residual Monomer (%)**
PS651	12	0.34	2059	1.42	20	
PS652	9	0.32	1995	1.17	19	
PS701	12.5	0.37	2285	1.17	22	4
PS702	11.5	0.40	2290	1.18	22	3
PS751	17.5	0.41	2424	1.21	23	4
PS752	18.5	0.39	2332	1.17	22	
PS753	6	0.25	2408	1.22	23	7
PS1	8	0.26	1580	1.46	15	3

In ^{1}H NMR, the integral of the signal is proportional to the quantity of protons that signal represents. This can be used to calculate the relative quantities of chemically distinct hydrogens in a given sample. By integrating the monomer and polymer peaks, the proportion of residual monomer in the purified sample can be determined, and hence the homopolymer purity can be quantified. With respect to Figure 4.3, the purity of the polystyrene macroinitiator PS701 was determined to be 96%. The two broad peaks from 1.16-1.24 ppm (**a**, **b**) and from 6.20-7.37 ppm

(**c**) were assigned to the hydrogens from the backbone and phenyl ring of polystyrene, respectively. The two hydrogens from the CH_2 on the vinyl groups of the styrene monomer are assigned to the signals at 5.24 ppm (**e**) and 5.76 ppm (**d**). The proton signals of the CH group (**f**) and of the phenyl ring (**g**, **h**, **i)** of styrene are overlapped with those of the aromatic protons of polystyrene (**c**). The ^{1}H NMR peaks from 0.6 ppm to 1.4 ppm are assigned to the methyl groups of BlocBuilder[13,14][15]. The percent residual monomer in the polystyrene macroinitiator was determined by integrating peak (**d**), which accounts for 1 proton and comparing it to the area of peak (**a, b**), which accounts for 3 protons using equation (4.1). The ^{1}H NMR spectrum of BlocBuilder® MA was also recorded to help with identification of the nitroxide and initiator peaks in the polystyrene macroinitiator spectrum and is shown in Figure 4.4. The presence of the small peak at 2.13 ppm is suspected to be due to slight impurities in the BlocBuilder® MA.

$$Residual\ monomer = \left(\frac{\frac{I\ [peak\ (d)]}{H's\ represented\ by\ monomer\ peak\ (d)}}{\frac{I\ [peak\ (d)]}{H's\ represented\ by\ peak\ (d)} + \frac{I\ [peak\ (a+b)]}{H's\ represented\ by\ peak\ (a+b)}} \right) \quad (4.1)$$

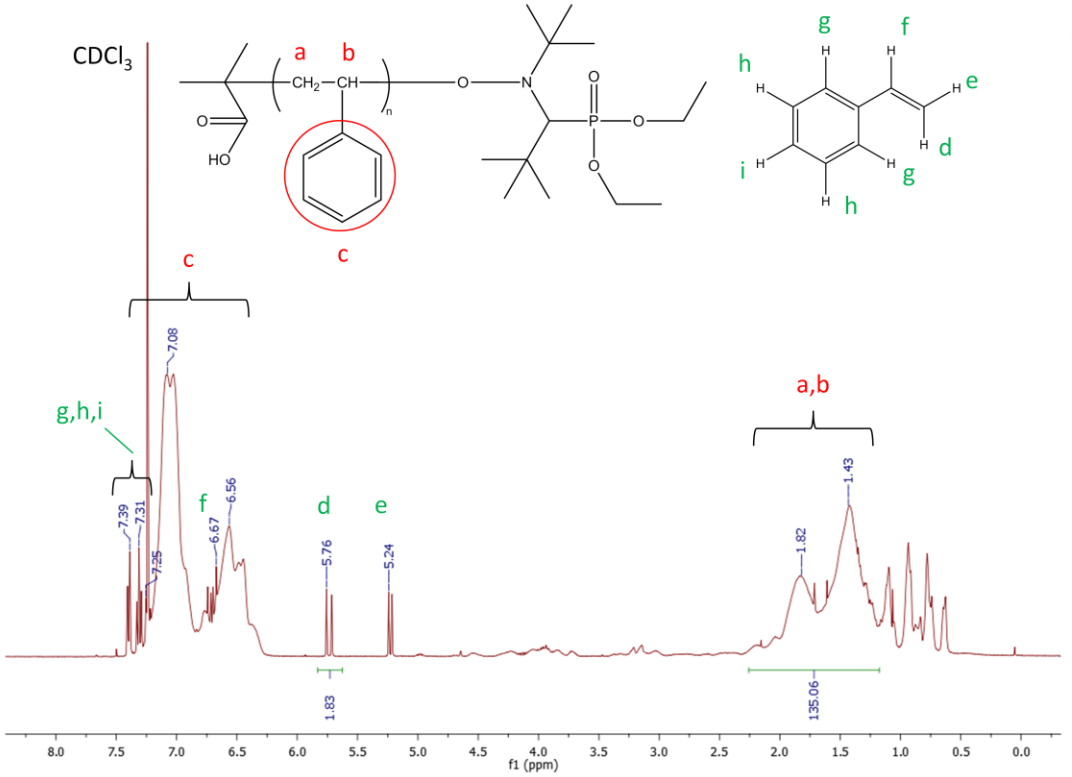

Figure 4.3: ^{1}H NMR spectrum of the polystyrene macroinitiator PS701 in $CDCl_3$.

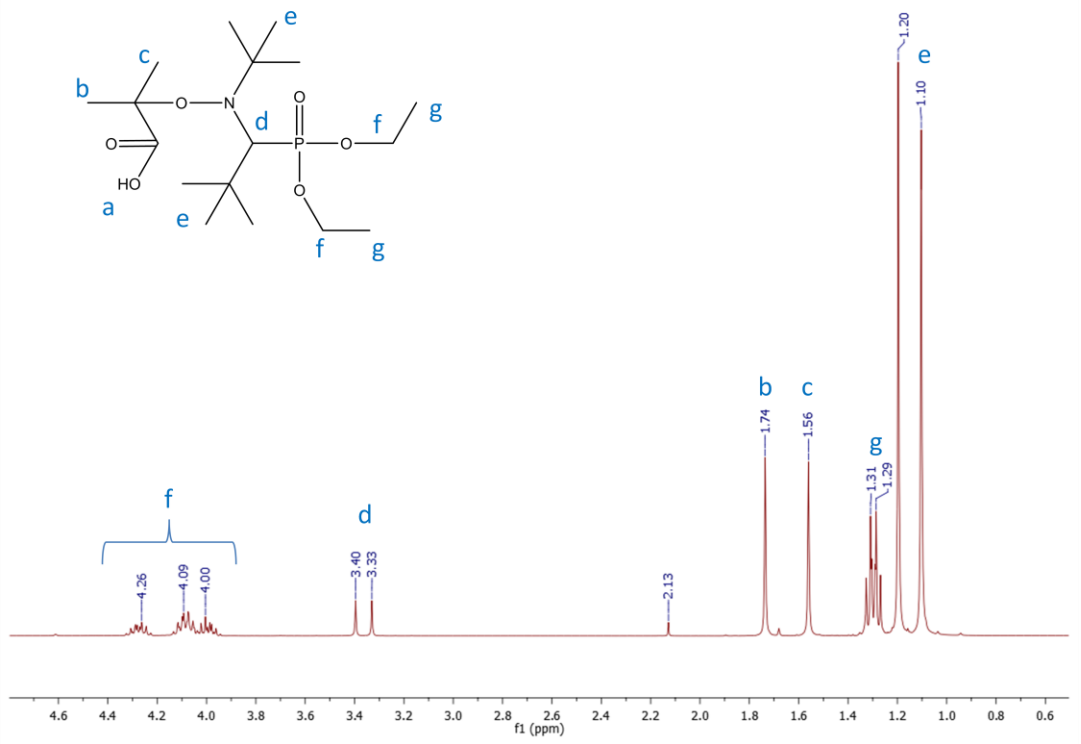

Figure 4.4: ^{1}H NMR spectrum of BlocBuilder® MA in $CDCl_3$.

To determine the extent to which the purity of the PSt macroinitiators would improve, two additional purification cycles were performed for PS753. The cycle of washing with methanol, filtering, and drying was performed for a total of three times resulting in an increase from 93% to 99% purity. It is important that the precipitated polystyrene macroinitiators be as pure as possible for use in the synthesis of the acrylic acid block to prevent unwanted random block sequences in the final diblock copolymer. The purity of the polystyrene block can be altered later by incorporation of known amounts of polystyrene and poly(acrylic acid) during synthesis.

The molecular weight of the purified polystyrene macroinitiators can be determined from the ^{1}H NMR spectrum as well. Although the initiator peaks coincide with the vinyl proton peaks of polystyrene, making it impossible to calculate the ratio of polymer to initiator chain ends, the nitroxide peaks can be of use. The termination of any number of initiator species will be accompanied by the release of the same number of free SG1 molecules. Precipitation of the polystyrene bulk solution in methanol will remove any residual monomer as well as very short chains and any terminated initiator or free nitroxide species. As such, the molecular weight can be calculated using the SG1 nitroxide peaks because the ratio of SG1 to initiator will remain the same as that as at the start of the polymerization after precipitation. Assuming that all chains are capped by an SG1 molecule at the end of the polymerization, all free SG1 species will be removed along with residual monomer during the precipitation and purification process since it is soluble in methanol. However, if there are dead polystyrene chains in the system, this calculation will overestimate the number of units per chain as they will not be capped by an SG1 molecule. Figure 4.5 shows the integrated ^{1}H NMR spectrum for the polystyrene macroinitiator PS701.

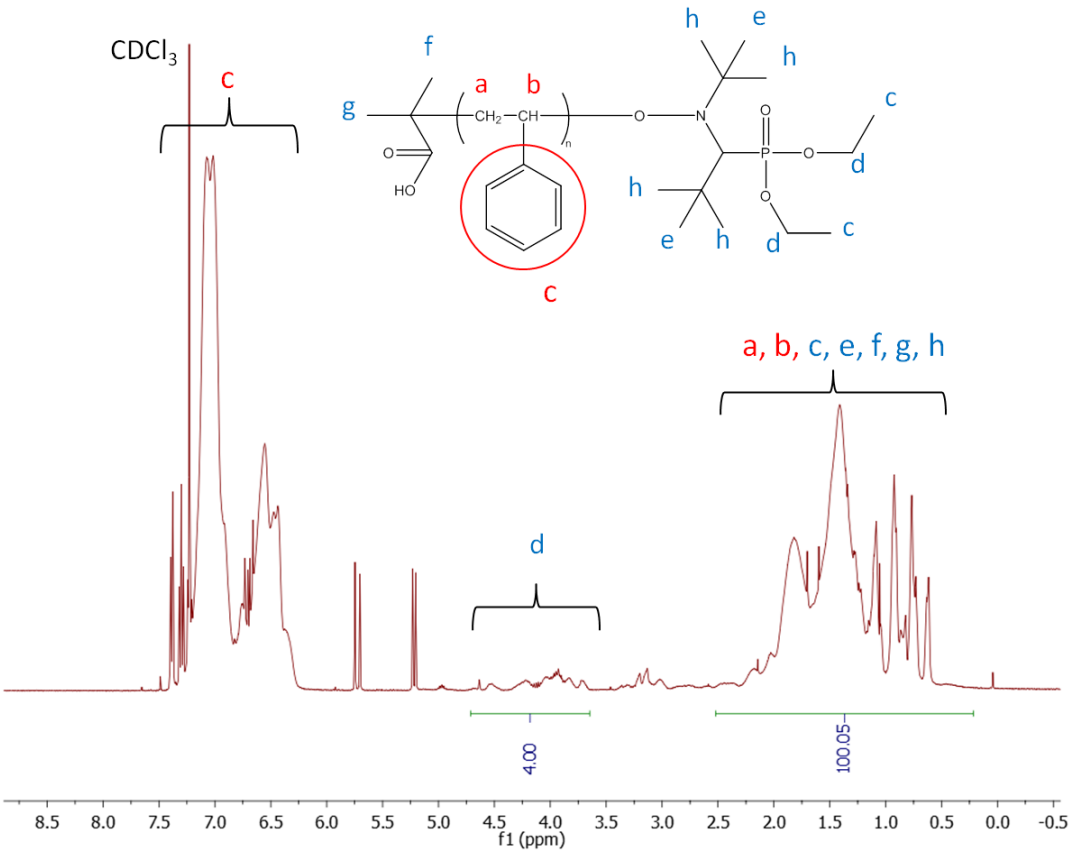

Figure 4.5: Integrated ^{1}H NMR spectrum of polystyrene macroinitiator (PS701) in $CDCl_3$ for calculation of the degree of polymerization.

The integration for the region **d** in Figure 4.5 accounts for four protons from the two CH_2 groups on SG1. The peaks for **c**, **e**, **f**, and **g** account for 30 protons in total. Subtracting the integrations corresponding to the SG1 and initiator methyl groups from the overall integration for the **c**, **e**, **f**, and **g** region including the methylene and methine protons from polystyrene (**a**, **b**) will give the integration for just methylene and methine protons. Dividing that value by the number of vinyl protons accounted for by that region will give the number of styrene units per polymer

chain. With respect to Figure 4.5, the degree of polymerization can be calculated using equation (4.2):

$$Degree\ of\ Polymerization = \frac{[(I[a+b+c+e+f+g]) - 30(I[1H])]/3}{(I[1H])} \quad (4.2)$$

where I[1H] is the integration per proton and I[a+b+c+e+f+g] is the integration of the region represented by peaks **a**, **b**, **c**, **e**, **f**, and **g**.

For PS701, the degree of polymerization calculated from the ^{1}H NMR spectrum is 23, which is very close to the value of 22 obtained by GPC, indicating minimal dead chains and thus validating this method.

4.3.2 Synthesis and Characterization of Polystyrene-*b*-poly(acrylic acid) Block Copolymers

The synthesized polystyrene macroinitiators were used to re-initiate the acrylic acid polymerization in 1,4-dioxane at 90°C. The feed rate of the acrylic acid was varied in an attempt to target a range of polydispersities. The final copolymers were chemically modified prior to molecular weight analysis by GPC by methylation to convert the poly(acrylic acid) block to a poly(methyl acrylate) block. To determine the composition of the final copolymers, titration and NMR spectroscopy were used. The resulting compositions were then used in the calculation of the final block copolymer molecular weight.

4.3.2.1 Identification of Polystyrene-b-poly(acrylic acid) Block Copolymers

A ^{13}C NMR spectrum was acquired to identify the presence of polystyrene and poly(acrylic acid) as shown in Figure 4.6. The assignments of the ^{13}C NMR resonance peaks are in agreement with those of the PSt-*b*-PAA block copolymers from literature[16] and indicate clearly the presence of the poly(acrylic acid) block.

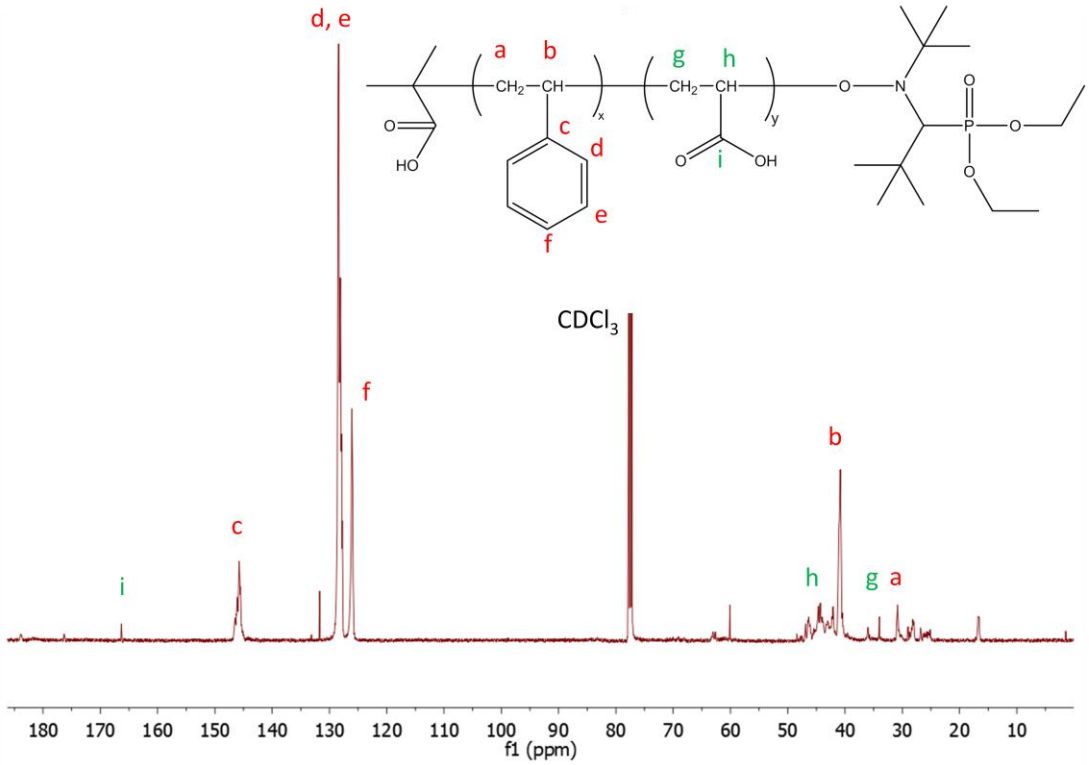

Figure 4.6: ^{13}C NMR spectrum of PSt-*b*-PAA copolymer (B20) in $CDCl_3$ taken at 500 MHz.

To further confirm the presence of poly(acrylic acid) in the final copolymer, a 2D Heteronuclear Multiple Quantum Correlation (HMQC) experiment was carried out. Both the HMQC spectrum of the polystyrene macroinitiator and that of the final block copolymer are shown in Figure 4.7. The peaks highlighted in red are assigned to the methylene and methine

protons of the polystyrene backbone as well as the methylene protons from the poly(acrylic acid) backbone. The peak highlighted in green is assigned to the methine proton from the poly(acrylic acid) backbone. The peak highlighted in blue is assigned to the dimers formed by the acrylic acid monomer. The presence of the green peak clearly shows that the chain extension of polystyrene with acrylic acid is successful. From the HMQC spectrum, it can be seen that the signal for the methine proton from poly(acrylic acid) is very close to the dimers peak and it is important that the entire signal of the poly(acrylic acid) backbone is incorporated in the integration for compositional analysis.

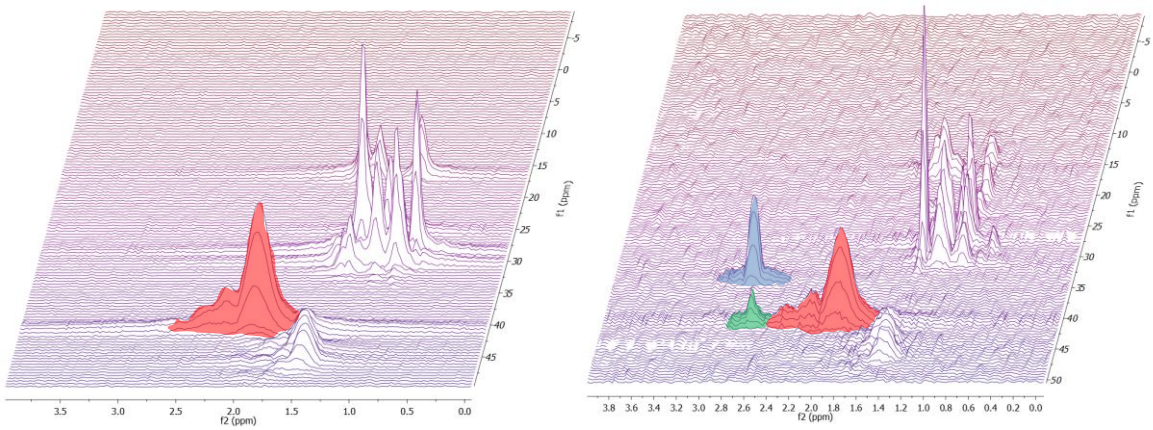

Figure 4.7: HMQC spectrum of polystyrene macroinitiator (left) and PSt-*b*-PAA block copolymer (right). The methine proton signal from the poly(acrylic acid) backbone is highlighted in green, while the blue peak results from dimers formed by the acrylic acid monomer.

4.3.2.2 Composition Analysis by Titration

A simple titration can be used to determine the weight fraction of acidic units in a given polymer sample. When using this method to determine the acid composition of PSt-*b*-PAA block copolymers, it is important to note that it does not truly reflect the poly(acrylic acid) composition in the copolymer due to the contribution of acidic groups from other sources. As the initiator part

of BlocBuilder also carries a carboxylic acid group, the calculated acidic content will be a slight overestimation of the quantity of acrylic acid polymer. Hence, one acid unit per chain would need to be subtracted from the total acid units per chain in order to give a correct estimation of the poly(acrylic acid) content. In addition, as verified by ^{1}H NMR in Figure 4.8, the final copolymers are not completely free of acrylic acid monomer. This means that the acrylic acid polymer content would also be overestimated as a portion of the acrylic acid in the titrated sample originate from the residual monomer and should not be included as part of the poly(acrylic acid) composition in the copolymer. This residual monomer content can be calculated from the ^{1}H NMR spectrum of the final block copolymer, which will be discussed in the next sections.

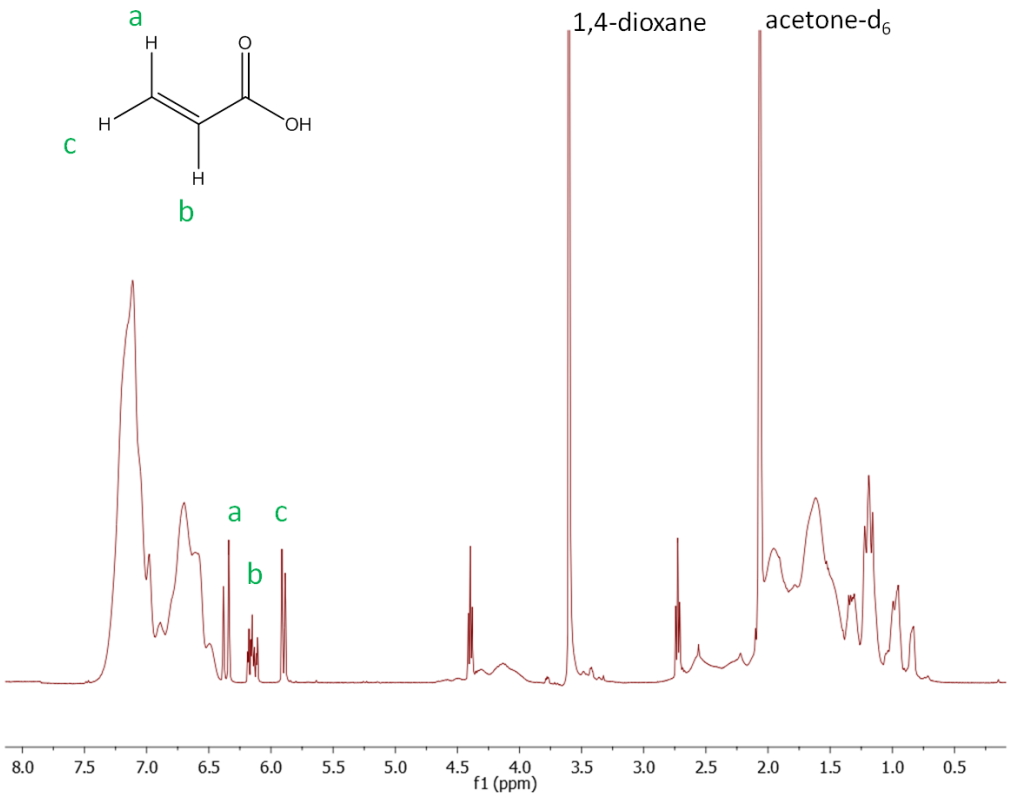

Figure 4.8: ^{1}H NMR spectrum of PSt-*b*-PAA copolymer (B16) in acetone-d_6. Acrylic acid monomer peaks are represented by peaks **a**, **b**, and **c**.

A useful parameter that can be obtained from titration is the acid value, which is expressed as the milligrams of potassium hydroxide (KOH) that is required to neutralize one gram of polymer. The acid value is used as a measure of the relative quantity of carboxylic acid groups in a polymer and is calculated using equation 4.3:

$$Acid\ Value = \frac{(mol\ equivalence\ NaOH)(MW_{KOH})}{(mass\ of\ copolymer)} \times \frac{1000mg}{g} \tag{4.3}$$

where MW_{KOH} is the molecular weight of potassium hydroxide and mol equivalence NaOH is the moles of NaOH required to neutralize the sample. It is important to note that the acid value does not represent the absolute acid concentration of a sample.

From the titration data, the weight fraction of acrylic acid in the sample can be calculated using equation 4.4:

$$wt.frac.Acrylic\ Acid = \frac{(mol\ equivalence\ NaOH)(MW_{AA})}{mass\ of\ copolymer} \tag{4.4}$$

where MW_{AA} is the molecular weight of acrylic acid. To determine the fraction of poly(acrylic acid) in the copolymer, the fraction of residual monomer would need to be subtracted from this value to give an accurate composition by weight. The titration method was tested against a PSt-*co*-PAA copolymer sample of known composition provided by BASF and the copolymer composition obtained matched that of the specifications, thus validating this method. The titration method is simple to perform, however the accuracy of the results obtained is highly dependent on the sample size and the volume chosen for the NaOH additions.

4.3.2.3 Composition Analysis by Nuclear Magnetic Resonance Spectroscopy

The copolymer compositions were analyzed using ^{1}H NMR spectroscopy. However, a direct compositional analysis from the ^{1}H NMR spectrum of the copolymer could not be obtained

due to overlapping of the polymer peaks. The chemical shifts of the methylene and methine protons of polystyrene and those of poly(acrylic acid) appear in the same range, from 1.0 to 2.5 ppm, as well as the methyl groups of the SG1 nitroxide, from 0.5 to 1.2 ppm. With the abundance of overlapping signals, it was impossible to integrate the individual polymer peaks for comparison. To overcome this problem, a subtraction method was used. The polystyrene macroinitiator was analyzed by ^{1}H NMR and GPC prior to re-initiation with acrylic acid. After the synthesis of the acrylic acid block, the final copolymer was also analyzed by ^{1}H NMR and GPC. Assuming negligible changes to the polystyrene block during chain extension and that all chains are living, the difference in the integration of the vinyl proton peaks in the 0.5 to 2.5 ppm range between both spectra can be attributed to the poly(acrylic acid) block.

As mentioned previously, from the ^{1}H NMR spectrum of the polystyrene macroinitiator, it can be seen that a small quantity of residual styrene monomer still remains in the purified product. To ensure that the residual styrene monomer plays a minimal part in the synthesis of the poly(acrylic acid) block and that the assumption of negligible change in the polystyrene block is valid, two polymerizations were carried out; one with polystyrene in 1,4-dioxane with acrylic acid at 90°C (EXPT1), and one with just the polystyrene macroinitiator in 1,4-dioxane at 90°C (EXPT2). Equal amounts of the same polystyrene macroinitiator were used in both experiments for direct comparison. Analysis by GPC show a clear difference in molecular weight distributions between the two polymers obtained after a 6-hour reaction period. A clear shift of the GPC trace of the copolymer (EXPT1) to the right can be clearly seen in Figure 4.9 as polymerization progressed. No change is observed in the molecular weight distribution of the polystyrene macroinitiator in 1,4-dioxane (EXPT2). There is also no tailing observed meaning it is safe to assume that all polystyrene chains are living and are re-initiated in the solution polymerization

with acrylic acid. This proves that the previous assumption regarding a negligible change in the polystyrene block is valid, enabling the use of the subtraction method in the ^{1}H NMR analysis.

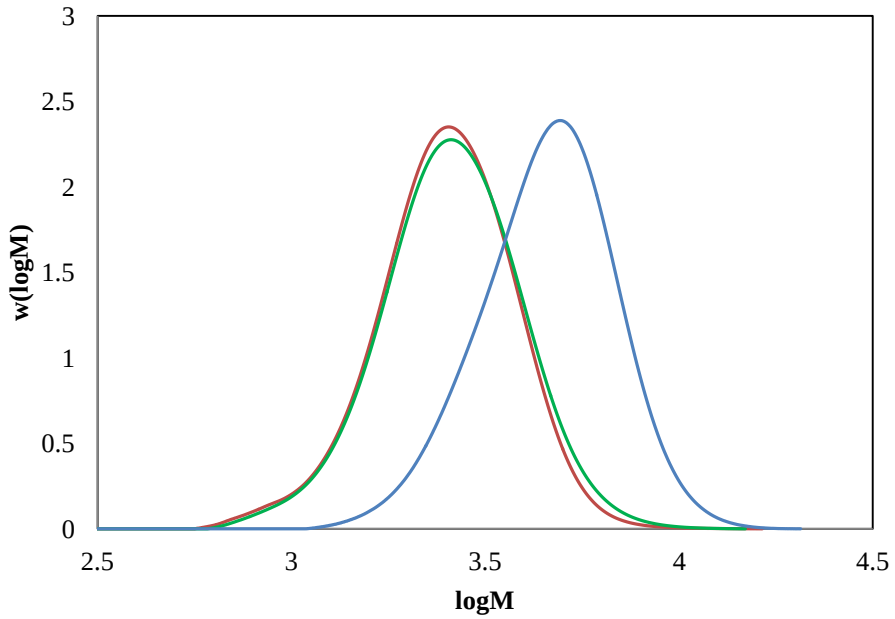

Figure 4.9: Molecular weight distributions of expts. PS702 (red), EXPT1 (green), and EXPT2 (blue) showing no effect of minimal residual monomer in the purified polystyrene initiator (red and green) and successful chain extension of the polystyrene block with acrylic acid (blue).

An accurate integration of the polystyrene macroinitiator peaks just prior to re-initiation in acrylic acid is necessary for the subtraction method. From the ^{1}H NMR spectrum of the polystyrene macroinitiator in Figure 4.10a, a slight overlap of the polystyrene backbone and the BlocBuilder signals is evident. In order to minimize the error from integration of the two separate regions, an integration of the entire region (0.5 to 2.5 ppm) was taken. The integration of the proton signals of the phenyl ring from the polymer is also overlapped with those from the monomer as well as that of the methine proton from the styrene monomer backbone. The integration for this region can be adjusted to reflect only that of the phenyl ring of polystyrene by

subtracting the portion contributed from the monomer. This was done by integrating one of the methylene proton signals (at 5.24 ppm and 5.71 ppm), multiplying the integration by 6 to account for 6 protons from the monomer in the phenyl region, and then subtracting this value from that of the entire phenyl peak region. The polymer peaks from the phenyl ring of polystyrene (6.25 to 7.46 ppm) accounts for 5 protons and the peaks of the polystyrene backbone accounts for 3 protons. An attempt to integrate only the backbone region in the NMR spectrum gave results that were very close to the theoretical amount. With the integration of the phenyl region set to 1.00, the backbone region should theoretically give 0.60, and an integration of 0.65 was obtained. This backbone region includes the signals from the two methyl groups of the initiator portion of BlocBuilder and a small portion of some of the methyl groups on SG1, which can explain why the value is slightly higher.

The ^{1}H NMR spectrum of the PSt-*b*-PAA block copolymer was compared to that of the polystyrene macroinitiator for compositional analysis. It would be helpful to see the signal of the carboxylic acid group from the acrylic acid in the ^{1}H NMR spectrum but this signal is absent due to the solvent used. The hydroxyl hydrogen should appear in the 10 ppm range but the signal is often very broad or not observed due to exchange with protic solvents. Aprotic solvents, such as DMSO, would allow the OH group to be visible, but polystyrene is not very soluble in DMSO.

Assuming that the phenyl peaks of the polystyrene block remain unchanged, the increase in the integration of the vinyl proton region can be attributed to the poly(acrylic acid) block. Figure 4.10b shows the ^{1}H NMR spectrum of the PSt-*b*-PAA block copolymer. Again, the integration of the phenyl region is set to 1.00, and the integration of the backbone and SG1 region

is obtained. For expt. B20, the integrations of the backbone and SG1 regions from the polystyrene macroinitiator and the final block copolymer are 0.91 and 1.07, respectively. This translates to an integration value of 0.37 for the three poly(acrylic acid) vinyl protons. From the ratio of the integration of poly(acrylic acid) to the entire copolymer, a poly(acrylic acid) composition of ~15 % was obtained.

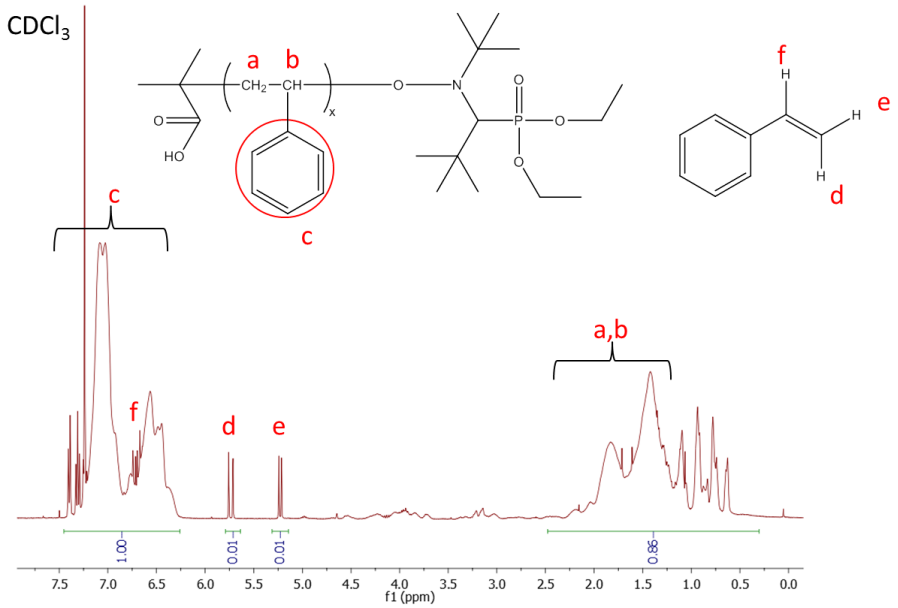

(a)

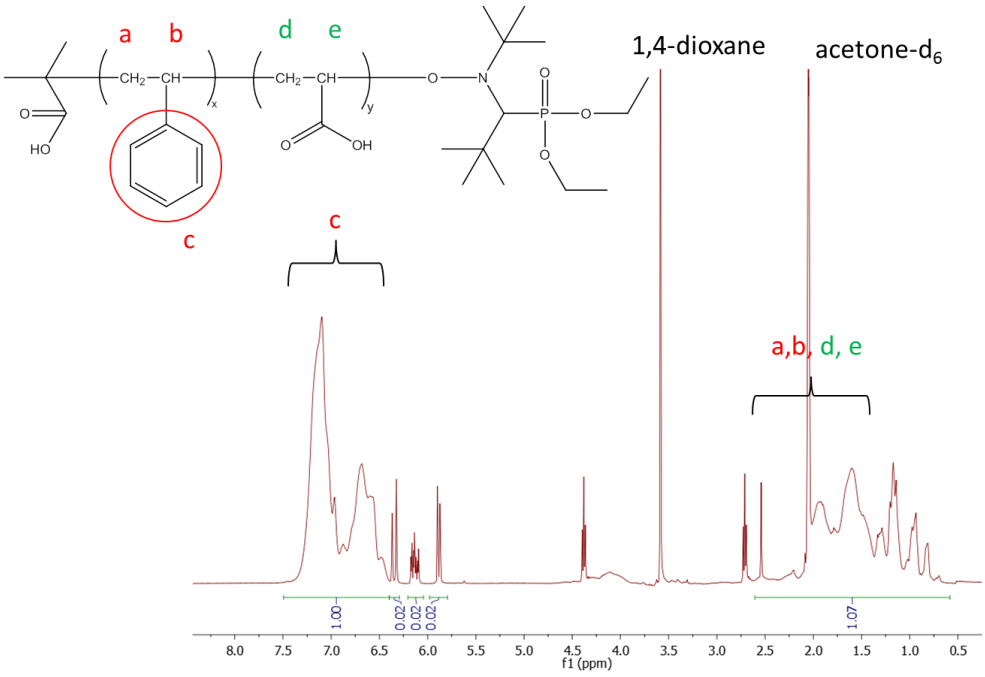

(b)

Figure 4.10: ^{1}H NMR spectrum of (a) polystyrene macroinitiator in $CDCl_3$ (PS701), and (b) PSt-*b*-PAA block copolymer in acetone-d_6 (B20).

When using $CDCl_3$ as the solvent, there is a slight overlap of one of the acrylic acid monomer peaks (6.5 ppm) with the phenyl proton peaks as shown in Figure 4.11 for expt. B17. By integrating the other two vinyl proton peaks of the acrylic acid monomer, an integration value for the overlapped methylene proton peak can be obtained as they are present in a 1:1:1 ratio. Subtraction of this portion from that of the total phenyl region will allow for an accurate estimation of the integration of the phenyl peaks of the polystyrene block. The final integration value for the phenyl region was then adjusted to 1.00 to allow for direct comparison with the ^{1}H NMR spectrum of the corresponding polystyrene macroinitiator. With an integration value of 1.102 for the backbone and SG1 region of the copolymer, the composition obtained was ~17% poly(acrylic acid).

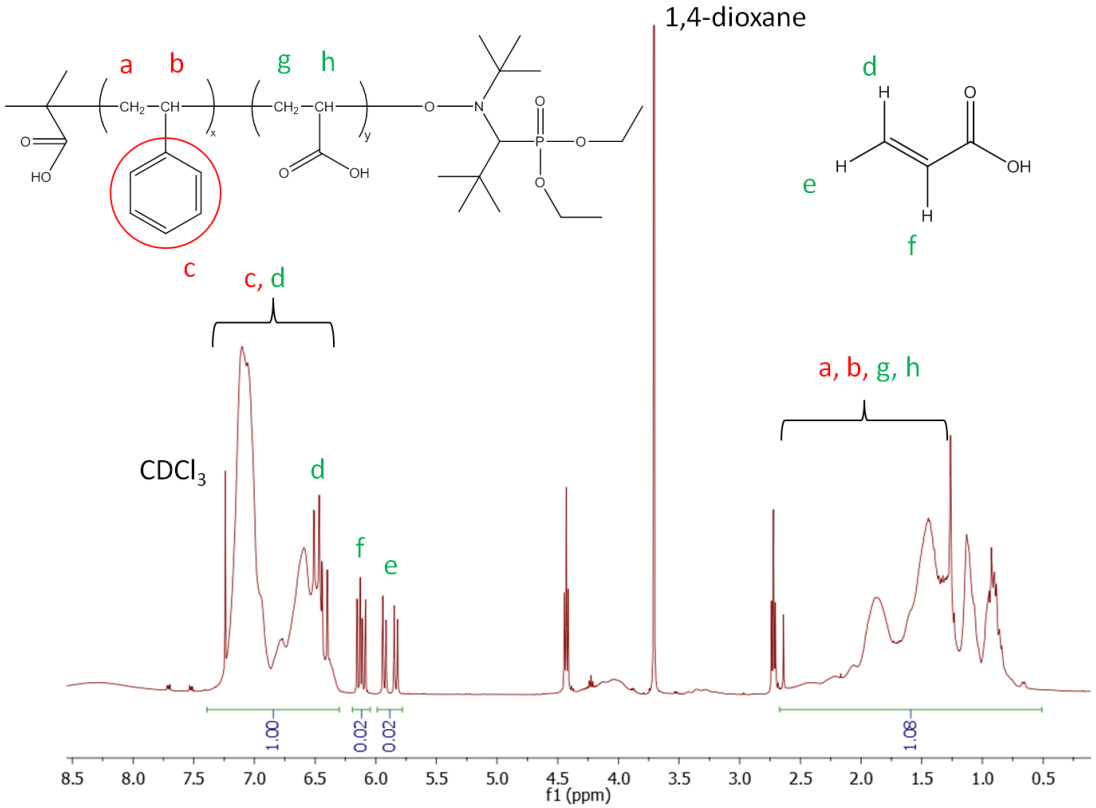

Figure 4.11: ^{1}H NMR spectrum of PSt-*b*-PAA expt. B17 in $CDCl_3$.

The integration of the acrylic acid monomer peaks and the estimated poly(acrylic acid) peaks also allows for the estimation of the residual acrylic acid monomer content in the final copolymer sample using equation (4.1), giving a measure of the purity of the final block copolymer. This residual monomer content was then used in the titration calculations discussed previously to account for the monomer groups neutralized by NaOH.

4.3.2.3 Copolymer Compositions

Copolymer compositions were determined by titration and ^{1}H NMR analysis. The titration method gives a weight percent of poly(acrylic acid) content and can be converted to a mole percentage for comparison to that obtained using the NMR subtraction method.

Table 4.4: Summary of copolymer compositions of PSt-*b*-PAA copolymers obtained by titration and ^{1}H NMR.

Expt.	**M_n[b] (g·mol^{-1})**		**Mole % PAA**		
	PSt	**PSt-*b*-PAA**	**Titration**	**^{1}H NMR**	**Difference**
B05	2332	6054	26.5	3.1[a]	23.44
B10	2059		9.8	4.6	5.21
B14	2059	3383	24.1	30.6	-6.51
B15	1580	3589	58.1	54.0	4.14
B16	2285	3280	30.2	23.1	7.05
B17	2285	3027	21.6	17.0	4.59
B20	2285	2643	26.5	15.5	11.04
B21	2290	4020	39.4	36.3	3.07
B24	2408		39.4	40.4	-1.03
B25	2408	3055	32.5	14.5	18.01

[a] Compositions calculated do not fulfill the assumptions for using the subtraction method.
[b] Number average molecular weight of PSt-*b*-PAA copolymers calculated from composition obtained by ^{1}H NMR.

As can be seen from Table 4.4, there are some discrepancies between the titration and NMR methods used to calculate the copolymer compositions. For the most part, there is an absolute difference of ~5% between the compositions obtained by both methods. For some of the samples, specifically expts. B05, B20, and B25, the compositions obtained by ^{1}H NMR spectroscopy were significantly different from that obtained by titration. Furthermore, some of the obtained compositions do not agree well with the copolymer molecular weights obtained. A main reason for these differences is that the calculation by ^{1}H NMR assumes that all chains from the polystyrene macroinitiator re-initiate in the acrylic acid polymerization. If there are any dead polystyrene chains in the system, the ratio from the integration of the phenyl region with respect to the polystyrene and poly(acrylic acid) backbone regions will not be reflective of the additional poly(acrylic acid) units because it would give a ratio with respect to the total polystyrene in the system, including those which have terminated. This means that the final composition calculated by ^{1}H NMR would be lower than the actual value if there are indeed dead polystyrene chains because there would be more acrylic acid units added on to each living chain. Therefore, caution must be taken when using the subtraction method to determine the copolymer composition and it is important to first analyze the GPC traces to see if there are any terminated chains. Figure 4.12 shows the molecular weight distribution for expt. B05 clearly showing the presence of dead chains in the re-initiated polymerization as indicated by the tail in the low molecular weight end of the GPC trace. In this case, the weight composition calculated by titration would be more accurate because it doesn't rely on the livingness of the polystyrene block.

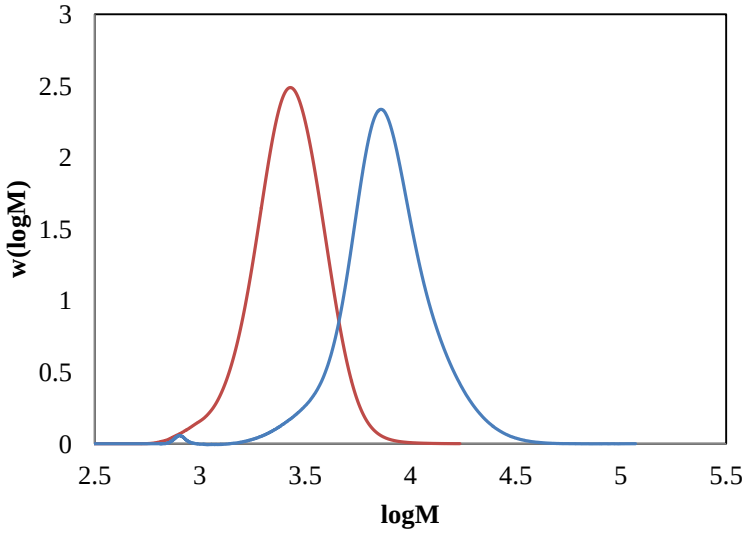

Figure 4.12: Molecular weight distributions of PSt-*b*-PAA copolymer expt. B05 (blue) and the corresponding polystyrene macroinitiator PS752 (red).

The copolymer composition can be obtained using both the titration and NMR subtraction methods. For the titration method, an accurate estimate of the residual monomer content is required for the calculation of the poly(acrylic acid) content as the percentage is based on the concentration of acidic groups of the sample. The carboxylic acid group of the initiator must also be taken into account and can be assumed to account for one unit per polymer chain. Depending on the length of the poly(acrylic acid) block of the copolymer chain, the error from not accounting for this carboxylic acid group may or may not be significant. The longer the poly(acrylic acid) block, the smaller the deviation from the true value. The same applies for the error resulting from inaccurate calculation of the residual monomer content. Comparison of the weight percent poly(acrylic acid) without accounting for the residual acrylic acid monomer

content show a maximum of ~4 % difference from that of the percentage obtained accounting for the residual monomer.

For the copolymer compositions obtained by the subtraction method using the ^{1}H NMR spectra, the accuracy of the method highly depends on the livingness of the polystyrene macroinitiator. Due to the overlapping peaks of the polystyrene and poly(acrylic acid) backbones, direct integration of the two regions is not possible for comparison. From the results obtained, as long as the molecular weight distributions show retention of a high degree of livingness, the copolymer compositions obtained are in relatively good agreement with those obtained by the titration method. Otherwise, the titration method would give a more accurate result.

4.3.2.4 Conversion

From the ^{1}H NMR spectrum of the block copolymer in Figure 4.11, it can be seen that there is still a significant amount of solvent left after drying. As such, the conversion of the poly(acrylic acid) block determined by gravimetry will not be accurate unless the portion of residual 1,4-dioxane is accounted for. Based on calculations of the sample at time zero for which the conversion should be zero (no conversion prior to addition of acrylic acid monomer), the residual 1,4-dioxane remaining in the sample after drying is approximately 20 %. Precipitation of the copolymer in a suitable solvent could further lower the amount of residual solvent in the sample but would interfere with the NMR subtraction method. The conversion can also be determined from ^{1}H NMR of the final copolymer solution. By acquiring a spectrum prior to drying, the proportion of residual acrylic acid monomer can be compared to the poly(acrylic acid) polymer peaks to obtain the conversion. This method however, relies on the accuracy of the

estimated poly(acrylic acid) backbone peaks by the NMR subtraction method. Figure 4.13 shows the ^{1}H NMR spectrum of the copolymer reaction solution prior to drying and the integrations used for the calculation of the conversion.

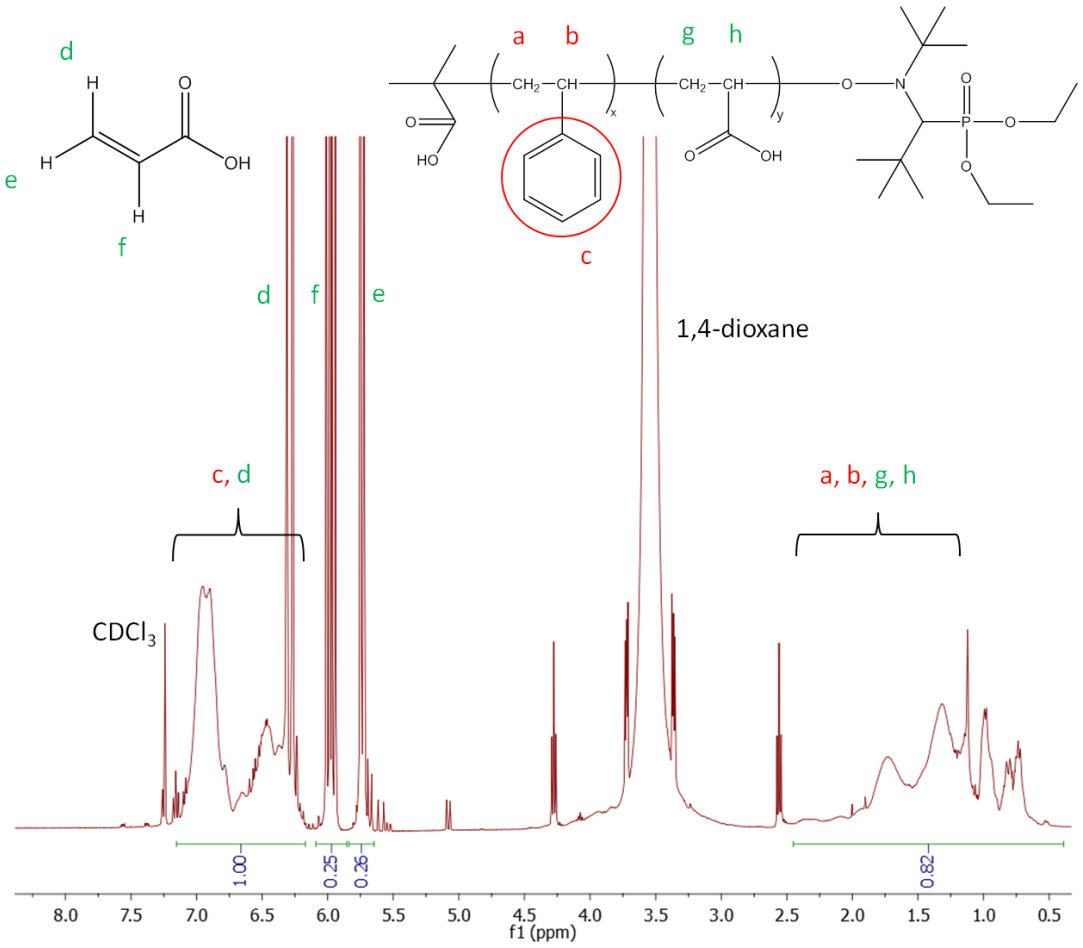

Figure 4.13: ^{1}H NMR spectrum of the PSt-*b*-PAA copolymer (expt. B17) reaction solution prior to drying in $CDCl_3$.

4.3.2.5 Varying Feed Conditions

In order to target a range of polydispersities and conversions of the final PSt-*b*-PAA block copolymer, the feed rate of the acrylic acid monomer and the duration of the

polymerization were varied. For the same polymerization period, the more moles of acrylic acid monomer available per mole of polystyrene, the faster the polymerization proceeded. As the degree of polymerization desired for the poly(acrylic acid) block is small, it is difficult to obtain the exact composition desired as a small change in the number of acrylic units added will have a large effect on the final composition. The copolymer compositions obtained by ^{1}H NMR spectroscopy were used in the calculation of the final molecular weight of the PSt-*b*-PAA copolymers. The number average molecular weight of the methylated polystyrene-*b*-poly(methyl acrylate) copolymer was adjusted to represent that of polystyrene-*b*-poly(acrylic acid) by accounting for the difference in molecular weight between the methyl acrylate and acrylic acid units. The polymerization conditions, compositions, and copolymer molecular weights obtained are presented in Table 4.5.

Table 4.5: Summary of formulations, experimental conditions, and molecular weights obtained for the PSt-*b*-PAA copolymers synthesized by SG1-mediated solution polymerization in 1,4-dioxane.

Expt	Reaction Time (hrs)	AA Feed Rate (mL/hr)	AA:PSt in Feed (mol:mol)	PSt-SG1			(PSt-PAA)-SG1			PAA Content		Acrylic acid Conv.[e]	Acid Value[d]
				M_n ($g \cdot mol^{-1}$)	DP_n	PDI	M_n ($g \cdot mol^{-1}$)[b]	DP_n	PDI	NMR (mol %)	Titration (wt %)[c]		
B05	4		85.18	2332	22	1.17	6054	52	1.27	3.1[a]	19.6		153
B10	4	3.1	61.24	2059	20	1.42				4.6	7.1	0.44	56
B14	4		55.77	2059	20	1.42	3383	18	1.15	30.6	17.8	0.29	139
B15	4	4.4	119.40	1580	15	1.46	3589	28	1.30	54.0	49.2	0.16	383
B16	6	6.0	35.93	2285	22	1.17	3280	14	1.11	23.1	22.9	0.53	178
B17	6	4.0	36.03	2285	22	1.17	3027	10	1.12	17.0	16.4	0.38	128
B20	4		35.18	2285	22	1.17	2643	5	1.17	15.5	20.3	0.19	158
B21	6		46.45	2290	22	1.18	4020	24	1.17	36.3	30.9	0.69	241
B24	5.5		39.49	2408	23	1.22				40.4	31.1		243
B25	4		38.17	2408	23	1.22	3055	9	1.23	14.5	24.5		191

[a] Compositions calculated do not fulfill the assumptions for using the subtraction method.
[b] Molecular weight data obtained by GPC after methylation of copolymers using TMS –diazomethane. M_n values adjusted for poly(acrylic acid) from poly(methyl acrylate).
[c] Titration gives wt. % after adjustment of residual acrylic monomer from ^{1}H NMR analysis by the substitution method.
[d] Acid value based on residual acrylic acid monomer from ^{1}H NMR analysis by the substitution method.
[e] Acrylic acid conversion determined from gravimetry with adjustment for ~20% residual 1,4-dioxane and acrylic acid monomer in sample after drying.

4.4 Conclusion

The synthesis and characterization of polystyrene-*b*-poly(acrylic acid) copolymers synthesized by NMP are presented. The synthesis of the polystyrene block by bulk polymerization followed by chain extension of acrylic acid by solution polymerization in 1,4-dioxane appears to be a good method for producing PSt-*b*-PAA copolymers of varying sizes. The length of each block and polydispersity can be adjusted by changing polymerization conditions such as reaction time, monomer feed rates, and the ratio of BlocBuilder® MA to monomer. Characterization of these block copolymers were achieved using titration and nuclear magnetic resonance spectroscopy. A simple titration method using phenolphthalein as indicator provided poly(acrylic acid) content on a weight basis after adjustment of residual acrylic acid monomer in the final sample. Copolymer analysis by ^{13}C NMR confirmed the successful addition of the poly(acrylic acid) block and compositions were obtained by ^{1}H NMR using a subtraction method. Residual monomer contents were also analyzed by ^{1}H NMR. With regards to the compositional analysis, obstacles that have yet to be overcome include improving the accuracy of the subtraction method which involves an accurate determination of the number of chains after copolymerization, and a method to analyze copolymer purity with regards to homopolymer blocks as the resonance peaks from ^{1}H NMR cannot provide such information due to the similar chemical structures.

The techniques for the synthesis and characterization of the polystyrene-*b*-poly(acrylic acid) block copolymers presented in this chapter will be used in the next step of the project to synthesize a range of copolymers with varying compositions and purity. The results achieved in this work demonstrate the ability to synthesize a wide range of copolymers with the option to

control the size of each block as necessary. The performance of these amphiphilic block copolymers will then be analyzed in terms of effectiveness for use as protective colloids in collaboration with BASF.

Acknowledgements

Financial support from the Natural Sciences and Engineering Research Council of Canada, Ontario Research Chair Program, and Queen's University is gratefully acknowledged. We thank Arkema Inc. for providing materials and BASF for financial support, their expertise and advice.

References

[1] S. Förster, M. Antonietti, *Adv Mater.* **1998**, *10*, 195-217.

[2] I. W. Hamley, "Developments in Block Copolymer Science and Technology", in: John Wiley & Sons Ltd., England 2004,.

[3] D. Bendejacq, V. Ponsinet, M. Joanicot, Y. -. Loo, R. A. Register, *Macromolecules.* **2002**, *35*, 6645-6649.

[4] K. A. Davis, K. Matyjaszewski, *Macromolecules.* **2000**, *33*, 4039-4047.

[5] J. Qiu, B. Charleux, K. Matyjaszewski, *Progress in Polymer Science.* **2001**, *26*, 2083-2134.

[6] T. E. Patten, K. Matyjaszewski, *Adv Mater.* **1998**, *10*, 901-915.

[7] L. Couvreur, C. Lefay, J. Belleney, B. Charleux, O. Guerret, S. Magnet, *Macromolecules.* **2003**, *36*, 8260-8267.

[8] G. Laruelle, J. François, L. Billon, *Macromol.Rapid Commun.* **2004**, *25*, 1839-1844.

[9] B. Lessard, S. C. Schmidt, M. Marić, *Macromolecules.* **2008**, *41*, 3446-3454.

[10] L. Couvreur, B. Charleux, O. Guerret, S. Magnet, *Macromol.Chem.Phys.* **2003**, *204*, 2055-2063.

[11] I. Cambridge Isotope Laboratories, **2010**.

[12] S. Beuermann, M. Buback, T. P. Davis, R. G. Gilbert, R. A. Hutchinson, A. Kajiwara, B. Klumperman, G. T. Russell, *Macromolecular Chemistry and Physics.* **2000**, *201*, 1355-1364.

[13] C. Lefay, J. Belleney, B. Charleux, O. Guerret, S. Magnet, *Macromol.Rapid Commun.* **2004**, *25*, 1215-1220.

[14] C. Burguière, C. Chassenieux, B. Charleux, *Polymer.* **2003**, *44*, 509-518.

[15] C. Bernhardt, F. Stoffelbach, B. Charleux, *Polym.Chem.* **2011**, *2*, 229-235.

[16] S. Chijiwa. Characterization of Polystyrene-*b*-poly(acrylic acid) Copolymer Micelles by Nuclear Magnetic Resonance Spectroscopy. M.Sc. Thesis, McGill University, July **2001**.

Chapter 5

Conclusions and Recommendations for Future Work

5.1 Conclusions

5.1.1 Decoupling of Target Molecular Weight and Particle Size in Nitroxide-Mediated Microemulsion Polymerization

In living radical emulsion polymerization systems, a strong dependence of the particle size on the target molecular weight through the initiator concentration has been observed. The effect of increased particle size when targeting lower molecular weights proves to be a challenge in synthesizing polymers with tailored properties. A range of conditions were explored to decouple the two effects to create colloidally stable polymer latexes at a solids content of 20 wt. % using low surfactant to monomer ratios. Using nitroxide mediated microemulsion polymerization of *n*-butyl acrylate, the extent to which these two effects can be decoupled was studied by varying the surfactant to monomer ratio (wt/wt), by varying the BlocBuilder to Na_2CO_3 ratio (mol/mol), by varying the monomer content in the seed stage, and by a semi-batch addition of the surfactant. Interestingly, it was found that increasing the surfactant to monomer ratio from 0.2 to 0.5 (wt/wt) led to an increase in particle size, opposite to what was expected, likely due to the increase in ionic strength contribution from the additional surfactant. An increase in the initial monomer content at the seed stage resulted in a decrease in the final particle size likely due to a higher number of nucleated particles as well as higher rates of polymerization owing to the segregation effect. Larger particle sizes can be obtained by increasing the portion of surfactant fed into the system over time as a result of fewer nucleated particles in the seed stage. Changing the molar ratio of BlocBuilder to Na_2CO_3 did not significantly change the final particle size provided there is sufficient base to provide buffering capacity to the system, although a large

excess of Na_2CO_3 is expected to lead to an increase in particle size due to ionic strength contributions. For the most part, the final molecular weights matched that of the theoretical, but deviation from the theoretical molecular weight was observed at a target M_n of 80,000 $g \cdot mol^{-1}$, resulting from chain transfer to polymer and new chain formation likely caused by impurities in Dowfax™ 8390 and *n*-butyl acrylate monomer. The polymerizations were controlled and living but the molecular weight distribution broadened with higher conversions. The effect of target molecular weight and particle size was successfully decoupled to a significant extent by varying process conditions and parameters and particle sizes from 20-100 nm were obtained for target molecular weights from 20,000-80,000 $g \cdot mol^{-1}$.

5.1.2 Synthesis and Characterization of Polystyrene-*b*-Poly(acrylic acid) Copolymers

The use of amphiphilic block copolymers as protective colloids is desirable for a wide range of applications. However the importance of very narrow molecular weight distributions and high purity of these copolymers in commercial applications is not clear. The work described provides a basis for the synthesis of polystyrene-*b*-poly(acrylic acid) copolymers for performance analysis. The synthesis of polystyrene-*b*-poly(acrylic acid) copolymers was realized by synthesis of the polystyrene block first, followed by re-initiation with acrylic acid by solution polymerization in 1,4-dioxane to yield the resulting block copolymer. This direct synthesis method provided a much easier way than traditional methods to produce PSt-*b*-PAA copolymers of varying lengths and compositions. Polymerization conditions such as reaction time, monomer composition, and the ratio of BlocBuilder® MA to monomer can be adjusted to vary the length of each block and polydispersity. Characterization of these block copolymers were achieved using titration and nuclear magnetic resonance spectroscopy for composition, and gel permeation

chromatography for molecular weight analysis. The composition analysis by ^{1}H NMR appears to give accurate results provided that the polystyrene macroinitiator maintains a high degree of livingness, which is assessed by GPC. Otherwise, the titration method proves to be a more accurate technique. The results presented demonstrate the ability to synthesize a wide range of copolymers with the option to control the size of each block as necessary. The work presented in this thesis serves as the first part of the project to determine the effectiveness of copolymers of varying degrees of purity, compositions, and polydispersities as protective colloids.

5.2 Recommendations for Future Work

Based on the research conducted in this thesis, the following recommendations for future work for each chapter are made.

Chapter 3 explored various methods to decouple the effect of target molecular weight and particle size in nitroxide mediated microemulsion polymerizations at low surfactant to monomer ratios in order to provide a set of conditions at which those two properties can be targeted separately. Although significant progress has been made and the two properties can be successfully decoupled to a significant extent, the following recommendations are made in an attempt to further increase this range.

1. Widen the range of surfactant concentration explored. At some point, further increase in surfactant should lead to a decrease in particle size as is usually observed. This would be helpful in identifying the point at which the stabilization mechanism changes in order to

better understand and exploit the use of different surfactant concentrations to target the particle size.

2. Attempt to decrease further the particle sizes obtainable for target M_n of 20,000 $g \cdot mol^{-1}$ as it still remains a challenge to target particle sizes of <40 nm of low molecular weight. The ability to synthesize particles of these specifications in NMP microemulsions could lead to new applications of nanolatexes.
3. Dowfax^{TM} 8390 has proved to be a very effective surfactant in our polymerizations in terms of rate and stability achieved. However, it would be interesting to see if different types of surfactant would result in the same magnitude of changes in particle sizes obtained as well as stability achieved in these microemulsion systems. Dowfax^{TM} 8390 is a disulfonated surfactant, with double the charge density compared to monosulfonated ones. It will be interesting to see if the effect of ionic strength will be as pronounced with the use of monosulfonated surfactants.

Chapter 4 described the synthesis and characterization of polystyrene-*b*-poly(acrylic acid) copolymers using nitroxide mediated polymerization for use as protective colloids. The following recommendations are made to improve the accuracy of the composition analysis.

1. Explore the use of other NMR techniques to try to improve the accuracy of the ^{1}H NMR subtraction method.
2. Determine a suitable method to analyze the copolymer purity with regards to homopolymer blocks. These cannot be distinguished by the ^{1}H NMR spectrum as the

proton resonances appear in the same region. It would be necessary to evaluate the quantity of homopolymer contamination in the copolymer sample for future analysis.

3. The use of a dual detector method in GPC (UV-VIS/DRI) may help in characterizing polystyrene and poly(acrylic acid) composition.

Appendix A

Surfactant Coverage Analysis

The surfactant coverage of the surface of the polymer particles was determined from a soap titration method by Maron et al.[1]. In this procedure, polymer latex samples were diluted to desired concentrations and known quantities of surfactant were added to the sample while measuring the surface tension between each addition. When surfactant is added to the latex solution, the surfactant molecules will either dissolve in the aqueous phase, diffuse to the polymer-water interface, or form micelles at concentrations above the CMC[2]. The surface tension will decrease with the addition of surfactant as they are adsorbed onto the particle surface until the solution reaches CMC at which point the surface tension will remain the same with further addition of surfactant. A plot of the surface tension and the mass of surfactant added is then used to determine the maximum amount of surfactant that can be added to the latex before particle saturation occurs. Figure A.1 and Figure A.2 show the soap titration plots for latexes from expts. S41 and S43, respectively. The point at which the slope of the line changes indicates the maximum amount of surfactant that can be added to the polymer latex solution before micellization.

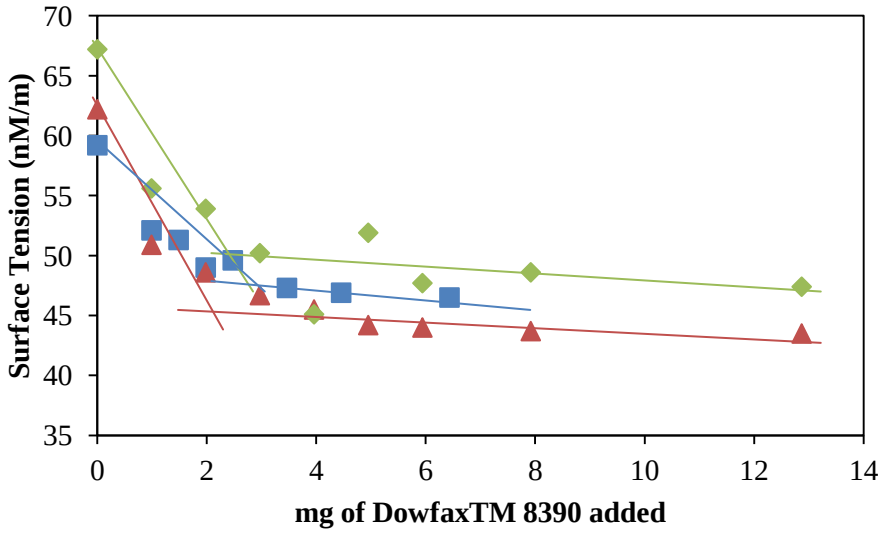

Figure A.1: Soap titrations for latex S41 at three different polymer concentrations: 1 mg·mL^{-1} (blue), 0.5 mg·mL^{-1} (green), and 0.25 mg·mL^{-1} (red).

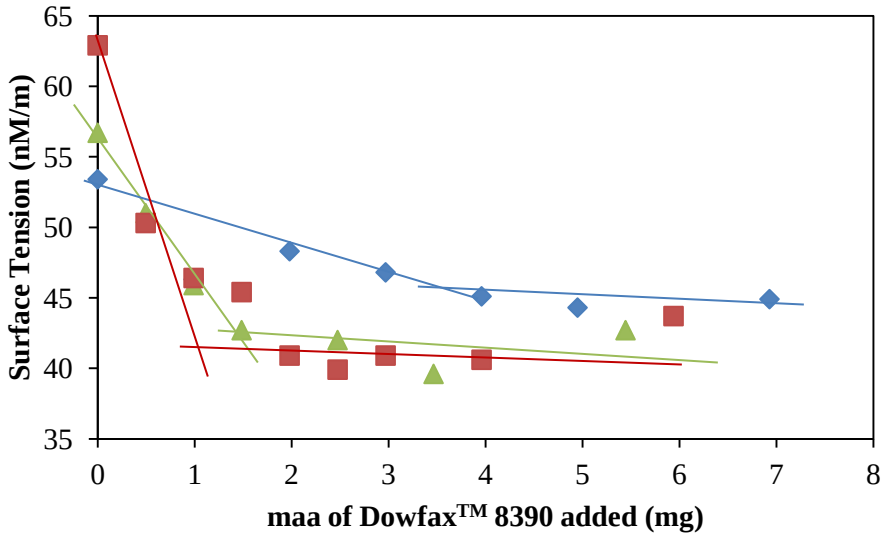

Figure A.2: Soap titrations for the latex of expt. S43 at three different polymer concentrations: 1 mg·mL^{-1} (blue), 0.5 mg·mL^{-1} (green), and 0.25 mg·mL^{-1} (red).

Using this information, the area that one surfactant molecule occupies on the particle surface (A_s) can be calculated as:

$$A_s = \frac{6}{S_t D_p N_A \rho} \qquad (A.1)$$

where D_p is the average particle diameter, N_A is Avogadro's number, ρ is the polymer density, and S_t is the moles of surfactant per gram of polymer particles at micellization determined experimentally. The value of S_t is the sum of the initial moles of surfactant per gram of polymer (S_i) and the mole of surfactant per gram of polymer required to reach the CMC (S_a). S_i and S_a are calculated as follows:

$$S_i = \frac{C_i}{m_o} \; and \; S_a = \frac{C_a}{m} \qquad (A.2)$$

where C_i is the initial surfactant concentration in moles per litre of latex, m_o is the initial polymer concentration in grams of polymer per litre of latex, C_a is the concentration of surfactant added and adsorbed in moles of surfactant per litre of latex, and m is the polymer concentration. Unadsorbed soap in the latex solution at the CMC (C_f) is accounted for using equation (A.3):

$$C = S_a m + C_f \qquad (A.3)$$

where C is the surfactant concentration at micellization obtained from the break point in the plot of surface tension against mass of added surfactant (Figure A.1 and Figure A.2). The slope and intercept of equation (A.3) are constant provided that the assumptions that the size of the particles or the adsorbing surface does not change hold true. A plot of C vs. m can be constructed to determine S_a and C_f as shown in Figure A.3 and Figure A.4.

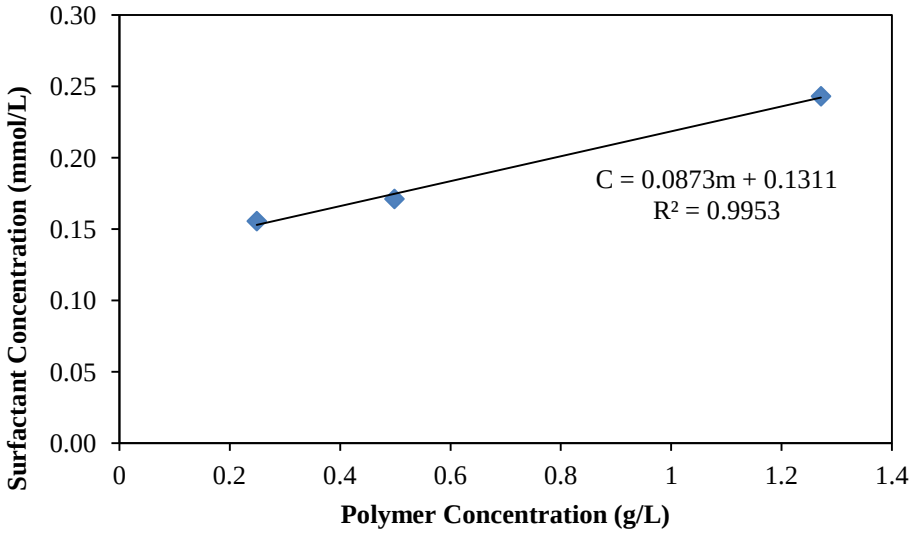

Figure A.3: Plot of surfactant concentration at micellization vs. polymer concentration for the latex of expt. S41at three different concentrations.

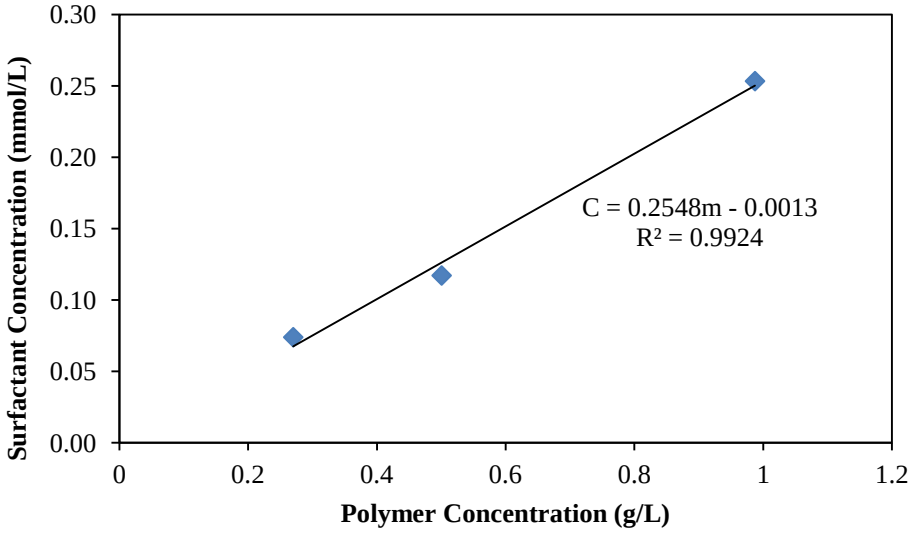

Figure A.4: Plot of surfactant concentration at micellization vs. polymer concentration for the latex of expt. S43at three different concentrations.

Using the value of S_t (S_i+S_a), the area that one surfactant molecule occupies on the particle surface can be calculated according to equation (A.1). The percent surfactant coverage is then calculated as:

$$\%\ Coverage = \frac{\left(\frac{m_s}{M_s}\right) A_s N_A}{\frac{6M_{pol}}{\rho D_p}} \qquad (A.4)$$

where m_s is the mass of surfactant, M_s is the surfactant molecular weight, A_s is the area occupied by one surfactant molecule, M_{pol} is the mass of the polymer. From this, the percent coverage calculated for expts. S41 and S43 are 83 % and 76 %, respectively.

References

[1] S. H. Maron, M. E. Elder, C. Moore, *J.Colloid Sci.* **1954**, *9*, 104-112.

[2] C. Fowler. Emulsion Polymerization Using Switchable Surfactants. M.Sc. Thesis, September **2011**.

Appendix B

Replicate Runs

In order to ensure that the particle sizes obtained from varying the process parameters are significantly different, three sets of replicate runs were carried out to determine the standard deviation between the measurements (conditions outlined in Table B.1).

Table B.1: Summary of conditions for the three sets of replicate microemulsion experiments.

	Target M_n ($g \cdot mol^{-1}$)	**S/M (wt/wt)**	**BB/Na_2CO_3 (mol/mol)**	**Mean Particle Diameter (nm)[a]**
R1	40000	0.2	0.4	41.68, 38.43, 43.46
R2	40000	0.5	0.4	64.95, 61.05
R3	80000	0.2	0.4	32.05, 34.07

[a] Particle size listed is the intensity average particle size (d_z) from the Malvern Nanosizer

Figure B.1 shows the replicate runs for target molecular weights of 40,000 and 80,000 $g \cdot mol^{-1}$. As observed, there is minimal batch to batch variation between the final particle sizes obtained.

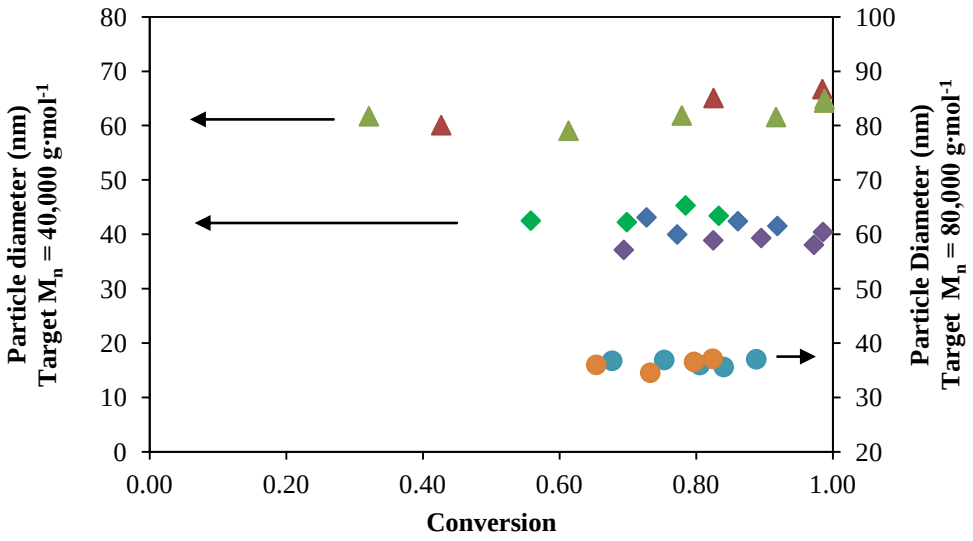

Figure B.1: Replicate runs showing consistent results with minimal batch to batch variation in particle sizes achieved for expts. R1 (◆), R2 (▲), and R3 (●).

Statistical analyses were also performed on the particle sizes obtained from varying each set of parameters discussed previously to determine if the differences in the particle sizes obtained are indeed significantly different. The two-sided Student's t-test was used to compare two population means at a time and against a significance level of 95%, the particle sizes obtained were indeed statistically significant. This means that the differences in particle sizes obtained are caused by the adjustment made to the process parameters. Table B.2 provides a sample of the statistical analyses carried out for one of the replicate sets and for the experiments with varied surfactant to monomer weight ratios from 0.2 to 0.5 at BlocBuilder/Na_2CO_3 molar ratio of 0.4 at a target M_n of 40,000 g·mol^{-1}.

Table B.2: Results from the two-sided Student's t-test performed at a significance level of 95% on replicate data set R1(R41-R43) and S/M variation experiments S41-S43 with BB/Na_2CO_3 = 0.4 at a target M_n of 40,000g·mol^{-1}.

Expt	Mean	Variance	Comparison	Degrees of Freedom	$T_{Statistic}$	$T_{critical}$[a]	P-value
R41	41.68	0.79	**R41, R42**	2.33	1.77	3.93	0.2193
R42	38.43	9.39	**R42, R43**	2.04	-2.77	4.26	0.1091
R43	43.36	0.09	**R41, R43**	2.43	-3.10	3.82	0.0900
S41	38.19	0.09	**S41, S42**	2.93	-18.96	3.26	0.0028
S42	45.49	0.36	**S42, S43**	4.00	-31.36	2.78	0.0001
S43	61.05	0.38	**S41, S43**	2.87	-57.73	3.32	0.0003

[a] $T_{critical}$ determined from t-distribution tables[1].

A 95 % confidence interval was also constructed for the set of replicates to determine the minimum significant difference in particle diameter and a value of 5 nm was obtained. The confidence interval is constructed using equation B.1:

$$Confidence\ Interval\ at\ 100 * (1-\alpha)\%\ significance = \bar{X} \pm t_{(1-\alpha/2, N-1)} \frac{s}{\sqrt{N}} \qquad (B.1)$$

where $\bar{X}$ is the mean, $t_{1-\alpha/2,\ N-1}$ is from the t-distribution tables, s is the sample standard deviation, and N is the number of samples.

References

[1] D. C. Montgomery, G. C. Runger, *Applied Statistics and Probability for Engineers*, John Wiley & Sons 2010.

Appendix C

Molecular Weight Distributions

(a) S41

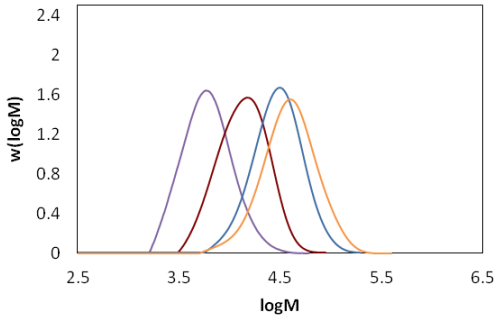

(b) S43

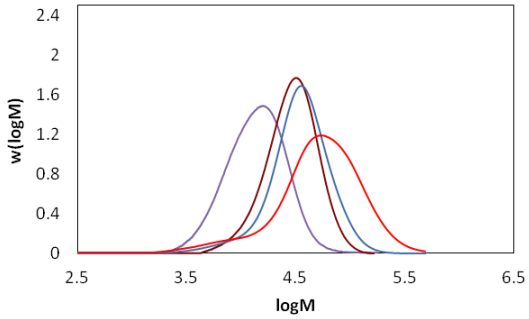

(c) S81

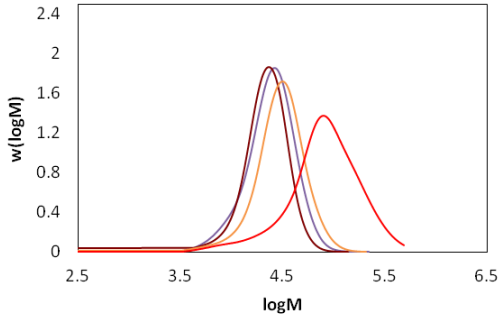

(d) M21

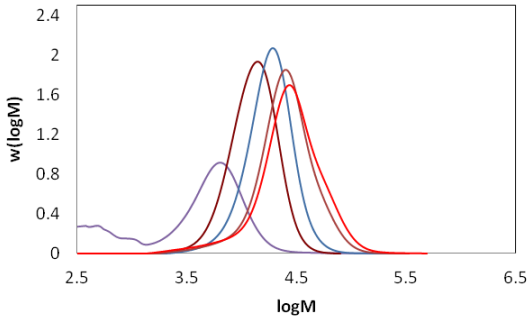

(e) M22

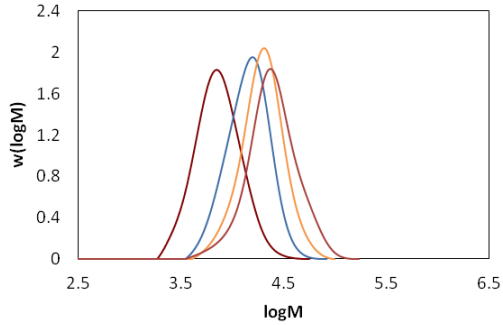

(f) M23

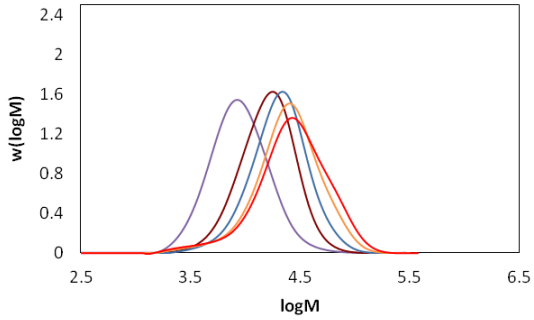

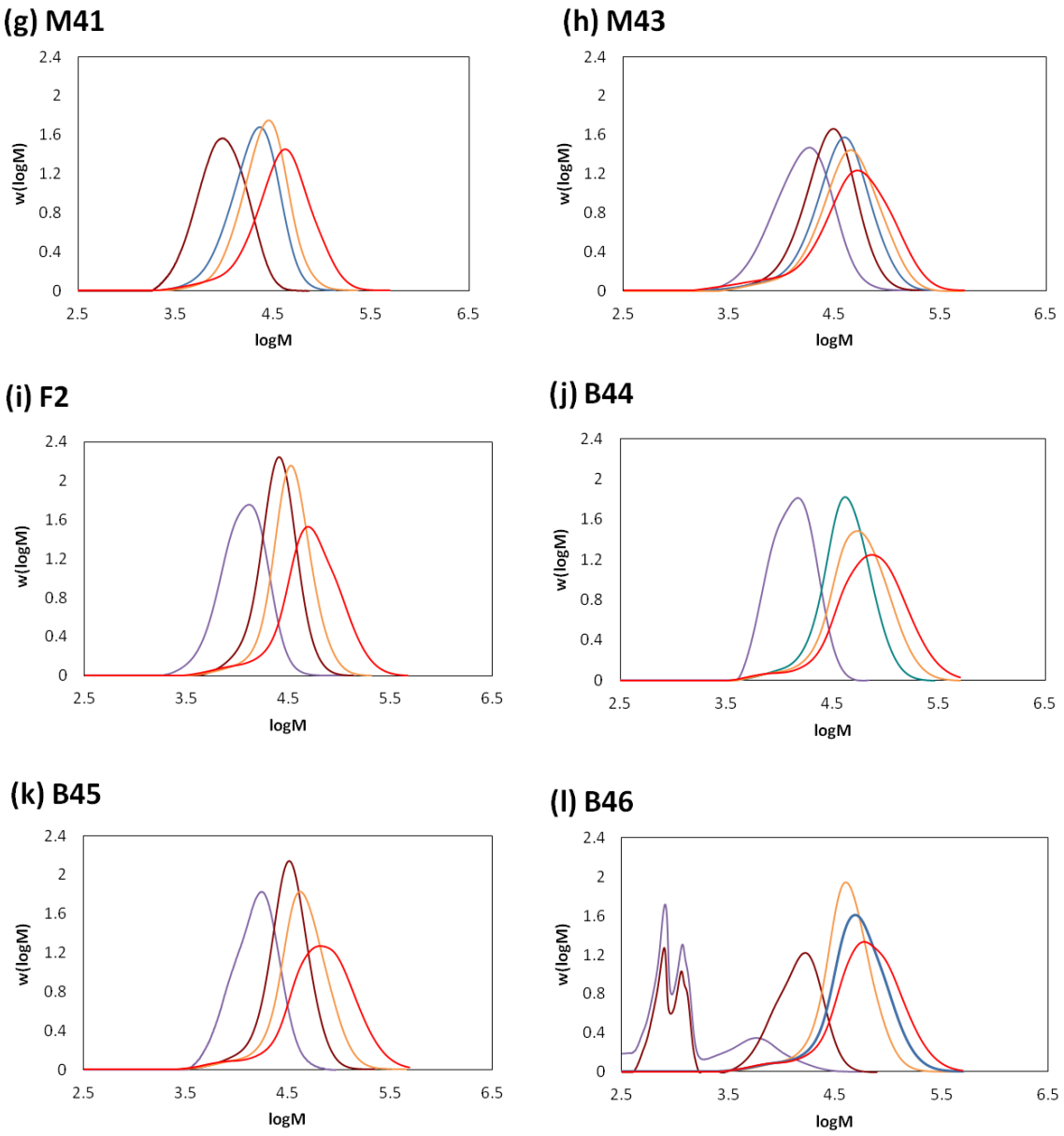

Figure C.1: Full molecular weight distributions for some of the SG1-mediated microemulsion experiments of *n*-butyl acrylate listed in Table 3.6. (a-c) S series of experiments for variation of the surfactant to monomer ratio. (d-h) M series of experiments for variation of initial monomer content in the seed stage. (i) F series of experiments for variation of the semi-batch addition of surfactant. (j-l) B series of experiments for variation of BlocBuilder to Na_2CO_3 ratio.